OPTIMISING THE HYBRID OPERATION TEMPERATURE WINDOW OF A HYBRID HEATING SYSTEM IN THE IRISH CLIMATE

A NUMERICAL SIMULATION STUDY OF AN AIR-WATER HEAT PUMP AND CONVENTIONAL GAS BOILER IN A RESIDENTIAL SETTING

DANIEL JAKOB
(18409686)

The thesis is submitted to University College Dublin in part fulfilment of the requirements for the degree:

ME in Mechanical Engineering
School of Mechanical and Materials Engineering
College of Engineering & Architecture
University College Dublin

SUPERVISOR: Prof. Donal Finn

25th April 2023

Daniel Jakob: *Optimising the Hybrid Operation Temperature Window of a Hybrid Heating System in the Irish Climate*, A Numerical Simulation Study of an Air-Water Heat Pump and Conventional Gas Boiler in a Residential Setting, © April 2023

SUPERVISOR:
Prof. Donal Finn

COLLABORATOR:
Dr Mohammad Saffari

HEAD OF SCHOOL:
Prof. Kenneth Stanton

ME in Mechanical Engineering Thesis 2023
School of Mechanical and Materials Engineering
College of Engineering & Architecture
University College Dublin
Belfield, Dublin 4, Ireland

Typeset in LaTeX, with LuaLaTeX and the classicthesis v4.6
FONTS:
main text font: TeX Gyre Pagella, math font: TeX Gyre Pagella Math, monospace font: Bera Mono
SOURCE AVAILABLE AT:
https://github.com/daniel-jakob/Thesis.

DECLARATION

Belfield, Dublin 4, April 2023

Daniel Jakob

Dedicated to my family.

CONTENTS

LIST OF FIGURES

LIST OF TABLES

ACRONYMS

COP Coefficient of performance
GHG Greenhouse gas
HHS Hybrid heating system
ASHP Air source heat pump
PE Primary energy
PEF Primary energy factor
HVAC Heating, Ventilation & Air Conditioning
PES Primary energy savings
SPF Seasonal performance factor
SCOP Seasonal coefficient of performance
RHI Renewable Heat Incentive
DHW Domestic Hot Water
AWHP Air-Water Heat Pump
HP Heat Pump

HHPS Hybrid Heat Pump System
RES Renewable Energy Share
TES Thermal Energy Storage
HDD Heating degree days
PID Proportional-integral-derivative
RMSE Root mean square error
CV(RMSE) Coefficient of Variation of Root Mean Square Error
NMBE Normalized mean bias error
SMAPE Symmetrical mean absolute percentage error
ACPH Air Changes Per Hour
BEM Building Energy Model

NOMENCLATURE

Abbreviations

%-age	Percentage
avg.	Average value
exp	Experimental
nom.	Nominal value
sim	Simulation/Simulated
temp.	Temperature

Subscripts

0	Nominal value of variable or parameter
v	Constant volume, when Referring to specific heat of a substance
i	Index variable
air	Referring to air
biv	The bivalent temperature of the HP
cut	The cut-off temperature of the boiler
elec	Referring to electricity
ext	Referring to external or ambient air
gas	Referring to gas
H	Referring to heat energy
HP	Referring to a/the HP

rad	Referring to radiation/radiative
tot	Total or cumulative value

Other Symbols

$\bar{Y}$	Average value [−]
Δ	Difference or "change in" operator [−]
$\dot{m}$	Massflow rate [$\mathrm{kg\,s^{-1}}$]
$\dot{Q}$	Heat or energy flowrate [$\mathrm{J\,s^{-1}}$] or [$\mathrm{kW\,s^{-1}}$]
$\dot{V}$	Volumetric flowrate [$\mathrm{m^3\,s^{-1}}$]
$\dot{W}$	Work flowrate [$\mathrm{J\,s^{-1}}$] or [$\mathrm{kW\,s^{-1}}$]
η	Efficiency [%]
$\hat{Y}$	Actual or reference value [−]
ts	Timestep index [−]
ρ	Density [$\mathrm{kg\,m^{-3}}$]
A	Area [$\mathrm{m^2}$]
B	Fuel consumption [kW]
C	Cost of fuel type [$\mathrm{€\,kWh^{-1}}$]
c	Specific heat capacity of a substance [$\mathrm{kJ\,kg^{-1}\,K^{-1}}$]
h	Heating value [$\mathrm{J\,kg^{-1}}$]
I	Carbon intensity [$\mathrm{g\,kWh^{-1}}$]
k	Scaling factor used in boiler model [−]
m	Mass [kg]
N	Total number of data points [−]
n	Exponent of heat transfer, used in the radiator model. Set to 1.3 [−]

p	Number of adjustable model parameters, for calibration purposes, ASHRAE suggests $p = 1$ $[-]$
Q	Amount of heat or energy transfer [J] or [kWh]
T	Temperature [°C]
t	Time [s]
U	Heat transfer coefficient $[\mathrm{W\,m^{-2}\,K^{-1}}]$
V	Volume $[\mathrm{m^3}]$
W	Amount of work transfer [J] or [kWh]
Y	Simulated or forecast value $[-]$
y	Control signal used in boiler model $[-]$

ABSTRACT

A full factorial parametric study was carried out on a numerical model of hybrid heating system consisting of an air source heat pump and a gas boiler. This thesis aims to use the `Modelica` modelling language to determine an optimal bivalent parallel operation temperature window for the hybrid heating system. A two-storey, residential home was modelled, verified and validated against the reference home, and year long simulations were performed to optimise the temperature window along two metrics: reducing carbon emissions and reducing annual running costs. All combinations of seven bivalent temperatures from minus two Celsius to four Celsius and six cut-off temperatures from five Celsius to ten Celsius were examine in year-long numerical simulations. The `Modelica-EnergyPlus` co-simulation was carried out via the `Spawn of EnergyPlus` utility.

The best performing combination in the sensitivity analysis was a bivalent temperature of one Celsius, and a cut-off temperature of five Celsius. This combination resulted the lowest carbon emissions and the lowest annual heating cost for the Irish climate studied—a temperate oceanic climate. The distribution of natural gas usage and electricity usage were very different to one another across the different temperature windows. Gas usage was greatest at bivalent temperatures of three and four Celsius. Electricity usage peaked at minus two Celsius and ten Celsius bivalent and cut-off temperatures, reaching a minimum at four Celsius and five Celsius bivalent and cut-off temperatures respectively.

Combinations with higher bivalent and lower cut-off temperatures were more sensitive to gas and electricity price changes, most likely due to their higher energy consumption overall. Combinations with bivalent temperatures that allowed the heat pump to operate below the temperatures at with frosting occurred on the heat pump evaporator coils resulted in up to 50% greater yearly on-off cycling rates. Seasonal coefficient of performance varied only slightly with varying bivalent operation window.

Keywords: Hybrid heating system, parametric study, numerical building energy modelling.

ACKNOWLEDGMENTS

Firstly, I want to express my greatest appreciation to my supervising professor, Prof. Donal Finn, for his invaluable guidance and feedback throughout the research project. His input and encouragement have been essential in shaping the direction of this project.

I also extend my gratitude to the project collaborator, Dr Mohammad Saffari, for his contributions to this work. His expertise in `EnergyPlus` (and accompanying software) and willingness to share data to carry out the analysis has been instrumental in the success of this project, and I am thankful for his enthusiasm to collaborate and share his knowledge.

I want to thank Dr Alessandro Maccarini for his `Modelica/Dymola` course in Copenhagen, Denmark, which provided me with a solid foundation in the subject matter. His dedication to teaching has been inspiring. Thank you to UCD for providing funding to visit Copenhagen, and software licenses. Thank you to Dr Michael Wetter and the Modelica Buildings Library team at Lawrence Berkeley National Laboratory for their work on progressing the building energy simulation field.

I cannot forget to acknowledge the unwavering support and patience of my family and friends, who have been a constant source of encouragement throughout my academic journey. Thank you to Linus Sebastian, Michael Stevens, Derek Muller, Hank Green, and my late grandfather Jürgen Bielstein for being the people who ultimately influenced me to pursue mechanical engineering.

Special thanks to fellow Modelica-enjoyer Matthew Duffy, my sauna-buddy Daniel Joyce and Cormac Moloney for being my debugging rubber duck. Thank you to the people of `Beach Gaf` for providing endless fun (and often seriously distracting me...).

Finally, thank you to my parents for giving me the opportunity to attend university, providing for me and always wanting the best for me. Thank you, I love you.

1

INTRODUCTION

1.1 CONTEXT

Largely, throughout the developed world, it is clear that residential energy usage accounts for a large share of total energy use, and of that, space heating and Domestic Hot Water (DHW) production account for the majority of final energy use. In the USA, Heating, Ventilation & Air Conditioning (HVAC) energy use is 50% of all building energy use and in China, HVAC energy use is between 50%–70% of building energy use [1]. It is estimated that by 2050, two thirds of all residential buildings will have a form of air conditioning unit, further increasing these percentage shares. Alone in 2021, space cooling demand rose by 6.5% [2]. In Europe in 2022, the residential sector was responsible for 27% of final energy consumption [3]. Domestic water heating and space heating collectively account for close to 80% of a household's energy usage in Europe. [4]. All of this is to say, energy use due to HVAC and DHW production are high and are expected to continue rising.

Of course, it must be noted that air conditioning naturally rose sharply in no small part due to the COIVD-19 pandemic and subsequent isolation rules in place in many parts of the world.

Climate change has directly affected heating and cooling design. ASHRAE highlight that for 1274 weather stations/observing sites worldwide with sound data between 1974 and 2006, the averaged design conditions (which are explained in Sec. 2.2) over all locations had changed by the following:

- The 99.6% annual dry-bulb temperature increased by 1.52 °C
- The 0.4% annual dry-bulb increased by 0.79 °C

- Annual dew point increased by 0.55 °C
- Heating degree days (base 18.3 °C) decreased by 237 °C d
- Cooling degree days (base 10 °C) increased by 136 °C d

As of writing, continental Europe is experiencing "the most extreme event ever seen in European climatology" with a mid-winter heatwave [6]

All of these changes the mentioned parameters point towards an increase in global temperatures. The effects of climate change are affecting how building cooling and heating design is carried out, due to the fact that cooling loads are, in general, becoming lower, while heating loads are generally increasing. Milder winters are allowing Heat Pumps (HPs) to be, ever so slightly more efficient throughout a heating season. Already, HPs have over recent years become more popular throughout Europe [7, 8], but this is more likely due to higher efficiencies and lower costs of newer models.

The so-called *electrification of heat* has been supported in the EU for some time now due to seeking carbon emissions reductions and also security of supply, which, due to events on-going as of the writing of this thesis, has indeed become more of an issue than previously thought... Electric heating devices such as HPs convert electricity into heat, creating the sought after link between building heating and the electrical grid [9]. However, this link will not come without growing pains, as more buildings rely on the electrical grid to provide electricity for heating, the electrical demand grows. Due to the nature of heating demand and weather/climate which generally affects large areas and subsequently a large number of houses simultaneously, the electrical grid would be of course put under large strain when a particularly cold spell of weather hits an area. These great peaks in energy demand are a problem when it comes to electrical grid deployment, as the real-time balancing of the grid becomes an increasingly difficult job with the large variability of renewable energy production methods such as wind. Vuillecard et al., Thomaßen, Kavvadias and Jiménez Navarro [10, 11] propose that Hybrid heating systems (HHSs) could alleviate these very

high energy demands from heating systems, could they manage to intelligently switch to primarily gas operation during peak energy demand periods.

In Ireland, the housing stock increased by just 0.4% between 2011 to 2016 [12]. Very few new houses are being constructed with the possibility for newer, more efficient space heating and/or hot water production systems and better, holistic insulation. A similar sentiment has been noted in other Western European countries, making this not a localised issue, but rather an international one [13, 14]. Thus, in order to reduce Primary energy (PE) consumption in any meaningful way, retrofits must be carried out on existing buildings. This includes adding insulation to attic spaces and/or walls of the house and the installation of more efficient heating systems. An advantage of HHSs is that existing buildings presumably already have a heat generator, be it a gas boiler or otherwise, which can be easily integrated into a HHS with the addition of a HP. Of course, plumbing works must be carried out and the HP itself has a relatively high barrier to entry in the form of a high upfront cost. Currently SEAI do not give grants for the installation of HPs as they do not deem them to be a renewable type of heat generator. This is partly true as HPs do use electricity to run, which, as discussed in Sec. 2.3, is generated mostly by non-renewable means in Ireland currently.

Heat transfer from low to high temperature regions does not occur through normal thermodynamic means. Refrigerators are special devices used to achieve this, utilizing the refrigeration cycle, with the vapour-compression refrigeration cycle being the most commonly used. The reversed Carnot cycle is the most efficient but is only an idealized theoretical model. HPs and air conditioners have the same components, and a single system can be used for both heating and cooling by adding a reversing valve to the hydronic circuit [16].

The performance of Air source heat pumps (ASHPs), or HPs in general, is very different to that of a traditional gas condensing boiler. The performance of a HP is almost entirely determined by the outdoor temperature and climatic conditions. The performance of a HP is described by the Coefficient of performance (COP) of the unit. This measure varies throughout a heating season, day and even from minute to minute. A HP with a COP of 3 for example, produces three units of heat energy for every unit of electricity supplied. This *extra* energy is being gathered from a renewable energy source — which in the case of Air-Water Heat Pumps (AWHPs) is the external air. The amount of non-renewable energy consumed by HP at any given time depends on the Renewable Energy Share (RES) of the grid. According to SEAI, the RES of Ireland for electricity is around 9.3%. This figure is expected to increase in the coming years/decades as more wind turbines are installed, other renewable energy generators are built, the Celtic Interconnector subsea line between Ireland and France, and multiple non-renewable energy plants are decommissioned.

Since the COP of an ASHP varies quite drastically over a heating season, the measure Seasonal coefficient of performance (SCOP) is often used to describe the performance of a HP over a year or a heating season. The SCOP is an important tool for measuring the performance of heat pumps because it provides a standardised way to compare the efficiency of different systems. The measure of SCOP and Seasonal performance factor (SPF) are quite similar in that they are both a ratio of the total electrical energy input to the total heat energy output of the HP, however, SCOP can also include other parts of the heating system

Frosting is detrimental to the performance of HPs [17]. During cold, humid weather, frost builds up on the evaporator coils on the outdoor component of the HP. Frosting dramatically lowers the heat conductivity between the coils and the ambient air, be-

ing essentially insulated by the frost. Frosting is a major concern in cool, humid climates, Ireland being one such climate.

A Hybrid Heat Pump System (HHPS) as opposed to monovalent systems, is a configuration of a HP in combination with a conventional gas boiler. During warmer days, the HP has sufficient heating capacity to provide all the energy needed to heat a space, while being very efficient, while on colder days, it may be not economical or ecological to run the HP. During these periods, the majority of the heating load is passed to the gas boiler, which is not affected by the ambient air temperature. A control system can be put in place to intelligently turn on and off the HP and gas boiler to better suit the current weather. An alternative-parallel bivalent system is where the predefined external temperatures for turning on/off the HP/boiler are not coincident, as discussed in Subsubsec. 2.1.3.1. This creates a temperature range wherein the HP and boiler are running simultaneously. This is the focus of this thesis: where lies the optimal crossover points for boiler-only operation, bivalent operation and HP-only operation, specifically for the Irish climate. This research has been carried out for other climate types. The Irish climate is unique in that the temperature range (during the heating season) is quite narrow, the humidity is quite high almost all year round (especially on the west coast) and the temperature is quite mild. Fig. 1.1 shows a heating duration curve, which are explained in Sec. 2.2, with the bivalent temperature and cut-off temperature overlaid. The red region shows the number of hours of the year where the boiler is active, to the left of the cut-off point, the boiler is the sole heat source of the HHPS, while to the right of the cut-off point and left of the bivalent point, the boiler and HP are producing heat. Right of the bivalent point, the HP is the sole heat producer.

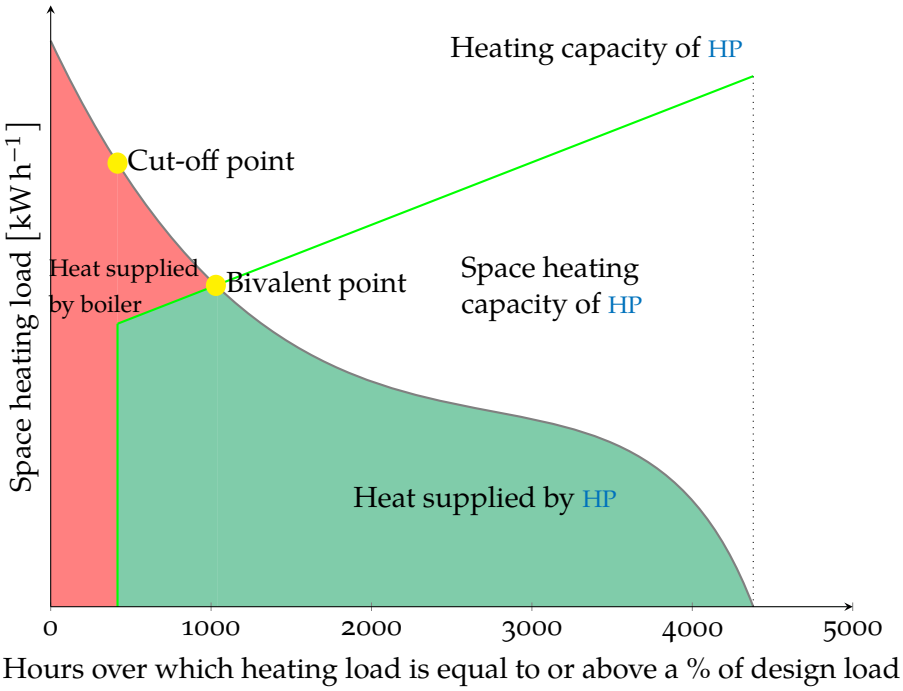

Figure 1.1: Hybrid operation representation via heating duration curve

1.2 OVERVIEW OF METHODOLOGY

Briefly, this thesis uses a numerical model of an Irish residential house (in `EnergyPlus`) coupled with a HHPS model developed in `Modelica` to co-simulate year long experiments. The model of the dwelling was based off a real house in Belturbet, Co. Cavan, and experimental values measured from the dwelling in-situ, over the course of a year and a half, were used to validate the house and heating system model. 42 year long experiments were simulated, each with a different bivalent operation temperature window, i.e., a sensitivity analysis was carried out, varying two parameters, the bivalent temperature of the HP, and the cut-off

temperature of the boiler. The affects of varying this window were analysed from an ecological basis and an economic basis.

1.3 AIM

The overall aim of this thesis is to create a `Modelica-EnergyPlus` co-simulation model of a reference residential building and HHS. Through this model, the dynamics of shifting and dilating the hybrid operation temperature window will be analysed in order to optimise the HHS along two dimensions: minimising CO_2 emissions and minimising annual heating costs. In other words, a parametric study with fixed-factor design will be carried out investigating the effects of varying the year-fixed hybrid operation temperature window, in annual simulations of the model. This analysis will first be carried out using the Irish market as a case study, and the results will be generalised to determine inflection points.

1.4 MOTIVATION

The operation, control and performance of HHSs consisting of AWHPs and traditional gas boilers has been moderately studied in the literature. This type of heating system has been simulated and tested in-situ in countries such as China [18], Japan and Korea [19, 20], North America [21], Germany [13] and other continental European countries [14, 17, 22–24], however, the research regarding efficient control of such a system in the Irish climate, namely a temperate oceanic climate, has not (or at the least only partially) been explored [9]. Ireland has a very changeable and mild climate, but the characteristic of note is its consistently high humidity. Humidity and low temperatures are the bane of HP operation and efficiency.

By achieving the aims mentioned previously, this thesis aims to contribute to the development of energy-efficient and cost-effective HHSs that have the potential to reduce Greenhouse gas (GHG) emissions and promote sustainable energy practices in the residential sector. The use of a rigorous and validated simulation model will enable a more accurate analysis of the system dynamics, allowing for the identification of optimal operational parameters and the potential for further optimisation in future research.

1.5 RESEARCH QUESTION

Research question: How can a year-static hybrid operation temperature window of a HHS be optimised to minimise both CO_2 emissions and annual heating costs in a typical Irish residential home.

1.6 THESIS LAYOUT

The thesis is structured as follows:

Chap. 2 provides a literature review on HPs, HHSs, Heating degree dayss (HDDs), PE, electrification of heating, controllers and control theory, and verification and validation of models.

Chap. 3 outlines the methodology used, including the experimental reference building, building and heating system models, sensitivity analysis design, and eco-economic assessment.

Chap. 3 focuses on the system model, including the location, form and fabric of the building, schedules, equipment and internal gains, and heating system.

Chap. 5 presents the results of the parametric study, specifically the parametric study design, energy consumption (electricity and gas), and performance indices.

Chap. 6 covers the eco-economic assessment, including analysis of the minimisation of the cost of annual heating, minimisation of CO2 emissions and optimising Primary energy savings (PES).

Finally, Chap. 7 presents the conclusions drawn from the study, as well as giving outlines for potential future work on the subject.

2

LITERATURE REVIEW

The literature review chapter provides a comprehensive overview of the relevant literature in the field of HHSs, including HPs, HDDs, PE, electrification of heating, controllers and control theory, and verification and validation of models. In particular, Sec. 2.1 focuses on HPs, covering the vapour-compression cycle, HHSs, bivalent operating modes, buffer tanks, frosting and defrosting. Sec. 2.2 examines HDDs and design temperatures, while Sec. 2.3 discusses into PE considerations. Sec. 2.4 discusses the electrification of heating, and section Sec. 2.5 discusses controllers and basic control theory, including Proportional-integral-derivative (PID) controllers, noise, and error. Finally, Sec. 2.6 examines the verification and validation of the model, including validation techniques, methodologies, statistical indices and their associated tolerances.

2.1 HEAT PUMPS

HPs work by harnessing the energy from low temperature sources such as air, water or the ground. HPs of any kind acquire energy from its surrounding environment in the form of low-temperature heat and *concentrate* it to heat comparatively minute volumes to its surroundings. This is achieved through a vapour compression cycle, explained in Subsec. 2.1.1. Under ideal conditions, AWHPs have extremely high COPs in the 3.5 to 4.5 range. This is of course from their ability to harvest the aerothermal energy from the outside air. The main downfall of AWHPs is that when the external air temperature is low, their COP is reduced

significantly. Due to this inherent disadvantage, HPs are essentially unfit be the sole space heating generator for almost all applications, depending on climates and design points. While HPs have the capacity to perform heating and cooling, this thesis and associated simulations do not consider the cooling of a building or home, and therefore is only concerned with heating and considers only the heating-season time frame of the year. The space-heating radiators found in existing homes are not suitable for cooling [13], the cold water in the radiators does not warm the room effectively and condensation on the radiator surface may become and issue.

Because the efficiency of HPs is so dependent on the constantly varying outside air temperature, the measure of SPF is typically used to characterise them when considering the performance over a certain heating period and is considered a more comprehensive metric to establish HP efficiency [8, 25]. The SPF represents the ratio of the total useful energy produced by the HP during a heating season, to the seasonal electricity consumption. For example, an SPF of 3 would mean that over a given year, the HP produced 3 units of heating energy for every unit of electrical energy provided [25]. Due to HPs extracting renewable energy from the surrounding air, the SPF is (or should be) always higher than 1, and generally is above 3. EU legislation states that in order to be eligible for the Renewable Heat Incentive (RHI), the SPF of a HP must be above 2.5 [26].

There are three main types of HPs for space heating (i.e., not air-conditioning): AWHPs, Ground-Water Heat Pumps and Hydro-Water Heat Pumps [27, 28]. Ground-Water HPs acquire their heat energy by exploiting the heat contained within the soil of the Earth. Soil, below a certain depth has a very consistent heat, only fluctuating mildly seasonally. The added benefit of this type is that soil below a certain depth will not freeze, which would cause frosting like in AWHPs. Hydro-Water HPs gain their

heat from water sources such as ponds, lakes or well-water. The temperature of water fluctuates far less than the ambient air temperature, meaning they do not extract as much energy as AWHPs on warmer days, however, during warmer days, the heating load of a residential home is much less than the peak load. Conversely, during very cold days, the water remains much warmer than the air, which is very beneficial during those high-load spells. These two types of HPs, due to their heat sources, have their merits, however, it is also due to their heat sources that they are relatively obscure and not commonplace. Installing these types of HPs is costly, complicated, time consuming and require permits to build. Due to these reasons, AWHPs are the most common form of HP sold in Europe [7].

HPs come in many different heat capacities, from single kilowatt units to extremely large units which can heat large multi storey office buildings. In residential home contexts, the largest HPs generally available are almost 300 kW, but usually fall in around the 5 kW to 20 kW range. If an ASHP were to be sized so large as to have the capacity to provide the entire heating envelope of a residential home during even the coldest expected temperatures, the ASHP would (aside from being prohibitively expensive), be so oversized that when temperatures are moderate, the HP would produce so much heat as to heat the space so quickly that it would have an extremely short on-off cycle [29]. Since the peak load for heating occurs for a very small number of hours during any given heating period, this would be very detrimental to the unit, specifically the condenser component. The frequent on-off cycling significantly reduces the longevity of the condenser, and would require replacement long before what would be expected [30]. Many manufacturers suggest that the number of on-off cycles should not exceed 6 per hour. To avoid this issue, AWHPs are specifically undersized. Various "design temperatures" can be calculated for a given location. For Dub-

lin, the design temperature which covers 99.0% of the annual heating is −0.7 °C. AWHPs are usually sized to meet a design temperature of 60%–70%, as opposed to more traditional space heaters, as is further explained in Sec. 2.2.

HPs tend to perform better when providing space heating through underfloor heating [25]. This is partly due to underfloor heating being more efficient in general than other, more traditional space heating methods, namely hot-water radiators. Another reason more applicable to HPs is that the (space heating) inlet water temperature for underfloor heating is much lower than radiators. This means the HP does not have to heat the circulating water as hot as it would with radiators. The temperature delta between water temperature inlet to the HP and the outlet is simply lower and therefore less energy has to be produced by the HP in the first place. However, retrofitting houses with underfloor heating is expensive and very intrusive to the building — as obviously (all) floors must be ripped up and coils must be placed and plumbed — which discourages many homeowners from performing this type of retrofit.

HPs for residential use are generally classified into two distinct product types: low-temperature and high-temperature, which refers to the flow temperature of the HP. Low-temperature HPs typically heat water to a maximum temperature of 35 °C, while high-temperature HPs typically heat water to a maximum temperature of 55 °C [31]. The flow temperature of a HP in a heating system plays a crucial role in the performance and efficiency of the system. It refers to the temperature of the fluid, typically water or refrigerant, as it flows through the HP's evaporator and condenser coils. A lower flow temperature in the evaporator coil allows the HP to absorb more heat from the source, increasing the energy provided to the in-pump loop which is passed to the condenser coils and subsequently the heat distribution/buffer tank loop [8]. The flow temperature is affected by the initial tem-

perature of the refrigerant and also how much electrical energy is being provided to the compressor.

The flow temperature also affects the overall temperature of the heating system, as it determines the temperature of the water or refrigerant that is circulated through the heating system of the building. A higher flow temperature allows the HP to provide more heat to the building, making it warmer. However, a higher flow temperature also results in a lower COP of the heat HP, meaning it is less energy efficient.

2.1.1 *Vapour-Compression Cycle*

The vapour-compression cycle is a process used in HPs and refrigeration systems to transfer heat from a low temperature heat source to a high temperature heat sink [16]. The cycle begins when a refrigerant, typically in a liquid state, is vaporised in an evaporator. As the refrigerant vaporises, it absorbs heat from the surrounding low temperature heat source, such as the air inside a refrigerator or the ground in a geothermal HP.

Next, the vaporised refrigerant is pressurised and moves through a compressor. As the refrigerant is compressed, its temperature and pressure increase. The hot, high pressure refrigerant vapour is then passed through a condenser, where it releases heat to the surrounding high temperature heat sink, such as the air outside a refrigerator or the air inside a home in a HP.

As the refrigerant gives up heat, it condenses back into a liquid. The liquid refrigerant is then passed through an expansion valve, where its pressure is reduced and it begins to evaporate once again. This reduction in pressure causes the refrigerant to absorb additional heat, which helps to further cool the low temperature heat source.

The refrigerant continues through the cycle, alternating between the evaporator, compressor, and condenser, until the desired level of heat transfer is achieved. In a HP, the cycle is reversed during the heating mode, transferring heat from the outside air to the inside of a home.

While the vapour-compression cycle is not identical to the Rankine cycle or the Carnot cycle, it shares some similarities and can be thought of as a practical implementation of these theoretical models.

The Rankine cycle is a thermodynamic cycle that describes the operation of a heat engine, such as a steam power plant [16]. The cycle consists of four processes: pressurisation, heating, expansion, and cooling. These processes are similar to those in the vapour-compression cycle, in which a working fluid (such as water or steam) is pressurised and heated, causing it to expand and generate work before being cooled and condensed back into a liquid.

Like the Rankine cycle, the Carnot cycle is a theoretical model of a heat engine that describes the maximum possible efficiency of a heat engine operating between two temperature reservoirs. The Carnot cycle consists of four reversible processes: isothermal expansion, adiabatic expansion, isothermal compression, and adiabatic compression. The efficiency of the Carnot cycle is determined by the temperature difference between the heat source and the heat sink, and it serves as a benchmark for the performance of real heat engines [16].

2.1.2 *HHSs*

A bivalent, hybrid HP heating system consists of a HP of some description and an auxiliary or supplemental heating source [32]. The HP type this thesis focuses on is a AWHP, and the auxiliary

heating source is a conventional condensing gas boiler. The overarching idea behind this dual heating source system for a home is: the (undersized) HP can provide heating to the home using electricity, rather than gas, as its energy input during milder periods of the heating season with minimal usage of the gas boiler, and during the more severe, colder periods of the season, the gas boiler can provide the majority of the heat required to keep the home at a comfortable temperature. AWHP performance is very weather dependent, as explained in Sec. 2.1, and during very cold, humid spells simply cannot provide enough heating capacity to maintain a comfortable temperature inside, unless it is wholly oversized, which has problems associated with it, described Sec. 2.1. Therefore, almost all of the literature agrees that an undersized HP with a "correctly" sized gas boiler is the most efficient system [14, 20–22]. Fig. 2.1 shows a schematic diagram of a HHS comprising of an AWHP, gas boiler, buffer tank, radiators, sensors, and controller. The blue line represents the "cold" water, which has just expelled its heat to the indoor rooms and is circulating back to the HP and gas boiler to be heated up again. This return water is typically in the range of 25 °C to 30 °C by the time it reaches the heating devices. The heating devices heat the water up a temperature in the range of 45 °C to 40 °C, where makes its way back to radiators to once again expel its stored heat to the indoor rooms, which for a comfortable temperature, are in the neighbourhood of 18 °C to 22 °C.

The controller of this system determines how much heat is being added to the circulating water by the two heating devices, the sum and also the share. During milder days, it is understandable that a lower quantity of heat is required to maintain the home at a comfortable temperature, while during colder days, more heating input is required. The AWHP can only run at full tilt, however, ideally, the controller can control the circulating water flowrate in such a way as to *step down* the heat output of the AWHP/gas

boiler to create the ideal heat flux from the radiators into the air of the rooms to maintain an optimal indoor temperature.

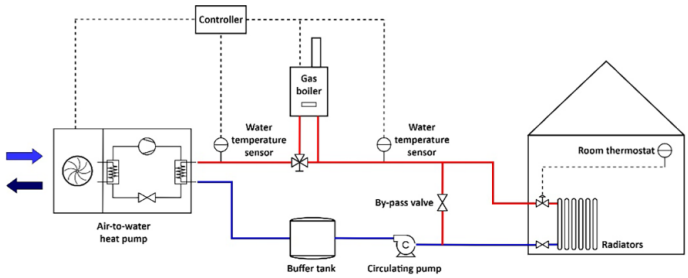

Figure 2.1: HHS with an AWHP and condensing gas boiler [14]

Heinen, Burke and O'Malley [9] concluded that HHSs that use a combination of electricity and gas as the energy source for the heating system can provide the greatest economic benefits when compared to other types of hybrid heating technologies in a combined power-residential heat system. The investment costs of these systems may vary depending on factors such as the size of the system, the specific technology used, and the cost of electricity and gas in the area. However, overall, a HHPS that utilises a combination of electricity and gas as the energy source is likely to have the most favourable cost-benefit ratio.

2.1.3 *Operating Modes of HHSs*

2.1.3.1 *Bivalent-Parallel Operation*

In monovalent systems the entire heat demand, regardless of ambient temperature is supplied with the HP, but there is hardly any reason to operate in this mode and requires an oversized HP.

In this study, the bivalent-parallel operation paradigm for a HHS is used, which is where a controller determines whether to solely run the HP or conventional gas boiler, or so run them in parallel. Buday [33] explains: at temperatures below a certain threshold (T_{cut}), only the boiler is used, see: domain 1 in Fig. 2.2. Between (T_{cut}) and a second threshold (T_{biv}), both the boiler and HP are used (domain 2). At temperatures above (T_{biv}), only the HP is used (domain 3). The second threshold (T_{biv}) is the temperature

at which the HP can meet the heat demand of the building, and (T_{cut}) is set to a value such that, when ambient temperatures are above this value, the HP is ecologically and economically efficient. The optimisation of the bivalent temperature, T_{biv}, is the crux of this thesis. The cut-off temperature can be calculated using the boiler and HP efficiency and the Primary energy factors (PEFs) of the heat sources.

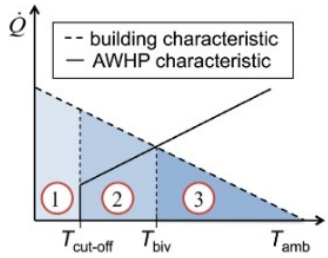

Figure 2.2: Bivalent-parallel operating scheme [13].

2.1.3.2 *Bivalent-Alternative Operation*

In bivalent-alternative operation, the controller has two options in contrast to the three outlined in Subsubsec. 2.1.3.1, either solely use the HP or solely use the gas boiler [33]. Below the set bivalent point, the heat demand is entirely provided by the auxiliary heating device, as seen in Fig. 2.3. Above the bivalent temperature, the heat demand is entirely provided by the HP. This operation places the T_{biv} and T_{cut} coincident [13, 33].

2.1.4 *Buffer Tank*

A buffer tank is a medium- to large-sized water vessel used in hydronic heating systems. It provides a large thermal inertia to the heating system-house system, which many small- to medium-sized houses, especially those with poor insulation, lack. Thermal inertia is a desired property of a building as rapid thermal fluctuations in ambient air are less of a concern when

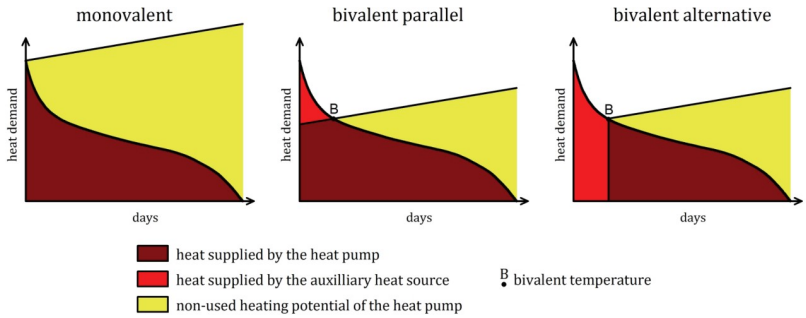

Figure 2.3: Types of bivalent HHS operation modes visualised through heating duration curves [33]. Note: T_{cut} is not clearly shown in this figure.

it comes to maintaining a comfortable thermal environment indoors. This effect is noticeable in large office/district buildings with high thermal inertias and plays a significant role in heating-capacity selection [5]. Furthermore, a buffer tank provides a "hydraulic switch" and allows for heat generation and heat distribution to be in separate loops. This opens up the option to have differing flowrates between the heat generation and heat distribution loops.

Buffer tanks have been found, when sized correctly and with an appropriate control strategy, to have a positive influence on the efficiency and performance on HHSs [13, 23]. The controller is able to make use of the HPs "most profitable working conditions" thanks to the presence of the buffer [34]. It has been found that when a buffer thank is present in the HP circuit, SPF increases as the size of the HP decreases [35]. Mugnini, Coccia, Polonara and Arteconi [35] confirmed this for all sizes of HPs simulated, the smallest buffer tank having a capacity of 200 L. Stiebel Eltron GmbH & Co. KG [30] suggest to size the buffer tank so large as to at least be able to defrost the coils.

ASHPs can experience negative effects when operated at partial load, such as on-off cycle deterioration. This is caused by losses in the start-up and standby stages, where there is a delay in

heating output and power consumption but no heat produced [36]. To prevent these losses and excessive on-off cycles, a buffer tank can be installed in series with the heat pump, providing the hydraulic switch mentioned earlier [36, 37]. In addition to protecting the heat pump from negative effects of partial load operation, the buffer tank also plays a role in maintaining indoor thermal comfort during reverse defrosting, as discussed in Subsec. 2.1.5.

The larger a buffer tank in volume, the larger its energy storage capacity. However, with a larger volume, and naturally larger cylinder and surface area, comes greater heat loss, which seem to correlate almost linearly [13]. This could be justified if other performance factors such as SPF or load factor were positively affected to offset this loss in heat, however this does not seem to be the case according to [23] and [13], which also found only a moderate reduction in on-off cycles with smaller tanks. This is partly to do with the thermal inertia of the building and return temperature controller. Klein, Huchtemann and Müller found that the volume of the buffer tank had very limited effect on the system performance. Dongellini, Naldi and Morini [14] sized their buffer tank just large enough such that the maximum number of on-off cycles was never greater than six per hour, resulting in a buffer tank with a volume of 79 L. This maximum on-off cycle figure was chosen based off their HP manufacturer guidelines.

2.1.5 *Frosting and Defrosting*

Frosting occurs in ASHPs in colder ambient temperatures resulting in issues for HPs. Frost build up depends on the ambient temperature, temperature of the surface in question and relative humidity. For HPs, a few ranges of temperatures at which frosting occurs has been found in the literature Sandström [38] finding a

range of −15 °C to 6 °C at a r.h. of ≈90%, while Kropas, Streckienė and Bielskus [39] found frost formation to begin when the ambient air temperature was below 3.5 °C with a r.h. of 88%. Frosting specifically occurs when the surface temperature of the fins on the air-side heat exchanger component (evaporator) are lower than the freezing point of the of the air. Water droplets start to form and collect on the fins. When the temperatures is below freezing or close to it, the water droplets freeze to the fins and build up a frosting. Frost, unlike snow, which both form from the freezing of water droplets, is not loose and must be scraped off or melted off. It will not *fall off of* a surface like snow might. This layer of frost acts as a layer of insulation and restricts the heat exchanger from transferring heat from the ambient air. Since these fins are typically closely packed, if the layering of frost continues and progressively builds up, the airflow around the fins decreases and so does convective heat transfer to the ambient air, further exacerbating the issue of insulation. All of this is to say that when frosting occurs in ASHPs, their performance declines severely, from a COP circa 3.25 to less than 2 with light- to medium-frosting [17]. Smaller HPs tend to be affected to a greater extent than larger capacity HPs [40]. Zhang, Jiang, Dong, Yao and Deng [41] found that the temperature of the air and surface of the fins, humidity, velocity of air are the main factors involved in frost formation.

Many treatments for frosting have been proposed and implemented into products. There is however no golden bullet solution, all of them advantages and disadvantages. Three main solutions are typically used when addressing the issue of frosting in ASHPs.

- Simple on-off defrosting: the HP is simply switched off when too much frost has formed on the outdoor component. The performance has been degraded to such a point that it is now economically advantageous to turn off the HP and wait for the frost to melt away. This however, takes

a long time and can negatively affect the thermal comfort of a home if no other heat production is used. The HP does not use any power during this off-cycle of course, retaining the COP of the HP—although, this may affect the overall system performance if a gas boiler needs to be used to provide the entire heating load of the home.

- Reverse cycle defrosting: this method is similar to the first method; the refrigerant is cycled in reverse and hot gas is forced into the heat exchanger. Recall that HPs and refrigerators differ only in objective. The HP now treats the outdoors as the "cold" sink and begins transferring heat from indoors to outdoors. Intuitively, one can see that this is quite detrimental to the SPF of the HP as the house is being actively cooled by the HP in order to heat up the outdoor coils and fins to melt away the frost, which in turn causes the auxiliary heater to work even harder to maintain a comfortable indoor temperature. The intention in this method is to melt the frost much quicker than the first method, allowing the ASHP to begin warming the home once again much earlier than the the simple on-off defrosting method.

- Resistive heating: electric resistive heaters are installed on/in the heat exchanger. This method works very well, quickly melting off frost and is a separate heating element to the HP and therefore does not interrupt the HPs cycles. Resistive heaters are very expensive to run and negatively affect the COP of the HP.

Amer and Wang [42] found that the reverse cycling method resulted in a higher average COP than the other two methods, over a series of multiple reverse cycle defrostings. Additionally, Bagarella, Lazzarin and Noro [22] found that a buffer tank can ensure thermal comfort during reverse cycle defrosting, due to being able to use the stored energy from the buffer tank to melt

the frost on the outdoor coils without actively cooling the indoor space due to the inherent decoupling of the heat production and distribution loops created by the buffer tank. Bagarella, Lazzarin and Noro [22] agreed with Dong, Deng, Jiang, Xia and Yao [43] that the *defrosting efficiency* of the reverse cycling method is around 60%. This is the ratio of energy supplied to the coils, to the actual energy transferred to the frost for melting.

2.2 HDD AND DESIGN TEMPERATURES

HDDs is a measure of the difference between the outside temperature and the inside temperature. HDDs are usually considered over a period of time, be it a month, heating season or entire year. A *base* temperature is chosen, typically around 12 °C to 21 °C which then determines when it is "cold" outside, or can be thought of as being the temperature above which heating is no longer considered to require heating. This base temperature can be chosen at will, and simply depends on what the person/institution deems to be *warm enough*. This measure can be used to quantitatively compare the heating demand of a given house in different locations/climates. The heating requirement of a specific building is directly proportional to the HDD [44].

To calculate the HDD for a certain day, three equations are used and are displayed from Eq. 2.1. Which equation to use is determined by the interaction between the base temperature and the maximum temperature recorded during that day.

$$\text{Degree days} = \begin{cases} t_{\text{base}} - \frac{1}{2}(t_{\text{max}} + t_{\text{min}}), & \text{if } t_{\text{max}} < t_{\text{base}} \\ \frac{1}{2}(t_{\text{base}} - t_{\text{min}}) - \frac{1}{4}(t_{\text{max}} - t_{\text{base}}), & \text{if } t_{\text{base}} > \frac{1}{2}(t_{\text{max}} + t_{\text{min}}) \\ \frac{1}{4}(t_{\text{base}} - t_{\text{min}}), & \text{if } t_{\text{base}} < \frac{1}{2}(t_{\text{max}} + t_{\text{min}}) \end{cases} \tag{2.1}$$

To calculate the Monthly degree days however, only the first of the three equations in Eq. 2.1 is made use of. This total is found by summing the daily temperatures differences and can be seen in Eq. 2.2.

$$\text{Monthly degree days} = \sum_{\text{month}} \left[t_{\text{base}} - \frac{1}{2}(t_{\max} + t_{\min}) \right] \quad (2.2)$$

Environmental Design: CIBSE Guide A. has chosen a base temperature of 15.5 °C. *2009 ASHRAE Handbook: Fundamentals* used a base temperature of 18.3 °C and determined an annual HDD of 3135 °C d for Dublin Airport, IE, N53°26′ W6°15′. Using the online tool `Degree Days.Net` [45] with a base temperature of 15.5 °C, a HDD figure of 2072.3 °C d was obtained for the same location.

Design temperatures are a measure how many hours/days a specified condition is exceeded. In the case of a heating design temperature, this would indicate how many days of the year or heating season are spent below a given temperature. *2009 ASHRAE Handbook: Fundamentals* [5] notes that this measure does not give an indication of the frequency or duration of these events, only a cumulative result is returned. According to *2009 ASHRAE Handbook: Fundamentals* [5], the 99.6% design temperature in Dublin Airport is −1.9 °C while the 99.0% design temperature is −0.7 °C. Traditionally, conventional gas boilers or resistive heaters were sized to design temperatures, meaning, for a chosen design temperature percentile (e.g., 99.0%), the heater could heat the building to thermally comfortable levels for 99% of the year, however during the 1% temperature lows, the heater would not be adequate. This calculates to the heater being undersized for ∼35 hours of the year.

$365 \times 24 = 8760\,\text{h} \Rightarrow 99.0\%\text{-}ile = 8760(100 - 99.0) = 87.6\,\text{h}$

In monovalent systems, the HP is sized in such a way as to be able to provided the entire heating load for a building at design con-

ditions. This results in the HP being positively over-dimensioned for the task [13]. An oversized heating system would be very inefficient due to frequent on-off cycling [32], which also results in rapid degradation of heating system components. Oversized heating systems also result in potentially uncomfortable indoor temperatures as rooms are unequally heated [21]. Finally, oversized systems have higher maintenance costs and significantly higher initial investment costs.

The concept of a *design-day* can be used to design heating configurations for homes, especially when performing numerical simulations on a model of the system [21]. A design-day file is a special weather file created with design conditions in mind. Based on the design temperature parameter, ASHRAE lays out a procedure to generate a 24-hour weather profile. These profiles represent the 0.4% to 99.6% extremes experienced for a particular location [5]. This weather data is used in simulations to determine the minimum size for a heater required for a house (for these particular percentiles of course).

for the purposes of the simulation(s) concerning this thesis, the 0.4 percentile, and any cooling-nessecary-temperatures for that matter, are not of concern as cooling is out of scope.

The "heating duration curve" can be devised for a specific climate and a specific HP where a curve is plotted on a chart with heating load [$\mathrm{kW\,h^{-1}}$] against number of hours the heating load is equal to or above a selected percentage of design load [46]. For example, as illustrated in Fig. 2.4, the blue line indicates 50% design load, and lands around 1300 hours on the x-axis. This means that for 1300 hours of the year/heating season, the heating load of the building is 50% of the design (or max) load. The balance point marked by the yellow circle is the point at which the HP is not longer able to provide the entire heating load required by the building. To the left of this point, the gas boiler will need to provide the remaining heat capacity to maintain a comfortable indoor temperature. If the AWHP size is increased, this balance point moves to the left, as the HP can provide the entire heating envelope of the building at lower temperatures.

Of course, for the sake of the diagram, the curves and lines in this figure are arbitrary (e.g., AWHP performance is not linear with outdoor temperature, and by proxy, heating load), but it illustrates how a HP may be sized to 60% of the design load of a building.

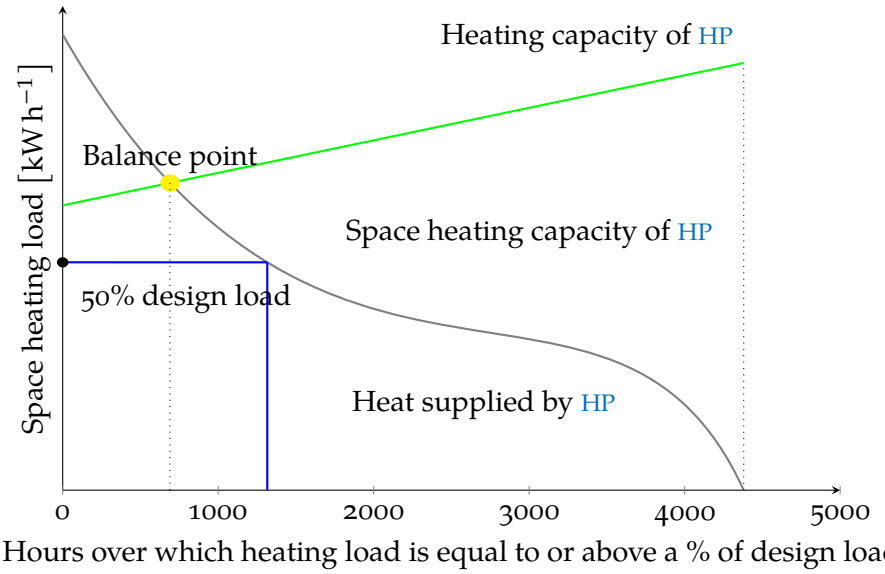

Figure 2.4: Example heating duration curve highlighting bivalent point. It shows the cumulative number of hours that a heating system needs to operate at various levels of heat demand

All of this is to say that there are many methods of determining and comparing the heating load of a building for a given climate, with which heating devices may be sized to in order to be able to (almost always) have the capacity to heat a building. A HHS is unique in that it is composed of two heating devices. The boiler, as stated before, is sized to a certain high-percentage design condition. This may be defined by the user/homeowner, convention, or by some set of standards set by a governing body (e.g., ASHRAE), and is typically a value in the region of 95% to

99.7%. On account of this, the AWHP can be sized smaller than compared to if it were the sole heating device.

2.3 PRIMARY ENERGY

PE is a term used in the fields of energy statistics and energetics. Sources of PE are those which have not been interfered with by humans, in other words, are the natural form of energy and are unprocessed. PE sources include: oil, natural gas, sunlight, wind, etc. PE stands in contrast to secondary energy, which can be thought of as the carrier of energy, which most commonly happens to be electricity, but can also be liquid forms of energy (e.g., diesel/petrol,), hydrogen fuel cells or (waste) heat. Following from PE, is PEF which connects PE to final energy, it is a measure of how much energy in total is required to produce a unit of *usable* energy [8]. The PEF is used to evaluate the environmental impact of a system by considering the primary energy consumption, which includes the energy required to produce and distribute the energy source, such as the energy used to extract and transport fossil fuels. For example, a hydroelectric power plant with a PEF of 1, means that the energy used to generate electricity is equal to the energy consumed. On the other hand, a coal-fired power plant with a PEF of 2.5, means that 2.5 units of PE are consumed to generate 1 unit of electricity. Therefore, hydroelectric power plants are considered more environmentally friendly than coal-fired power plants. [47] found that with a suitably high diffusion of RES in an electrical grid, significant PES can be obtained through the use of HPs for space heating and can overall promote energy savings in buildings, in turn reducing CO_2 emissions [8].

Fig. 2.5 is a Sankey diagram which breaks down the flow of energy in Ireland in 2020 from PE on the left by fuel type, and final energy on the left, by sector. It also highlights the energy

losses associated with energy production and transmission. It requires energy to convert natural gas or oil to electricity, while energy losses corresponding to renewable energy production are dismissed, as the energy source is of course *free*.

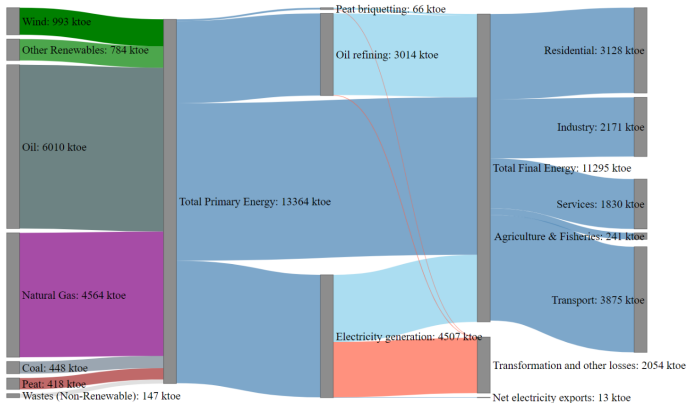

Figure 2.5: Sankey diagram showing PE by fuel type on left and final energy by sector on right [48].

PES is difference between the amount of energy consumed by the original device (whatever it may be) and the amount of energy consumed by the new device. In relation to this thesis, it will be taken to be the savings of the new heat generation system compared to the old system (conventional gas boiler as sole heat production). Knowledge of the PEF, PES and the make-up of the fuel types and shares in the PE, i.e., the RES, can indicate how much CO_2 is consumed at any instance with a heating system [47], and is the foundation of the techno-ecological model of this thesis.

The RES of an electrical grid refers to the proportion of electricity generated from renewable energy sources, such as solar, wind, hydro, geothermal, and biomass, compared to the total electricity generation. It is a measure of how much of the electricity being consumed by a country or region is coming from renewable sources. For example, if an electrical grid generates 50 GW of

electricity and 20 GW of it is generated from renewable sources, the RES of that grid is said to be 40%.

The RES is an important metric to measure the progress towards decarbonization and the reduction of greenhouse gas emissions in the energy sector. Governments and international organisations have set targets for the increasing share of renewable energy in the electricity mix as a means of reducing the dependence on fossil fuels and reducing the emissions of greenhouse gases [49]. Knowing the RES of an electrical grid can also help understand the potential for further integration of renewable energy sources and the necessary investments in infrastructure and technology to achieve the goals set by the government or international organizations. In addition, the RES of an electrical grid can also impact the stability of the grid and the integration costs, it is important for grid operators and policy makers to consider this metric when planning for future energy systems [49].

2.4 ELECTRIFICATION OF HEATING

The EU has now for a number of years been pushing for the electrification of heating throughout the union. This has been identified as a clear means to achieve decarbonisation goals, as concerns over global warming become greater. As noted in Sec. 1.1, the residential sector contributes 27% of the final energy consumption, while residential domestic water production and space heating contributes to 80% of that. In Ireland, residential heating accounted for 53% of CO_2 emissions from heating. However, across all sectors, heating and cooling are responsible for half of all final energy consumption in the EU [50]. Therefore, it is clearly evident that decarbonisation of the heating/cooling sector is vital to a) reaching EU targets of lowering CO_2 emissions and b) improving air quality and the reduction of harmful

emissions [51]. Although, switching to electrically driven heating systems does not automatically or inherently reduce the carbon emissions, merely, it changes the source of the energy; the electricity must also be decarbonised for this to be the case.

SEAI [48] carried out a comprehensive study on the Irish electrical grid performance as it relates to renewable energy sources and to heating/cooling. According to the report: the share renewable energy to that of the the total energy used in 2020 was 13.5% (having missed the EU target of 16%); the share of renewable energy used specifically in heating/cooling was just 6.3%, its target having been 12%; energy from renewable sources grew by 8.9% over the previous year, and the total installed wind energy capacity grew by 4.1%, from 4130 MW to 4310 MW (in the Republic). Overall, the residential energy CO_2 emission has trending downwards over the past decade and a half, falling by 25% since 2005, and the CO_2 intensity of electricity generation is half of its value in 2005, standing at 300 g kWh^{-1}. These are good signs for the electrification of heating, because in order for the electrification of heating to result in a decarbonising of heating, the electricity production must at least have a lower emission intensity compared to if no electrification process were to take place, but ideally have the prospects of becoming a very low/zero CO_2 intensity matter.

Emission intensity is a measure of how much CO_2 is released per unit of energy produced

2.5 CONTROLLERS AND CONTROL THEORY

Control theory is concerned with the control of dynamic systems with with a desired goal in mind, which is called the reference. A controller manipulates the inputs to a system, usually denoted u, in such a way as to alter the output variables or states, y, of the system to follow a given reference. Disturbances, d, to a system are expected, yet unforeseen inputs to a system which

may significantly alter the outputs state. There are two main types of controller, feed-forward, and feedback controllers [52].

A feed-forward controller, also known as an open loop controller, controls the system without knowing the current state of the system [53]. This is possible if disturbances are either eliminated, or wholly understood and accounted for. Complete knowledge of the dynamics of the system being controlled would be required and captured by a mathematical model, either by physics and first principles, or by system identification (a model is fitted to data) [53]. The dynamics of the system are inverted by the controller and fed to the system as inputs. Any error in the inversion process results in undesired system states.

However, they would they no longer qualify as disturbances, and would simply be considered as inputs, but that is by the by.

Feedback controllers, also known as closed loop controllers are a *much* more common form of controller. The current system state is known to the controller, and the reference and current state information is used to determine the appropriate control inputs. In doing so, a feedback controller inherently changes the dynamics of a system. Feedback controllers usually make systems more stable, however, there is the possibility of making systems less stable and even unstable through controllers [52]. There are many types of feedback controllers, the most common and well understood kind being a linear feedback controller called a PID controller, or just a PID. Linear controllers assume the general behaviours of the system to be linear. Although, even if the dynamics of system are not, in fact, linear, a PID will still likely be able to control the system appropriately and reach the reference state [54].

In a HHS, controllers are used to manage the operation of the different heating technologies and ensure that they are used in the most efficient and effective way possible [17, 22, 23, 35, 47, 55]. The controllers in a HHS are typically responsible for a number of tasks, including monitoring the temperature inside and outside the building, determining the best heating techno-

logy to use based on the current conditions, and controlling the operation of the heating technologies to maintain a comfortable and consistent temperature.

For example, when the outside temperature is cold, the controller may determine that it is most efficient to use the gas furnace to heat the building. When the outside temperature is mild, the controller may determine that it is more efficient to use the HP, which uses less energy than the gas furnace. Very advanced controllers may also use predictive algorithms and weather forecasts to anticipate changes in temperature and adjust the heating system accordingly by storing a lot of heat in the buffer tank during a warm period right before a cold period [55].

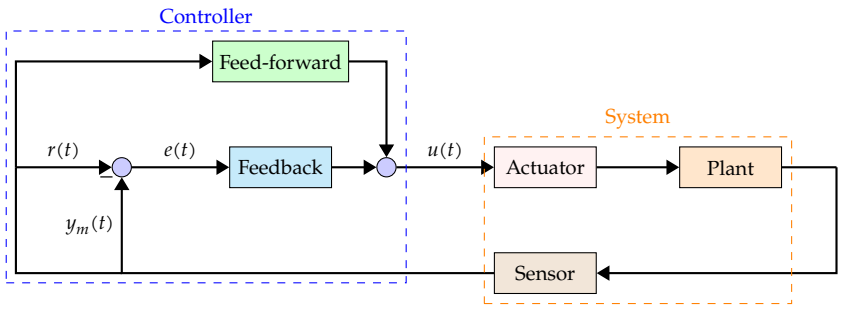

(a) Basic feed-forward/feedback hybrid controller [56]

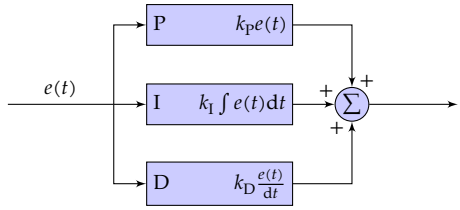

(b) The workings of a PID controller [57]

Figure 2.6: Representative block diagrams of a hybrid controller system and a PID controller

2.5.1 *PID Controllers*

PID controllers are a type of feedback control system that are commonly used in a wide variety of systems to maintain a desired output or setpoint. The acronym refers to the three components of the control algorithm used by the controller. PID controllers work by continuously calculating an error value that represents the difference between the desired setpoint and the current output of the system. Panda and Sujath [54] explains that this error value is then used to calculate and apply a correction to the system, based on the three components of the PID algorithm:

- The proportional component applies a correction proportional to the error value. This allows the controller to quickly respond to large errors and make large corrections.
- The integral component applies a correction based on the accumulated error over time. This helps to eliminate steady-state errors and ensure that the system eventually reaches the desired setpoint.
- The derivative component applies a correction based on the rate of change of the error. This helps to dampen the system's response and prevent overshoot and oscillation.

PID controllers are used in a wide variety of systems, including mechanical systems like motors and actuators, temperature control systems, and chemical process control systems. They are often preferred over other control algorithms because they are relatively simple to implement and can provide stable and accurate control of the output of the system.

2.5.2 *Noise and Error*

Noise and error are common sources of problems in control systems. Noise refers to random variations in the output of the

system that are not caused by the control signal, while error refers to the difference between the desired setpoint and the actual output of the system [54]. Noise and error can have a number of adverse effects on the performance of a control system, including reduced accuracy and stability, as well as increased oscillation and overshoot. To deal with noise and error in control systems, a number of different approaches can be used. One approach is to use a filter to remove noise from the output of the system signal. This can be done using a low-pass filter, which removes high-frequency noise, or a high-pass filter, which removes low-frequency noise [52]. Another approach is to use a model-based control algorithm, which uses a mathematical model of the system to predict the output of the system and apply appropriate control signals. This can help to reduce the effects of noise and error by using the model to compensate for them . Furthermore, another approach is to use a robust control algorithm, which is designed to be resistant to the effects of noise and error. Robust control algorithms typically use a combination of feedback and feed-forward control, as well as advanced control techniques like gain scheduling and optimization, to achieve robust performance in the presence of noise and error.

2.6 VERIFICATION & VALIDATION OF MODEL

Verification and validation are two important processes that are used to assess the credibility and reliability of a simulation model. While these terms are often used interchangeably in common parlance, they have distinct meanings and serve different purposes.

Verification is the process of ensuring that a simulation model is implemented correctly and accurately represents the underlying mathematical equations, assumptions, and physical phenomena. Verification ensures that the simulation code is free from coding

errors and that the numerical algorithms are implemented correctly, and confirms whether the model behaves as the modeller expects. This process involves checking the model against analytical solutions or known results and comparing the simulation output with the expected results [58].

Validation, on the other hand, is the process of determining whether a simulation model accurately represents the real-world system it is intended to simulate. Validation involves comparing the model output to real-world observations and data to assess the accuracy of the model in predicting system behaviour. This process also involves assessing the sensitivity of the model to input parameters and assumptions. The underlying values of the model (e.g., insulation thickness, floor tile conductivity, etc.) are altered and calibrated to fit the real-world data [59].

Building Energy Models (BEMs) must undergo verification and validation due to various sources of uncertainty arising naturally as a result of converting a real-life problem to a mathematical model to a numerical model. Four sources of uncertainty particular to BEMs are identified by [60, 61] as:

- Specification uncertainty arises from incomplete or inaccurate specifications of the building or systems being modelled.
- Modelling uncertainty results from simplifications and assumptions of complex physical processes.
- Numerical uncertainty is introduced during the discretisation and simulation of the model.
- Scenario uncertainty comes from external conditions imposed on the building, such as outdoor climate conditions and occupant behaviour.

2.6.1 *Validation*

The validation process of a BEM is a crucial step in ensuring that the model accurately predicts the energy performance of the building. Calibrating a building involves adjusting the energy model to better reflect reality [60, 62]. This is done by comparing measured data to simulated data, and performing an uncertainty analysis to determine how well they match. Although real and measured data can be similar, there may still be errors in the simulation [63]. Various factors, such as weather [64] or occupancy, can introduce uncertainty, along with envelope uncertainties. The 'ASHRAE Guideline 14-2014' [63] provides a comprehensive framework for validating BEMs. This guideline outlines a step-by-step process for validating the simulation model and includes criteria for evaluating the accuracy of the model. The validation process involves comparing the model results with actual building energy consumption data and performing statistical analysis to determine the level of accuracy. In the validation process used in this thesis, three statistical tools or indices are employed to evaluate the accuracy of the simulation model in this thesis. The first two are suggested by ASHRAE while the last is used as its properties are distinct from the first two and provides a useful measure of absolute error.

Coefficient of Variation of Root Mean Square Error (CV(RMSE)) is a statistical tool used to determine the degree of error between the simulated and actual data and is a commonly used tool in the validation process of BEMs because it takes into account the variability in the actual data [63]. It calculates the Root mean square error (RMSE) as a percentage of the mean of the actual data, which makes it a useful metric for evaluating the accuracy of the model across a range of operating conditions. A lower CV(RMSE) value indicates that the model is a better predictor of the actual building energy performance. The CV(RMSE) tool is particularly

useful when comparing the performance of different models or when assessing the impact of different input parameters on the accuracy of the model. Coakley, Raftery and Keane [60] said: "[CV(RMSE)] allows one to determine how well a model fits the data by capturing offsetting errors between measured and simulated data. It does not suffer from the cancellation effect.". The formula for CV(RMSE) is given by Eq. 2.3.

$$\text{CV(RMSE)} = \frac{100}{\bar{Y}} \sqrt{\frac{\sum_{i=1}^{N} (Y_i - \hat{Y}_i)^2}{N - p}} = \frac{\text{RMSE}}{\bar{Y}} \tag{2.3}$$

Normalized mean bias error (NMBE) is another statistical tool used in the validation process, measuring the bias of the model. It provides a measure of the difference between the mean of the simulated and actual data as a percentage of the actual data [63]. A zero NMBE value indicates that the model is unbiased, while a positive or negative NMBE value indicates overestimation or underestimation, respectively. The NMBE tool is useful in identifying systematic errors in the model, which can occur due to incorrect model assumptions, data input errors, or other issues. It helps to identify the direction and magnitude of the bias, which is important for developing strategies to improve the accuracy of the model. The formula for NMBE is given by Eq. 2.4.

$$\text{NMBE} = \frac{100}{\bar{Y}} \frac{\sum_{i=1}^{N} (Y_i - \hat{Y}_i)}{N - p} \tag{2.4}$$

Symmetrical mean absolute percentage error (SMAPE), first proposed by Makridakis [65] and approved by many [66–68], is a statistical tool that measures the absolute percentage difference between the simulated and actual data. Unlike the previous two tools, SMAPE is symmetric and thus gives equal weight to overestimation and underestimation. A lower SMAPE value in-

dicates higher model accuracy. It is an extension of the MAPE method which has the flaw of being asymmetric in its treatment of over- and underprediction of the actual value, overpredictions being penalised harder than underpredictions. There are three common definitions of SMAPE, each with different properties, however, this thesis chooses to use the definition which outputs values as a percentage error between 0% and 100% as this is most easily interpretable and comparable. The formula for SMAPE is given by Eq. 2.5.

$$\text{SMAPE} = \frac{100}{N} \sum_{i=1}^{N} \frac{|Y_i - \hat{Y}_i|}{|\hat{Y}_i| + |Y_i|} \tag{2.5}$$

'ASHRAE Guideline 14-2014' [63] suggest different tolerances for data calibrated by monthly or by hourly data for the CV(RMSE) and NMBE statistical methods. ASHRAE suggests tolerances of <15% for CV(RMSE) and ±5% for NMBE for comparisons done by a monthly basis. A simulation is said have high levels of model prediction performance if absolute percentage error values outputted by SMAPE are less than 20% and great levels if less than 10%.

2.7 CONCLUSION

In this literature review, the fundamental concepts behind the operating principles of HPs was described, the dynamics of HHSs were described, the effects of the different operating modes and physical phenomena were detailed, and Heating-system design was studied. The reasoning behind (future and current) policies pushing for HP adoption were explained along with the basics of control theory were. Finally, the verification and validation of numerical simulation models was discussed along with the statistical models to be used later on in the thesis. The literature surrounding HHSs and HPs is vast, however, perhaps the most

succinct—and perhaps discouraging—statement/expression in the literature is: "numerical findings are generally idiosyncratic to geographical contexts, time horizons as well as assumptions on costs, policies, and technology availability" [69]... Rauschkolb, Modi and Culligan [21] explain how small variations in the price of natural gas can shift fossil fuel-only systems from being the best economic choice to the worst.

After the literature review, it was found that there is a significant gap in research regarding the bivalent operation temperature window and its impact on HHPS. Very few papers have explored this topic, making it a crucial area of investigation. Additionally, the few studies available have primarily focused on continental climates and not on the temperate oceanic climate.

3

METHODOLOGY

3.1 OVERVIEW

This chapter presents the research methodologies employed in this thesis. Sec. 3.1 gives a general overview of the study, including a flow chart of the main steps. Secs. 3.2 and 3.3 give an overview of the reference building being modelled and the implemented heating system respectively. Sec. 3.5 gives an introduction to the ecological and economic models used to quantify the different hybrid operation temperature windows along with a brief overview of the market context. Finally Sec. 3.6 provides a conclusion to the methodologies chapter.

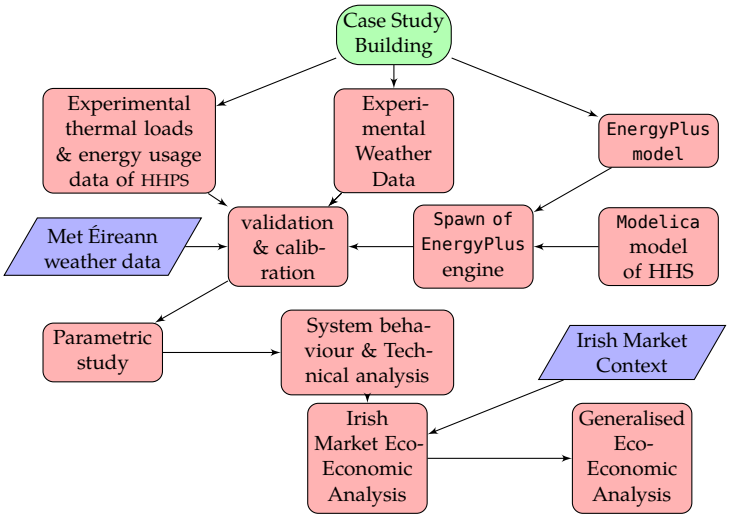

Figure 3.1: Flowchart methodology

3.2 EXPERIMENTAL REFERENCE BUILDING

This thesis uses as reference a building model produced for and used by a Master's thesis by Keogh [31]. The building itself will be described in detail in Sec. 4.2. Briefly, it is a detached house located in a residential area of Belturbet, Co. Cavan. The building envelope was modelled and the data is stored in a `.idf`-file which is interpretable and parsable by `EnergyPlus` and subsequently through the use of the `Spawn of EnergyPlus` utility provided by the Buildings Library [70], can be co-simulated in `Modelica` and `EnergyPlus` [71]. The aforementioned data contained in the file consists of the geometry of the house; its walls, floors, ceilings, roofs, etc, the thermal envelope properties; material and insulation thicknesses, thermal properties (e.g., conductivity, heat capacity), various simulation specific parameters and keys, and finally the internal gains models including activity schedules and heat densities.

A brief history of the dwelling: in September 2014 a Daikin Altherma integrated hybrid HP system was installed in the house. The dwelling underwent a minimal retrofitting between December 2014 and February 2015. The insulation and air tightness of the building were improved and low temperature optimised aluminium radiators were fitted which allow for lower temperature supply water to effectively heat a room, ultimately allowing for higher COPs from the HP. The infiltration rate was decreased to 0.5 Air Changes Per Hour (ACPH), however, for the sake of the `EnergyPlus` model, this was increased to 0.8 ACPH to account for no interzonal air movement or door and window openings. The improved thermal properties of the building resulted in a reduction of 475 watts per month in the heating load of the house. The average energy consumption decreased by 44.5% [31]. All comparisons between the model and the reference house will

be carried out post-minimal retrofit as it is generally not recommended to run a HP in poorly insulated/inefficient homes.

3.2.1 *Experimental Measurements*

Experimental measurements were carried out on the real-life dwelling pre-, during, and post-retrofit. Many data variables were logged, the main ones which this analysis is concerned with being: heating circuit water supply temperature and return temperature in celsius, volumetric flowrate of the heating circuit in cubic metres per hour, electricity power for HP in watts, outdoor temperature in celsius and gas volume in cubic metres. The data was collected on at ten-minute intervals, but reduced to hourly resolution for the purposes of the data analytics. These measurements are used in the verification process in Subsec. 3.3.2.

3.3 BUILDING AND HEATING SYSTEM MODELS

3.3.1 *Verification*

For the purposes of model verification, a series of small simulation runs were carried out to test whether the model was behaving as expected. It was noted during the early runs of the simulation, the air in `zone3_floor1` was dramatically increasing in temperature during a certain day in early January. It was discovered that this was due to relatively high levels of direct and horizontal solar irradiation entering the room through the large, southerly facing window. The first verification test consists of loosely quantifying the solar irradiation energy gain into the room with the existing window from the model, and comparing this to a simulation run where the window was purposely shrunk to circa one tenth of its original area.

The ubiquitous heat capacity equation was utilised in quantifying the irradiation gain:

$$Q = mc\Delta T \tag{3.1}$$

Where Q is the heat energy in watts, m is the mass of air in the room, c is the specific heat capacity of air ($c_{v_{\text{air}}} = 0.718\,\text{kJ}\,\text{kg}^{-1}\,\text{K}^{-1}$) and ΔT is the change in temperature of the air in the room (i.e., difference between temperature at a chosen time in hours leading up to the event, and the peak temperature after the bulk of the irradiation of the simulation day). The mass of air in this room was found by taking the volume ($31\,\text{m}^3$) and multiplying it by the density of air at a mean temperature ($\sim 1.204\,\text{kg}\,\text{m}^{-3}$). The heat gained by the room with the large window was found to be 527.8 kJ while with the small window it was found to be 58.1 kJ. This is to be expected as a larger window would justly allow more irradiance to (semi-)directly into the room.

The next test was to check if heat was being conducted through the interior walls of the building. A room was chosen, and its temperature was purposely raised to an unnatural level of 60 °C. One would expect that the temperature of the adjacent rooms would increase by means of conduction. The test involved comparing the adjacent room temperatures to the corresponding room temperatures in the case where the chosen temperature of the room was not artificially raised. The temperature was found to increase an average of 16 °C across the 4 neighbouring rooms.

Door and window openings were not modelled as part of this simulation. The air infiltration rate was increased slightly to compensate for this. However, this also means interzonal airflow was also not modelled.

3.3.2 *Validation*

3.3.2.1 *Climate*

Climatic weather data was obtained from the OneBuilding weather database [72] in the `.epw` filetype and produced by ASHRAE.

The weather data file used in this study is a product of an amalgamation of representative monthly weather data from a year occurring between 2020 and 2008 for each of the twelve months. This weather data was collected by the Clones weather station Operated by Met Éireann, located 16.5 kilometres away from Belturbet.

The weather data contains various weather properties, such as dry bulb temperature, wet bulb temperature, dew point temperature, relative humidity, wind speed, wind direction, global horizontal irradiance, direct normal irradiance, diffuse horizontal irradiance, and atmospheric pressure, all of which are used in `EnergyPlus` in the envelope simulation. The data is presented in an hourly interval. `EnergyPlus` and `Modelica` (via `Weather-Data.Bus` `Modelica` model provided by the Buildings Library) linearly interpolate the hourly data to give data at the appropriate/chosen timestep of the simulation.

To evaluate the accuracy of the weather data file, the temperature values obtained from the weather file were compared to the temperature measured during the in-situ retro-fitting as well as historical temperature data for the year of 2015 provided by Met Éireann from the Ballyhaise weather station. Ballyhaise is also in Co. Cavan and is approximately 10 kilometres from Belturbet. The three sets of data were resampled to hourly intervals for comparison. The NMBE and SMAPE model uncertainty indices discussed in Subsec. 2.6.1 will be used to determine the uncertainty of the climatic model, the CV(RMSE) will however not be used as it is not applicable or suitable for the purpose of describing the variability of climatic data.

According to 'ASHRAE Guideline 14-2014' [63], when comparing hourly data, the appropriate NMBE tolerance is $\pm 10\%$. When the NMBE comparing the Met Éireann data and the measured data in-situ in Belturbet is computed, a value of -9.369% is obtained, which falls within the acceptable range. When the NMBE

comparing the measured Belturbet data and the climatic data from the `.epw`-file is computed a value of 9.764% is obtained, which also falls within the acceptable range, simply on the other side of the range. When the SMAPE values are computed for the same comparisons, values of 10.938% and 19.518%. Both of these values are considered to indicate that the data has sufficient agreement and predicts the behaviour well. Fig. 3.2 shows a plot of the three dry-bulb temperature data series overlaid one another, against the hour for each day of the year from 0 to 8760.

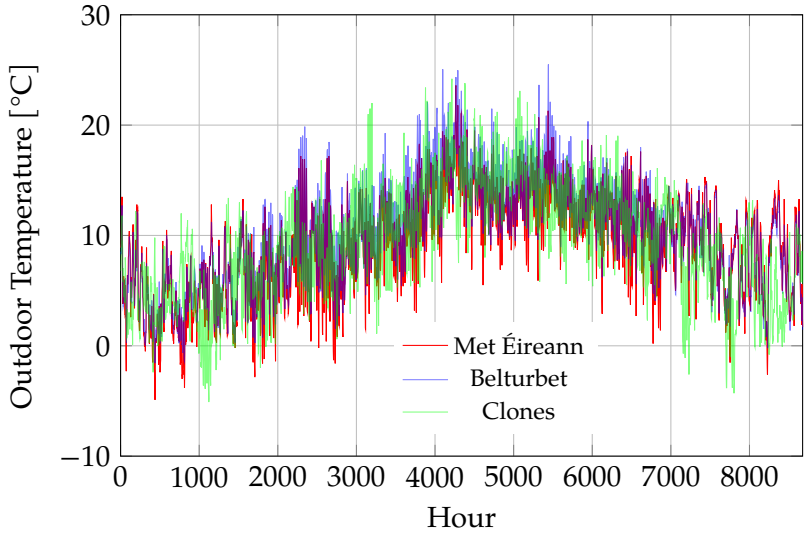

Figure 3.2: Year long comparison of the three dry-bulb temperature series. Met Éireann Clones weather station vs. experimental data from Belturbet vs. `.epw`-file based off of Clones data

Table 3.1: Summary of statistical indices results for climatic data validation

Statistical Index	Met Éireann vs. Belturbet	Belturbet vs. `.epw`-file	Tolerances
NMBE	−9.369	9.764	±10%
SMAPE	10.938	19.518	10%–20%

The comparison of temperature values using these statistical metrics revealed that the weather data obtained from ASHRAE was in good agreement with the in-situ temperature measurements in Belturbet and the historical metrological data from Met Éireann in Clones, with SMAPE and NMBE values which lay within the appropriate tolerances respectively. This indicates that the weather data file was a reliable source of climatic data for the study, and the statistical metrics used provided a robust method for evaluating the accuracy of the data.

3.3.2.2 *HHS Model*

The validation of the BEM was performed by comparing values obtained from the simulation with the experimental data collected from the building described in Subsec. 3.2.1. Two validation steps were carried out for the building. First, the idealised space heating load was compared. From the heating circuit water flowrate and temperature differentials it is possible to determine the nigh-ideal heating load of the building. The simulated heating loads were obtained by running a year long simulation of the BEM and using an idealised heat source to maintain the temperature of the rooms at 21 °C at all times. Secondly, an energy consumption comparison was carried out, comparing the electricity and gas consumption of the simulation and the experimental values separately, and then the combined fuel usages. It should be noted that the reference house had no night setback temperature—rather the indoor temperature was maintained at (20.0 ± 0.5) °C. This was only reflected in the `Modelica` model for the validation phase. The in-situ Daikin Altherma 3 HHPS had a cut-off temperature of 2 °C.

The validation criteria used to assess the accuracy of the model were based on 'ASHRAE Guideline 14-2014' [63], using the three statistical indices explained in Subsec. 3.3.2, these indicators measure the deviation between simulated and measured values,

as well as the direction and magnitude of the bias. A monthly calibration approach was adopted, meaning the CV(RMSE), NMBE and SMAPE values were calculated for each month using Eqs. 2.3 to 2.5 respectively.

For the space heating load a CV(RMSE) of 9.483% was achieved, which is under the ASHRAE suggested 15.0% for monthly data comparisons. The NMBE was calculated to be 0.02242%, well under the suggested 5% threshold, meaning the model did not systematically over- or underpredict the space heating load. The SMAPE value came to 6.061%, which is under the generally accepted 10% threshold for very good predictions. Fig. 3.3 shows a clustered bar chart comparing the simulation and experimental space heating values for all heating months.

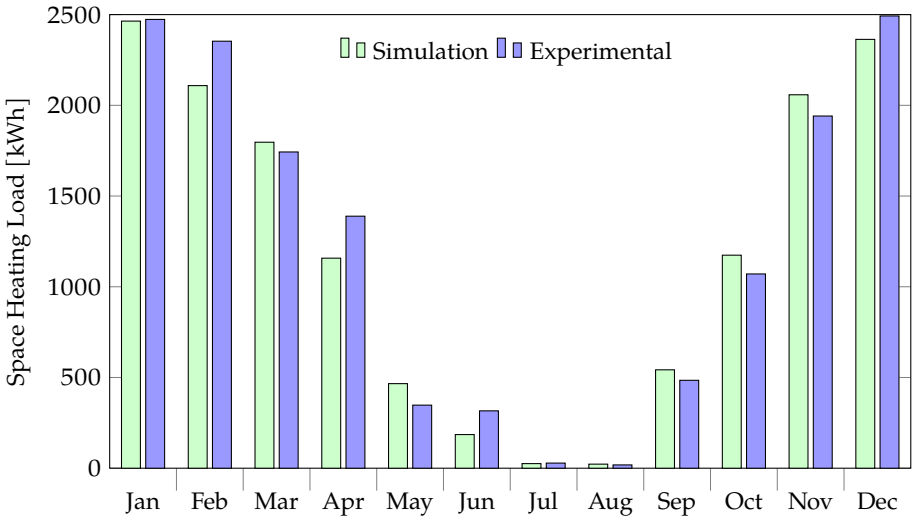

Figure 3.3: Space heating load for dwelling broken down by month: experimental vs. simulation

The electricity and gas energy usage for the simulation and experimental values were also compared. The CV(RMSE) evaluated to: 13.933 for the gas and 11.499 for the electricity and the NMBE came to 0.490 and 3.841 for gas and electricity respectively, which are below the thresholds set by the ASHRAE guidelines

for monthly calibrations. The SMAPE was 10.817 for gas and 6.305 for electricity which is also below the commonly agreed upon threshold. Fig. 3.4 shows a stacked, group bar chart of the electricity and gas usage for the experimental and simulation. It can be seen that the two sets of data are in good agreement. Tbl. 3.2 shows a summary of the statistical indices results for the three heating system validation comparisons.

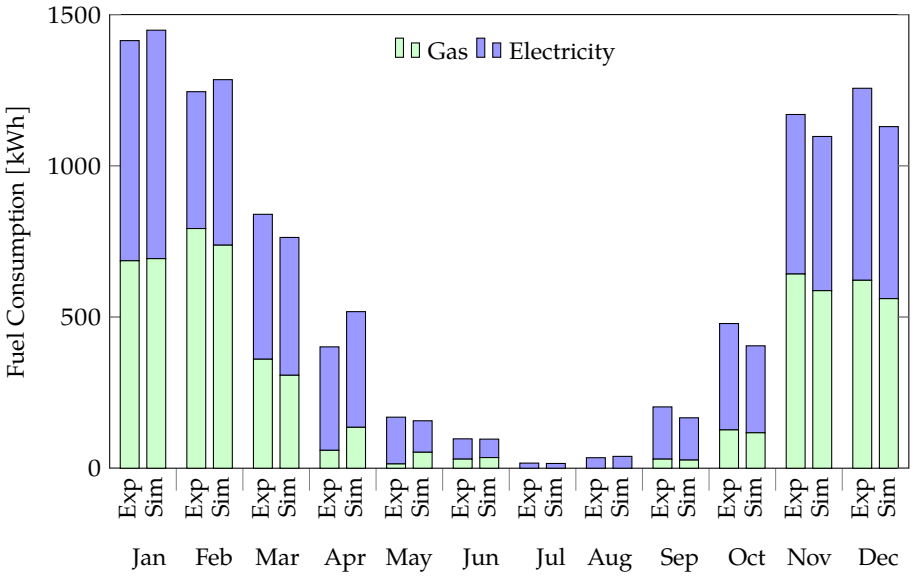

Figure 3.4: Energy usage for space heating broken down by energy type and by month, comparing experimental values to model values

Table 3.2: Summary of statistical indices results for model calibration and the corresponding tolerances

Statistical Index	Space Heating	Electricity	Gas	Tolerance
CV(RMSE)	9.483	11.499	13.933	15%
NMBE	0.022 42	3.841	0.490	$\pm$5%
SMAPE	6.061	6.305	10.817	10%–20%

The Daikin Altherma HP catalogue specifies that when producing hot water for space heating at 35 °C, an SCOP of 3.26 will be achieved for the model of HP being simulated [73]. When the HHS `Modelica` model was altered to strictly produce 35 °C hot water, the HP model provided by the IDEAS library reached an SCOP of 3.17, which comes to a percentage change of just 2.76%. This is accurate enough for the purposes of this analysis and confirms that the model should accurately represent the in-sutu HP. For the subsequent sensitivity analysis in Chap. 5, the temperature which the HP is producing water at is not fixed, and instead is allowed to be controlled by a space heating water supply temperature curve as described in Subsubsec. 4.5.5.1. This affects the COP positively and negatively depending on whether the demanded water supply temperature is greater or lower than 35 °C, however, overall, the SCOP is negatively affected. However, having the HP sometimes produce water at a higher temperature results in the boiler having to carry out less heating on that hotter water to "top it up" to the demanded water supply temperature, resulting in less gas usage.

3.4 SENSITIVITY ANALYSIS

A full factorial parametric study was carried out on the bivalent parallel operation temperature window of modelled HHS. This analysis aims to evaluate the effect of varying the bivalent temperature and cut-off temperature on the total cost of fuel and electricity for the heating system, in addition to assessing its PEF and CO_2 emissions. First, some fundamental preliminary steps must be completed before carrying out the sensitivity analysis. Choosing/identifying the parameters to be varied: it was discovered from the literature review that an optimising of the hybrid operation temperature window has not been carried out for the Irish climate, and not in any comprehensive way for other climates either. ASHP manufacturers may have carried out

proprietary research regarding this, however, such data is not available openly. Defining the range of values for each parameter: it is understood from Daikin's user manuals that they use a cut-off temperature of 2 °C and a bivalent temperature of 7 °C, which gives a good starting point. Knowledge gained from the literature review and Daikin's specifications manual for the HP being modelled, it is understood that the performance of a HP dramatically decreases with temperature due to diminishing COP and frosting effects, therefore a lower bound of −2 °C was chosen. For the bivalent temperature, an upper bound of 10 °C was chosen, as if it were much higher, the desired effects of running the HHS solely with the HP would be quite limited, almost defeating the purpose of the HP entirely. The upper bound for the cut-off temperature was set to 4 °C and finally the lower bound of the bivalent temperature was subsequently set to 5 °C to avoid creating a bivalent alternative operation hybrid system with the bivalent temperature and cut-off temperature being equal.

Next the resolution of the parameters was to be decided. This is typically determined based on the available computational resources and the desired level of detail in the analysis. Intervals of 1 °C were chosen, resulting in a resolution of 6 for the bivalent temperature and 7 for the cut-off temperature. With this, a matrix that specifies all possible combinations of values for each parameter can be drawn. Then the simulations must be ran one-by-one, varying the parameters in sequence and systematically. A graphical representation of the bivalent operation window can be seen in Fig. 3.5. It takes as an example a cut-off temperature of 7 °C and a bivalent temperature of 0 °C, meaning, when the outdoor temperature is between 0 °C and 7 °C, bivalent-parallel operation is occurring.

A brief technical analysis of the system's performance and its operation will be carried out to conclude the sensitivity analysis

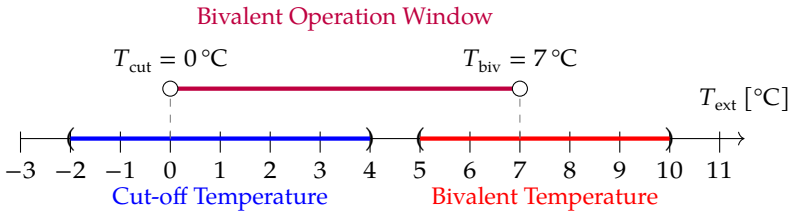

Figure 3.5: Representation of the bivalent operation window. An example is showcased of bivalent operation if the external temperature is between 0 °C and 7 °C.

chapter. The SCOP will be calculated for each parameter-level combination, and the on-off cycling of the HP will be investigated.

3.5 ECO-ECONOMIC ASSESSMENT

The eco-economic assessment chapter deals with showcasing the results gathered from the 42 total simulation runs and performing the analysis. This paper is seeking to answer two questions: what is the optimal temperature window to minimise cost, and what is the optimal temperature window to minimise environmental impact. The economic analysis involves determining the hourly consumption of gas and electricity by the two heating devices and determining the overall cost of running the heating system for the year. The price of gas does not fluctuate, only changing at most a couple of times in a year, however, the price of electricity fluctuates on an hourly basis due to Time-of-Use tariffs. The cost of heating for a a given timestep for this analysis was simply the sum from time $ts = 0$ to $ts = N$ of the sum of the products of cost of energy type at time ts by consumption over the time interval, given by Eq. 3.2, where B is the fuel consumption in kilowatts and C is the cost of the fuel type in cent per kilowatt-hour for a given fuel (at a given time ts, if electricity). N is number of timesteps in the simulation, typically around 180 000 due to timesteps of three-minute intervals being chosen.

The first term is multiplied by the difference between the time corresponding to timestep *ts* and the previous timestep. This is done to integrate over time.

Afterwards, an attempt will be made to generalise the economic findings by varying the prices of gas and electricity to different rates. What effect this has on the annual cost of operation will be looked into.

$$\text{Total Annual Cost} = \sum_{ts=0}^{N} \left(B_{\text{gas}_{ts}} C_{\text{gas}} + B_{\text{elec}_{ts}} C_{\text{elec}_{ts}} \right) (t(ts) - t(ts-1)) \tag{3.2}$$

As for the ecological component, similarly to the economic assessment, the Irish market will be taken as a case study, and then an attempt at generalisation will be made. To calculate the CO_2 used over the course of a year, similarly to Eq. 3.2, except the energy values of the HP and boiler are multiplied by the energy sources' respective carbon intensity values, in grams of carbon dioxide per kilowatt-hour of energy produced.

$$\text{Total Annual } CO_2 = \sum_{ts=0}^{N} \left(B_{\text{gas}_{ts}} I_{\text{gas}} + B_{\text{elec}_{ts}} I_{\text{elec}} \right) (t(ts) - t(ts-1)) \tag{3.3}$$

3.6 CONCLUSION

In conclusion, a residential, two-storey house located in Cavan, Ireland was used as a reference to build a numerical model from. The house model was created using the likeness of the dwelling: the thermal constructions, geometry and thermal envelope were modelled. Experimental measurements were taken of the thermal energy demand of the house and energy usage

broken down by energy type. A numerical model of a HHS was created in `Modelica`, using a Daikin Altherma 3 HP as a reference, and a weather model created from data originating from the Clones weather station was used as the climatic model. The dwelling-HHS composite model was verified and validated against the experimental measurements, falling within agreed upon tolerances provided by ASHRAE and the literature in general. A parametric study was designed to capture how varying the bivalent operation temperature window of the boiler-HP system would affect the system performance. Various other smaller models were designed, including internal gains from persons, lighting, etc., a frosting model and a HHPS-capable controller model.

4

SYSTEM MODEL

4.1 TIMESTEP AND SOLVER

A nominal timestep of 3 minutes was chosen, as this results in a very accurate simulation run. The dynamics of the model are accurately captured by a timestep of 180 seconds. The timestep value used in the simulations in the literature is sparse, however, Roccatello, Prada, Baggio and Baratieri [23] use five-minute timesteps, while Dongellini, Naldi and Morini [14] use timesteps of 30 seconds, Klein, Huchtemann and Müller [13] also use timesteps of 3 minutes. The `Dymola` built-in `Radau II-A` solver was used, as this is recommended by the Buildings Library Best Practices [74], which also suggests a tolerance of 1×10^{-6} for "faster and more robust simulation for thermo-fluid flow systems".

The `Radau II-A` solver uses the user-inputted timestep as a nominal value, but can dynamically decrease the timestep in order to maintain stability or accuracy. Thus, even though there are 175 200 three-minute intervals in a year, during each simulation run there tends to be circa 180 000 timesteps.

4.2 LOCATION

The reference house that the building model is based off of a hipped dormer, two-storey residential house located in Belturbet, Cavan, a small town close to the Republic of Ireland and Northern Ireland border, about 125 kilometres from Dublin. The ref-

erence house lies at an elevation of 80 metres and is Easterly facing. The dwelling is located in a residential estate, and is thus classified as being located in an urban environment.

4.3 FORM AND FABRIC

The reference model has a floor area of 160 square metres, 93 square metres of which are downstairs, i.e., "exterior floor", a gross roof area of 173 square metres and a total external wall surface area of 139 square metres. There are 21 exterior windows of varying sizes in total and thirteen rooms, seven downstairs and six upstairs. The ceiling height is a uniform 2.5 metres throughout the model. All rooms except for one were considered to be unconditioned, the exception being a very small box room on the ground floor which was interpreted to be a utility room of sorts. The void zones were also unconditioned. The building model geometry and thermal properties were created during previous works by Keogh [31]. A floor plan schematic can be seen in Fig. 4.1, showing the ground floor and first floor room layouts and windows. A 3D rendered model of the house can be seen in Fig. 4.2. All building model data is contained in a `.idf`-file, an input data file interpretable by `EnergyPlus`. This file contains data about the geometry of the building, envelope construction, thermal and physical properties of the constructions, building and occupancy schedules, internal gains, outside air infiltration to void zones and various other data regarding the simulation process e.g., timestep.

4.3.1 *Thermal Properties of Constructions*

4.3.1.1 *Minimal Retrofit Model*

Tbl. 4.2 details the specifications of the exterior wall construction for the minimal retrofit model, from outside to inside.

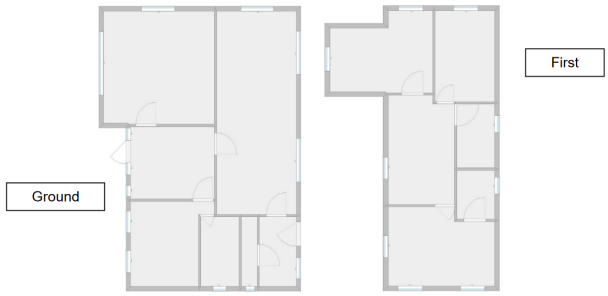

Figure 4.1: Dwelling floor plan, ground and first floor

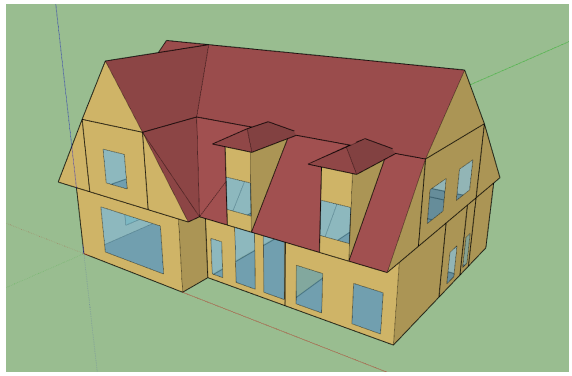

Figure 4.2: 3D Model of Reference Building, rendered in `SketchUp` via the `Euclid` plugin

Tbl. 4.3 details the specifications of the exterior floor construction for the minimal retrofit model, from top to bottom. The exterior floor is the floor which lays on top of the foundations and therefore conducts heat from the inside of the house to the ground. It consists of concrete at the bottom, insulation board, an air cavity and floor tiles on top.

Tbl. 4.4 details the specifications of the pitched roof construction for the minimal retrofit model, from outside to inside. This construction is applied to the bulk of the roof and consists of clay tile, an air cavity, insulation board and then plasterboard.

The dormer roof provides no insulation and is only in place to protect the inside spaces from wind and rain. Its specifications can be read in Tbl. 4.5.

Table 4.1: Summary of U-Values

Building Model	U-Value $[\mathrm{W\,m^{-2}\,K^{-1}}]$				Infiltration Rate [ACPH]
	Exterior Wall	Pitched Roof	Exterior Floor	Exterior Glazing	
Minimal Retrofit	0.31	0.16	0.25	2.15	0.8

Table 4.2: Exterior Wall Construction

Layer	Thickness [m]	Density $[\mathrm{kg\,m^{-3}}]$	Heat Capacity $[\mathrm{J\,kg^{-1}\,K^{-1}}]$	Conductivity $[\mathrm{W\,m^{-1}\,K^{-1}}]$
Rainscreen	0.01	7824	500	30
Insulation	0.085	43	1210	0.03
Air Cavity	0.15	–	–	–
Gypsum board	0.019	800	1090	0.16

4.4 SCHEDULES, EQUIPMENT AND INTERNAL GAINS

Internal gains in the context of an energy building simulation of a residential home refers to the heat generated within the envelope by people, appliances, and lighting.

People generate heat through their activities and body heat, while appliances generate heat through their operation. Lighting

Table 4.3: Exterior Floor Construction

Layer	Thickness [m]	Density $[\mathrm{kg\,m^{-3}}]$	Heat Capacity $[\mathrm{J\,kg^{-1}\,K^{-1}}]$	Conductivity $[\mathrm{W\,m^{-1}\,K^{-1}}]$
Acoustic Tile	0.0191	368	590	0.06
Air Cavity	0.15	–	–	–
Insulation	0.085	43	1210	0.03
Concrete	0.1016	1280	840	0.53

Table 4.4: Pitched Roof Construction

Layer	Thickness [m]	Density [kg m^{-3}]	Heat Capacity [J kg^{-1} K^{-1}]	Conductivity [W m^{-1} K^{-1}]
Clay Tile	0.025	1900	800	0.84
Air Cavity	0.15	–	–	–
Insulation	0.162	43	1210	0.03
Gypsum board	0.019	800	1090	0.16

Table 4.5: Hipped Dormer Roof Construction

Layer	Thickness [m]	Density [kg m^{-3}]	Heat Capacity [J kg^{-1} K^{-1}]	Conductivity [W m^{-1} K^{-1}]
Clay Tile	0.025	1900	800	0.84
Air Cavity	0.15	–	–	–
Roofing Felt	0.005	960	837	0.19

generates heat due to the inefficiencies in converting electricity into light, and light ultimately being converted to heat energy.

In energy building simulation, internal gains are important to consider because they can significantly affect the energy balance of the building. If the internal gains are high, the building may require less heating, which can lead to energy savings. Conversely, if the internal gains are low, the building may require more heating, which can lead to increased energy consumption and costs [75].

Table 4.6: External Glazing Construction

Layer	Thickness [m]	Transmittance [kg m^{-3}]	Conductivity [W m^{-1} K^{-1}]
Inner Pane	0.003	0.783	0.4
Argon Gas	0.20	–	–
Outer Pane	0.003	0.783	0.4

Internal gains are typically modelled as a heat input to the building, which is then factored into the overall energy balance of the building. The magnitude of internal gains is typically calculated based on the number of occupants, the types and number of appliances, and the lighting levels in the building.

4.4.1 *Occupancy Gains*

The magnitude of these gains depends on factors such as the number of occupants, their activity levels, and the duration of their stay in the building. It was decided that a house of the size of the reference home was sized for a total of four persons.

In order to accurately model occupancy gains in a BEM, it is important to use typical occupancy profiles in conjunction with typical metabolic rates for different tasks. A typical occupancy profile is a representation of the number of occupants in the building over time, while a typical metabolic rate is a measure of the heat generated by a person due to their physical activity. Different tasks require different amounts of energy, and therefore result in different levels of heat generation. For example, a person sitting quietly may have a lower metabolic rate than someone performing strenuous physical activity.

Buttitta and Finn [75] developed a stochastic occupancy model which generates hourly occupancy schedules for up to five different types of occupancy profiles of residential buildings for an entire year, based off of data gathered from London, UK. For this thesis, an occupancy profile was chosen which represented the largest share of the population, and two schedules were drawn, one for the weekdays and one for the weekends. These schedules depict the number of persons occupying the dwelling at each hour of the day, and the weekday schedule is detailed in Tbl. 4.7. The table shows the fraction of the (four) occupants in the home

at the corresponding time interval. For the weekend schedule, it was assumed that all occupants remain home all day.

Table 4.7: Weekday Occupancy Schedules

Time	Fraction of Occupants
00:00 → 06:50	1.0
06:50 → 07:30	0.75
07:30 → 08:20	0.5
08:20 → 18:20	0.0
18:20 → 24:00	1.0

'ANSI/ASHRAE Standard 55-2010: Thermal Environmental Conditions for Human Occupancy' [76] details the metabolic rate of people performing various tasks, given in Met units, as well as watts per square metre. An activity level schedule was quasi-arbitrarily assembled and is detailed in Tbl. 4.8. The table, which is very similar to the occupancy schedule in nature, shows the metabolic rate in watts per square metre for the corresponding time interval. `EnergyPlus` takes this metabolic rate and multiplies it by a value of $1.8\,\mathrm{m}^2$, deemed to be the standard surface area of a typical adult. As a reference, a rate of $40\,\mathrm{W\,m^{-2}}$ corresponds to sleeping, $50\,\mathrm{W\,m^{-2}}$ to $90\,\mathrm{W\,m^{-2}}$ are non-strenuous activities such as lounging, reading, etc. and above $100\,\mathrm{W\,m^{-2}}$ corresponds to activities such as walking briskly and beyond.

4.4.2 *Lighting*

In the past, internal gains from lighting used to be a significant contributor to the overall heat load of buildings. This was largely due to the widespread use of inefficient incandescent light bulbs, which generated a significant amount of heat as a byproduct of their operation. In fact, it was not uncommon for incandescent

Table 4.8: Activity Schedules

a Weekday Activity Schedule

Time	Metabolic rate $[\mathrm{W\,m^{-2}}]$
00:00 → 06:50	40
06:50 → 08:20	120
08:20 → 18:20	0.0
18:20 → 22:00	120
20:00 → 23:10	75
23:10 → 24:00	40

b Weekend Activity Schedule

Time	Metabolic rate $[\mathrm{W\,m^{-2}}]$
00:00 → 01:00	75
01:00 → 07:20	40
07:20 → 09:30	75
09:30 → 24:00	120
20:00 → 23:10	75
23:10 → 24:00	40

bulbs to emit more heat than light, resulting in a significant waste of energy and contributing to higher cooling loads in buildings.

However, with the gradual adoption of more efficient lighting technologies such as LED bulbs, internal gains from lighting have become much less of a concern. LED bulbs are significantly more efficient than incandescent bulbs, converting a higher percentage of their energy input into light rather than heat. This means that they generate far less waste heat, resulting in lower cooling loads and reduced energy consumption. ISO 17772-1:2017 presents lighting schedules and load density profiles for single family residential homes, and are reproduced in Tbl. 4.11a.

4.4.3 *Plug Loads and Equipment*

Plug loads in a residential home refer to the energy consumed by appliances and devices that are plugged into electrical outlets, such as televisions, computers, and kitchen appliances. Equipment internal gains in a residential home refer to the heat generated by the operation of various equipment and appliances,

such as refrigerators, ovens, and water heaters. This heat can contribute to the overall heat load of the home, particularly during periods of high use. ISO 17772-1:2017 gives details regarding standards for schedules and load density profiles for equipment gains and plug loads, and is reproduced in Tbl. 4.10, showing the fraction of the load thought to be "active" at the corresponding time. The nominal lighting load is given to be 2.07 $\mathrm{W\,m^{-2}}$ and nominal equipment load is given to be 1.92 $\mathrm{W\,m^{-2}}$.

Table 4.10: Lighting, Plug Loads and Equipment Gains Schedules and Load Densities [77]

a Lighting Schedule

Time	Fraction of nom. value
00:00 → 07:00	0.251
07:00 → 11:00	0.749
17:00 → 23:00	0.251
23:00 → 24:00	0.749

b Equipment Schedule

Time	Fraction of nom. value
00:00 → 08:00	0.625
08:00 → 10:00	0.875
10:00 → 12:00	0.625
12:00 → 16:00	0.750
16:00 → 18:00	0.625
18:00 → 20:00	0.875
20:00 → 22:00	1.0
22:00 → 24:00	0.750

4.5 HEATING SYSTEM

Fig. 4.3 shows an overall diagram view of the HHPS, along with controller and frosting model. Appendix B goes into detail regarding the individual blocks that comprise the `Modelica` model. On a high level, in the bounded box labelled 1 are the boiler, HP, house model and various valves pertaining to the hydronic system. In the box labelled 2, is the controller and active state

machine. Box 3 houses the frosting model, and box 4 contains the radiators, valves, room temperature sensors and P-controllers.

4.5.1 *ASHP*

The ASHP model was imported from the IDEAS library [78].Performance table data obtained from Daikin for a low-temperature, modulating AWHP was used in the modelling of the heat pump. By interpolating the data in the table, the model is able to determine the heating power, electricity usage, and COP based on the condenser outlet temperature and the ambient temperature. The HP has a nominal heating power of 7177 W at a test condition of 2/35 °C (air/condenser temperature), with a COP of 3.17 at this condition and a COP of 2.44 at a test condition of 2/45 °C for full load operation. The heat pump can operate at leaving water temperatures up to 55 °C.

The COP of the AWHP model is calculated by the ratio of heat energy transferred to the passing water to the electrical power used. This is given by Eq. 4.1.

$$\mathrm{COP}_{\mathrm{HP}} = \frac{\dot{Q}_{\mathrm{H}}}{\dot{W}_{\mathrm{elec}}} \tag{4.1}$$

The SCOP of the HP is calculated by taking the ratio the total heat energy imparted to the water to the total electrical energy used by the HP over the course of the year and is given by Eq. 4.2.

$$\mathrm{SCOP}_{\mathrm{HP}} = \frac{Q_{\mathrm{H,\,tot}}}{W_{\mathrm{elec,\,tot}}} \tag{4.2}$$

The model uses modulation to introduce some hysteresis to avoid quick-succession, repeated on-off cycling. The HP turns off when the modulation drops below 20% and turns on when the modulation exceeds 35%. Heat losses to the surroundings are

taken into account to produce a dynamic model, all the while maintaining the performance as per Daikin's data [79].

4.5.1.1 *Frosting Modelling*

The model provided by IDEAS library does not include frosting effects. Thus, a simple model for the repercussions of frosting on the ASHP was developed in the `Modelica` model. A conditional timer block and greater-than-threshold block were used to identify whether the outdoor temperature had been less than 2 °C for an aggregate of 60 minutes, resetting the timer only if the outdoor temperature had exceeded 4 °C for a contiguous 5-minute period. If this 60-minute condition was met, the ASHP was turned off, no matter the modulation level, for 10 minutes. This is intended to introduce a "penalty" to the HP for operating under cold conditions. The approximate values were taken from Sandström [38]. To account for energy loss due to a reverse-cycling defrosting of the HP, A secondary, model-only boiler was fired for such a period as to consume approximately 500 000 J of energy. This energy was summed with the consumption of the primary boiler. This figure was calculated using data from Sandström [38] and the 60% defrosting efficiency figure mentioned in Subsec. 2.1.5.

4.5.2 *Radiators*

The `RadiatorEN442` radiator model from the Buildings library [70] was used. Each of the twelve conditioned rooms was assigned a radiator. The nominal heat flow for a radiator in room i was determined by taking the nominal total heat flow of the system, $Q_{\text{flow, nom}}$ and multiplying it by the ratio of the volume of room i, $V_{\text{room, }i}$ to the total conditioned room volume, $V_{\text{rooms, tot}}$. The radiator model uses five discretised elements to perform a discretised element method heat transfer calculation. The model

parameters were altered to only produce convective heat transfer to the room i.e., no radiative heat transfer as the `EnergyPlus` compatible `ThermalZone` model has no radiative heat input. The convective heat transfer was modelled with Eq. 4.3.

$$Q^i_{\text{conv}} = \text{sign}(T^i - T_{\text{air}})(1 - f_{\text{rad}})\frac{UA}{N}|T^i - T_{\text{air}}|^n \tag{4.3}$$

Where T^i is the water temperature of the element, T_{air} is the temperature of the air in the room, f_{rad} is the fraction of the heat converted to radiation, set to zero in this model, n is the exponent of heat transfer, set to 1.3, and UA is the UA-value of the radiator which is numerically solved for the given nominal data values.

4.5.3 *Thermal Storage Tank*

The thermal storage tank `Thermal.Storage` model from the Buildings library [70] was used in the HHS model. The model uses ten stratified layers (`nSeg = 10`) to model to dynamics of the temperature gradient of the water within the tank. The storage tank was fixed to contain 0.5 m^3 of water, or 500 L, with 10 cm of insulation thickness and a height of 1.7 m. The tank was assumed to be located in the aforementioned unconditioned room, with heat losses occurring from the tank to the room. Two temperature sensors are connected to the tank, one at the top of the water volume (volume index 1) and one at the bottom of the water volume (volume index `nSeg`).

4.5.4 *Boiler*

The boiler model `BoilerPolynomial` from the Buildings library was utilised to model the natural gas boiler component of the HHS. A constant efficiency of 90% was used as this best matched

the efficiency of the reference house boiler. A nominal mass flowrate of 0.25 kg s^{-1} was inputted, which had been calculated through Eq. 4.4.

$$\dot{m}_{\text{boiler, nom}} = \frac{k\dot{Q}_{\text{nom}}}{\Delta T_{\text{boiler loop}} c_{\text{water}}} \tag{4.4}$$

The coefficient k is simply a scaling factor that affects the mass-flow rate and downstream variables.

The rate of heat produced by the fuel is calculated using Eq. 4.5, where $y \in [0, 1]$ is the control signal, determined by the HHS logic control outlined in Fig. 4.5, $\dot{Q}_0$ is the nominal heating power, set to 10 kW, and η_0 is the nominal efficiency.

$$\dot{Q}_{\text{fuel}} = y\frac{\dot{Q}_0}{\eta_0} \tag{4.5}$$

Eq. 4.6 determines the heat transferred to the passing water. η is the efficiency at the at instantaneous operating temperature and $\dot{Q}_{\text{ext}} > 0$ is the heat loss to the ambient. The boiler has a boundary condition of its heat port which is connected to the air of the unconditioned zone where the boiler is assumed to be installed.

$$\dot{Q} = \eta\dot{Q}_{\text{fuel}} - \dot{Q}_{\text{ext}} \tag{4.6}$$

Eq. 4.7 gives the mass flowrate and the volumetric flowrate of the fuel, where h_{fuel} is the heating value of the fuel, and ρ_{fuel} is the density of the fuel, 845 kg m^{-3}. Since a condensing gas boiler is being used, the higher heating value of gas (4.26×10^7 J kg^{-1}) is being used.

$$\dot{m}_{\text{fuel}} = \frac{\dot{Q}_{\text{fuel}}}{h_{\text{fuel}}} \quad ; \quad \dot{V}_{\text{fuel}} = \frac{\dot{m}_{\text{fuel}}}{\rho_{\text{fuel}}} \tag{4.7}$$

4.5.5 *Heating System Behaviour*

Fig. 4.5 is an flowchart diagram which depicts (a slightly non-nuanced version) the system behaviour of the HHS implemented in `Modelica`. On a high level, there are two separate control systems, one for producing the hot water using the boiler and the HP and depositing it in the Thermal Energy Storage (TES), and one for distributing the hot water throughout the radiators via the control of the valves, henceforth dubbed "heat generation loop control" and "radiator loop control" respectively. It must be noted that the reference house whose data the model calibration was based off, did not have a night setback, however, the final model did include a night setback. During the day, the room setpoint is 21 °C, while at night the setpoint is 16 °C.

4.5.5.1 *Heat Generation Loop Control*

The heat generation loop starts when both of the following conditions have been met: the average room temperature is less than 18 °C, and the water temperature of the buffer tank is less than the demanded supply water temperature. Then either one or both of the heating devices are activated. If the outdoor temperature is greater than T_{biv} (nominally 7 °C), the boiler is prevented from turning on, and if the outdoor temperature is less than T_{cut} (nominally 2 °C), the HP is prevented from turning on. This temperature window results in the bivalent parallel hybrid operation.

The demanded water supply temperature curve changes depending on the outdoor temperature. If the temperature is greater than the bivalent temperature, the supply curve is calculated based off of the nominal post-HP water temperature of 35 °C, and the time-dependent room setpoint temperature, otherwise the supply curve is calculated using the values of the nominal post-boiler water temperature of 50 °C. During bivalent oper-

ation, the HP heats up the circulating water to 35 °C, and the boiler "tops up" the water to the demanded supply temperature using a PD-controller. The two supply temperature curves can be seen in Fig. 4.4.

4.5.5.2 *Radiator Loop Control*

Conceptually, this aspect of the heating system decides whether both the outdoor temperature is low and the P-controllers are outputting a higher than threshold level signal, determines the appropriate water supply temperature and subsequently mixes the supply and return water to achieve this setpoint, and controls the individual valve opening positions to distribute the supply water proportionally to the rooms depending on their temperature and percentage of total conditioned volume of the particular room.

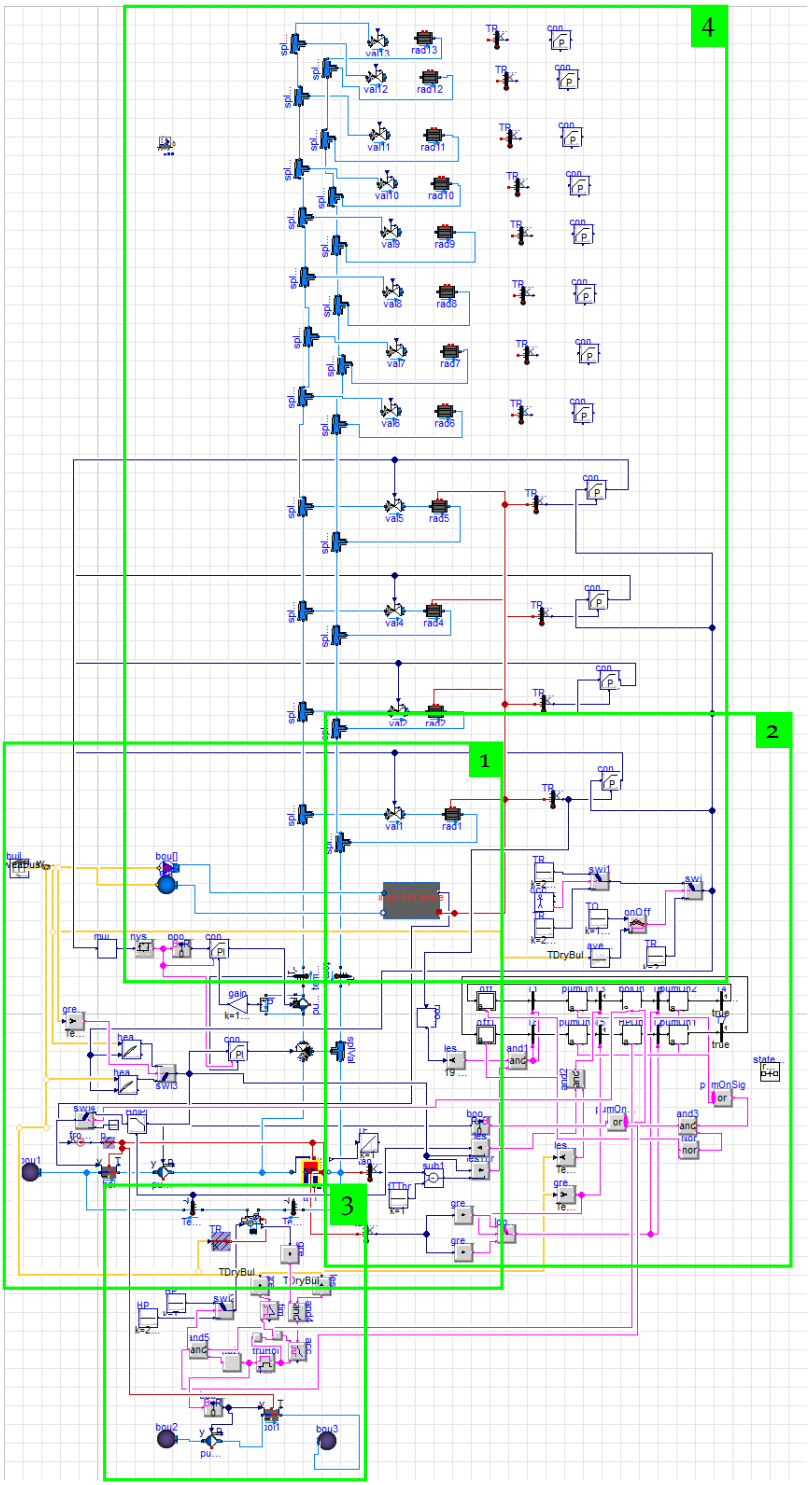

Figure 4.3: `Modelica` diagram view of implemented system

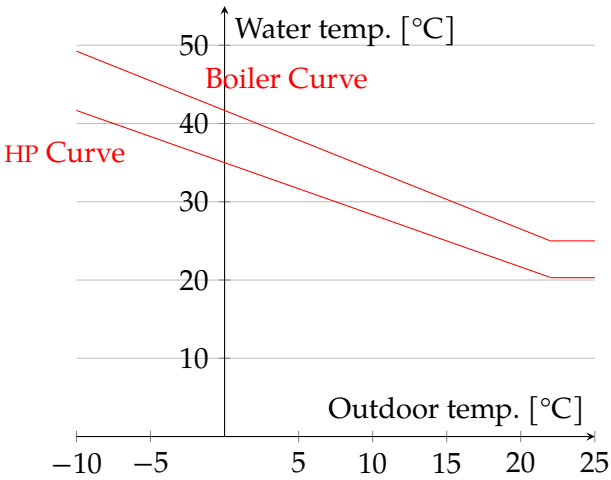

Figure 4.4: Supply temperature curves, demanded water temperature against outdoor temperature

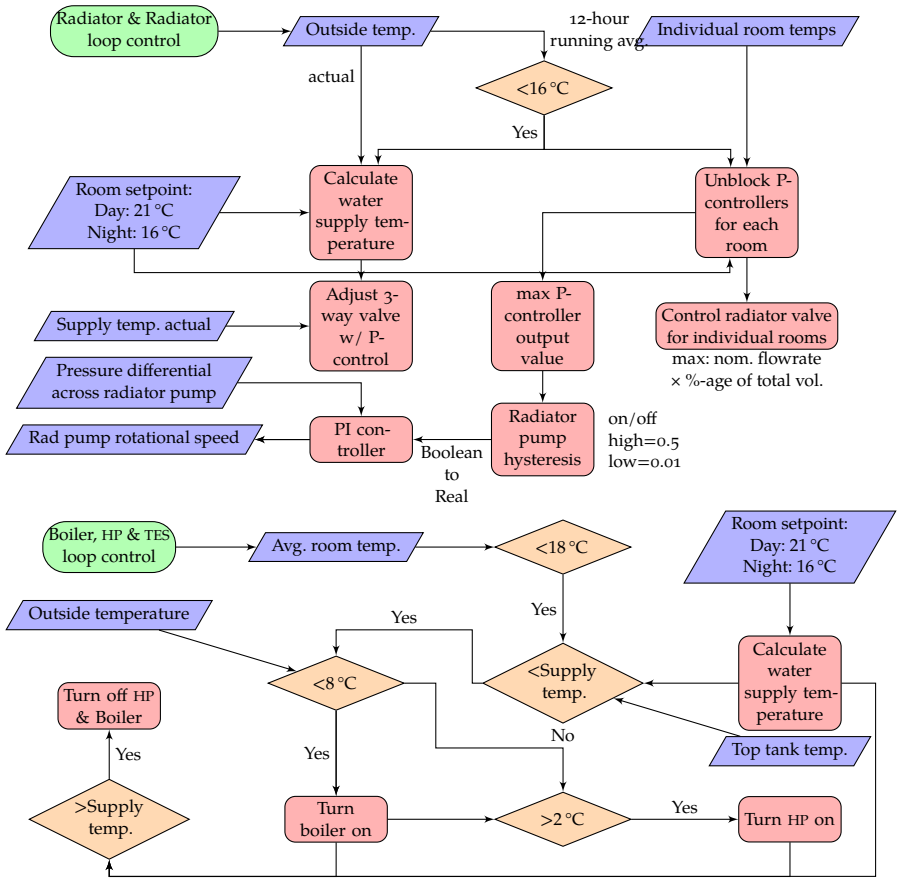

Figure 4.5: Flowchart diagram of HHS behaviour

5

SENSITIVITY ANALYSIS

A sensitivity analysis, also referred to as a parametric study, is a technique utilised in simulation modelling to assess the impact of varying parameters on the outcomes of the model. The process involves iteratively running the simulation multiple times with systematic modifications to input parameters and can enable the identification of critical parameters that exert the most substantial influence on the model outcomes, and also, in particular, identify the optimal pair of values of the parallel operation temperature window.

In this thesis, an exhaustive or full factorial sensitivity analysis has been performed on the bivalent parallel operation temperature window of a HHPS as opposed to other sampling methods such as a Latin Hypercube approach or Monte Carlo Sampling. The analysis evaluates the impact of altering the bivalent temperature and cut-off temperature on the total cost of fuel and electricity for the HHS over the course of a year in the economic assessment, as well as on the PE used and CO_2 emissions in the ecological assessment. The approach adopted in this research allows for a comprehensive examination of the system, by identifying the factors that are critical in determining the optimal operation of the system, while also providing insights into potential cost savings and environmental benefits.

Although full factorial designs can be computationally expensive and time-consuming, this approach was chosen as the dimensionality of the parameter space is very low at just two, and the resolution, or number of levels, being simulated for the two

parameters is also relatively low. This enables a full factorial parametric study to be carried out given the complexity of the model and the computational resources available.

5.1 PARAMETRIC STUDY DESIGN

As discussed in Sec. 3.4, the two parameters were varied with a non-uniform resolution. The bivalent temperature was varied from 5 °C to 10 °C, while the cut-off temperature was varied from −2 °C to 4 °C, giving a resolution of 6 and 7 respectively. The increment size (the step size between the resolution levels) was fixed at 1 °C for both parameters sweeps, as it resulted in an acceptable level of granularity between the various simulation runs. For the sake of brevity, a notation will be introduced to denote the certain parameter-level combination being discussed in a given sentence/paragraph. This idea will be denoted by $\{X, Y\}$, where the first number refers to the bivalent temperature and the second number refers to the cut-off temperature, not to be confused with the bivalent and cut-off temperature level indices e.g., the cut-off temperature level parameter of 10 °C has an index of 1, 9 °C has an index of 2, etc. When it is desired to refer to a certain column or row of the upcoming carpet plots, a tilde will be used to denote that the corresponding parameter levels are all being referenced, e.g., $\{-2, \sim\}$ would be used to refer to all cells corresponding to a bivalent temperature of −2 °C. If multiple rows or columns are to be referred to, a right-arrow will be used in order to be discernable to a minus sign, e.g., $\{-2 \rightarrow -1, 6\}$ would refer to the two cells corresponding to a cut-off temperature of 6 °C and bivalent temperature of −2 °C and −1 °C.

5.2 ENERGY CONSUMPTION

As the two parameters were varied, the energy consumption of the two energy sources changes of course, in magnitude and their respective share of the total energy consumption. Tbl. 5.1 and Tbl. 5.2 show heatmaps of the year-total gas consumption and electricity consumption, in kilowatt hours, for each of the parameter-level combinations respectively. The bivalent temperature is varied in the horizontal direction, while the cut-off temperature is varied in the vertical direction. The heatmaps are coloured, with red cells representing high values and green cells representing low values Some general and relatively obvious first impressions from the heatmap reveal that the level of gas consumption falls off dramatically between the levels corresponding to 1 °C and 4 °C of the bivalent temperature, from a high of 3996.7 kWh to 2215.6 kWh, which also happen to be the minimum and maximum gas consumption values for the gas consumption carpet plot overall. It can be intuited that when the HP turns off at higher outdoor temperatures, that the gas boiler must operate longer/more frequently to heat the dwelling. Once the bivalent temperature parameter is less than 1 °C, the level of gas consumption rises again, though much slower than from the other direction. This can be understood by considering that when the HP is forced to operate at these lower temperatures, the HP must be defrosted more often, which of course requires energy from the boiler, as a reverse-cycling model was implemented. This results in the consumption of gas increasing moderately.

When considering the electricity consumption heatmap, it is perhaps easier to interpret than the gas consumption heatmap. For lower levels of bivalent temperature, more electricity is consumed, as the HP naturally has simply more opportunities to operate, especially that during colder spells, where more heat-

Table 5.1: Year-total gas consumption carpet plot for each parameter-level combination [kWh yr^{-1}]

T_{cut} \ T_{biv}	−2	−1	0	1	2	3	4
10	2357	2315	2284	2251	2586	3237	3997
9	2366	2318	2287	2266	2605	3249	3907
8	2402	2351	2334	2244	2587	3275	3839
7	2416	2352	2340	2276	2564	3367	3902
6	2390	2364	2350	2216	2552	3358	3966
5	2424	2386	2380	2276	2543	3353	3996

ing is required. For lower values of cut-off temperature, less electricity is used, as the boiler is allowed to operate during colder temperatures, thus the heating system simply requires less input from the HP. The highest value of electricity consumption observed is 4347 kWh and the lowest value is 3425.4 kWh for parameter-level combinations of $\{-2, 10\}$ and $\{4, 5\}$ respectively.

Table 5.2: Year-total electricity consumption carpet plot for each parameter-level combination [kWh yr^{-1}]

T_{cut} \ T_{biv}	−2	−1	0	1	2	3	4
10	4347	4320	4270	4229	4130	3902	3675
9	4312	4286	4235	4189	4088	3862	3669
8	4249	4224	4169	4153	4049	3809	3649
7	4186	4170	4104	4078	3994	3716	3570
6	4140	4116	4053	4050	3949	3662	3497
5	4073	4050	3989	3974	3902	3604	3425

Tbl. 5.3 shows the carpet plot for the year-total energy consumption for the heating system, i.e., the sum of the electricity and gas consumption, again, in kilowatt hours. It can be seen that similarly to Tbl. 5.1, the overall energy consumption is greatest for the parameter-level combinations where the bivalent temperature is 3 °C or greater. There is a sharp decline in energy consumption from $\{4 \rightarrow 2, \sim\}$, likely as the gas consumption figures dominate this region of the table. In the region of the table

where the bivalent temperature is less than 0 °C, the total energy consumption is mildly greater than in the middle region of the table. This is due to the electricity consumption increasing as discussed previously. The maximum and minimum values are 7671.86 kWh and 6249.63 kWh for parameter-level combinations of {4, 10} and {1, 5} respectively.

Table 5.3: Year-total energy consumption carpet plot for each parameter-level combination [kWh yr^{-1}]

T_{cut} \ T_{biv}	−2	−1	0	1	2	3	4
10	6704	6636	6554	6480	6716	7139	7672
9	6678	6604	6522	6454	6693	7111	7576
8	6651	6574	6502	6397	6637	7084	7488
7	6601	6522	6444	6354	6558	7083	7472
6	6530	6480	6402	6265	6502	7021	7463
5	6497	6437	6368	6250	6445	6957	7421

5.2.1 *Performance Indices*

5.2.1.1 *SCOP Variation in Parametric Study*

As the hybrid operation temperature window shifts, and contracts and expands, the performance of the HHS changes due to the changing of the modes of heating active at a given a temperature and the dynamics between the operation of the gas boiler, ASHP and building model at large. As discussed in Subsec. 4.5.1, the SCOP of the HP can be thought of as the average COP of the ASHP over the course of the year or heating season. For this analysis, the entire year is being considered. The COP will be greatly affected by the outdoor temperatures the HP is operated at, thus, the COP will be highly dependent on the bivalent temperature parameter being varied throughout the sensitivity analysis. It will also be minorly affected by the cut-off temperature due to the aforementioned system dynamics. The SCOP for this analysis

is calculated using Eq. 4.2. The tabulated results are found in Tbl. 5.4.

Table 5.4: SCOP values for each parameter-level combination

T_{cut} \ T_{biv}	−2	−1	0	1	2	3	4
10	3.07	3.07	3.08	3.07	3.07	3.11	3.13
9	3.06	3.07	3.07	3.06	3.07	3.1	3.12
8	3.06	3.06	3.06	3.05	3.06	3.1	3.11
7	3.05	3.05	3.06	3.05	3.05	3.09	3.1
6	3.05	3.05	3.05	3.04	3.05	3.09	3.1
5	3.05	3.05	3.05	3.04	3.04	3.09	3.1

Note: the colours in this table are the opposite to Tbls. 5.1 to 5.3.

At first the results from Tbl. 5.4 may be confounding for two main reasons, first that the SCOP values change only very slightly with the different parameter-level combinations, and secondly, the lowest SCOP measured occurs in what was previously found to be the parameter-level combination, {1, 5}, with the overall lowest energy consumption and a middling electricity consumption.

A simple explanation for the SCOP hardly changing as a function of the bivalent temperature and is because there simply are very few opportunities for a low outdoor temperature to greatly affect the overall COP value of the HP. As can be seen from the outdoor temperature plot in Fig. 3.2, there are rarely times throughout the year where the ambient temperature drops below 0 °C. Thus, when the COP is averaged over the full 8760-hour year, the few number of hours where the COP is low due to low outdoor temperatures hardly cause an affect, but is still detectable. If however, one were to perform the SCOP calculation for the months where the outdoor temperatures do fall below 0 °C, greater variances would be found.

However, there is another compounding phenomenon occurring which is perhaps downplaying the negative effects of low

outdoor temperatures affecting the COP, which is the effect of frosting on the time under which the HP is operating at, at lower temperatures. The frosting of course only occurs when the outdoor temperature is low, and due to the frosting model described in Subsubsec. 4.5.1.1, the HP operation is blocked for a set time to emulate defrosting. This results in the HP simply operating less at these temperatures, reducing the negative consequences on the COP. This explains why the COP is generally lowest at $\{1, \sim\}$.

5.2.1.2 *Number of HP Cycles Variation in Parametric Study*

The number of on cycles for a HP over the course of a year is closely linked to the temperature below which it will be blocked from operating, i.e., its bivalent temperature, due to frosting effects. This is due to the fact that as the HP operates in cold weather, frost builds up on its outdoor unit, reducing its efficiency and eventually, the controller shuts off the HP to perform a defrost cycle. Tbl. 5.5 shows a heatmap of the number of on-cycles. A clear delineation can be seen when the bivalent temperature decreases past 3 °C. This is due to the frosting model activating at outdoor temperatures less than 2 °C. The HP can be thought of as being interrupted when the ambient temperature is less than 2 °C for longer than 60 minutes, leading to more regular on-off cycles, restarting the HP after the 10-minute defrosting period. There is a 50.9% increase in number of on-off cycles when comparing the value at $\{4, 10\}$ to $2, 5\}$. There appear to be anomalous values at the $\{-1, 10\}$ and $\{0, 6\}$ combinations, for which there is little explanation other than pure chance.

Time series plots can be seen in Figs. 5.1 to 5.3, of a ten-day period from the 19^{th} of March to 29^{th} of March. This period was chosen quasi-arbitrarily, with the only criteria being a period where the temperature drops below 2 °C multiple times for extended periods. Three series are shown in each, the water temperature of the supply and return radiator loop, and the outdoor tem-

Table 5.5: Annual number of HP cycles for the different parameter-level combinations

T_{cut} \ T_{biv}	−2	−1	0	1	2	3	4
10	1015	836	957	941	911	776	731
9	1020	997	962	946	916	783	750
8	1024	1006	967	976	938	794	782
7	1044	1035	991	990	964	795	791
6	1076	1053	777	1031	990	820	804
5	1103	1082	1039	1058	1037	850	821

perature. At the bottom of each is a small subplot which shows the HP on-off cycling. Figs. 5.1 and 5.2 show parameter-level combinations where the HP operates below 2 °C, while Fig. 5.3 does not. From the cycling subplot it can be seen that in Figs. 5.1 and 5.2, the HP restarts many many times around the 20th, 21st, 23rd and 25th. This matches up with the outdoor temperature dropping below 2 °C from the plot above. Constant on and off cycling incurs cycling losses which can amount to large amounts of energy and are detrimental to the lifespan of the HP [36, 37].

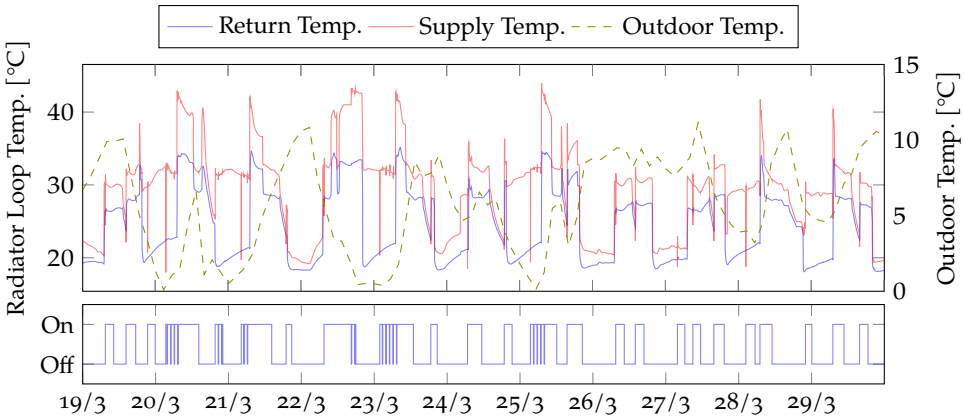

Figure 5.1: Supply and return water temperature overlaid with external temperature with subplot of HP on-off cycles for $\{-2, 5\}$ parameter-level combination for 19th to 29th March

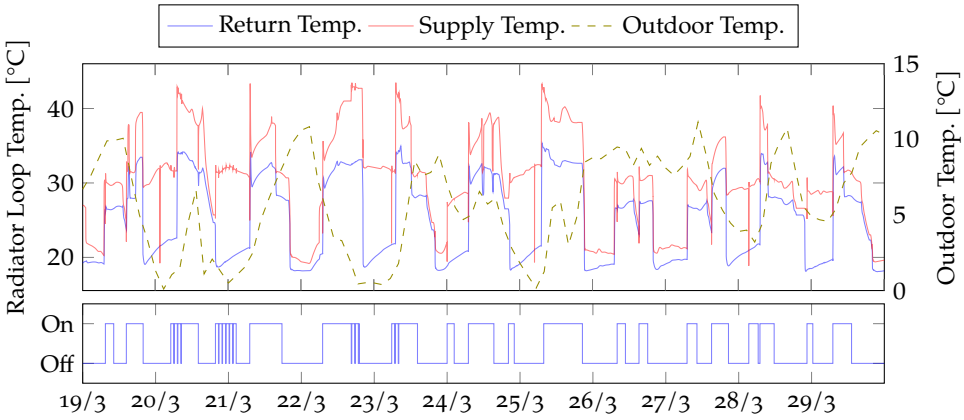

Figure 5.2: Supply and return water temperature overlaid with external temperature with a subplot of HP on-off cycles for $\{1, 7\}$ parameter-level combination for 19th to 29th March

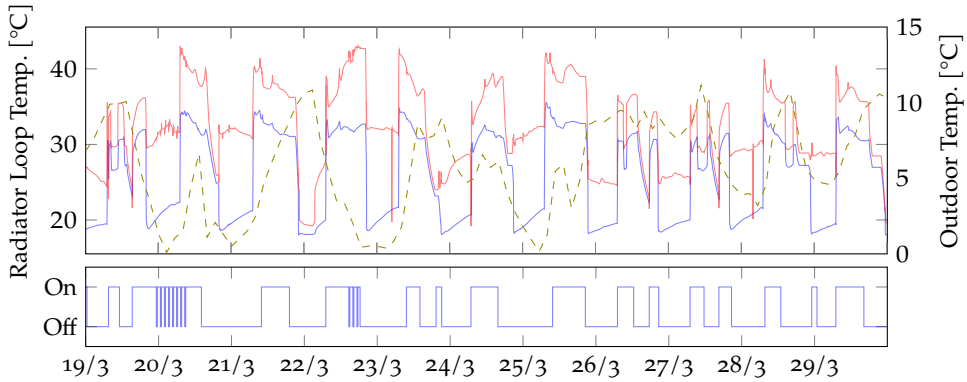

Figure 5.3: Supply and return water temperature overlaid with external temperature with a subplot of HP on-off cycles for {4, 10} parameter-level combination for 19th to 29th March

6

ECO-ECONOMIC ASSESSMENT

Wir müssen wissen. Wir werden wissen.
We must know. We will know.

— David Hilbert

The ecological-economic assessment of a HHS involves an analysis of the environmental and economic impacts associated with its operation. Such an assessment can provide insights into the effectiveness of the HHS in achieving the dual goals of reducing GHG emissions and minimising operational costs. The optimisation of the hybrid operation temperature window is a critical component of this assessment, as it has the potential to significantly impact both the ecological and economic performance of the system. By determining the optimal temperature range for the HHS, it is possible to achieve a balance between reducing energy consumption, minimising carbon emissions, and ensuring comfortable indoor temperatures. This chapter presents a detailed analysis of the ecological and economic benefits of optimising the hybrid operation temperature window and discusses the key factors that influence the optimal temperature range.

6.1 ECONOMIC ASSESSMENT

The economic assessment was carried out to identify the most cost-effective hybrid operation temperature window for the HHS through the parametric study explained in Chap. 5. To achieve this, the Irish market was used as a case study. The typical cost

of natural gas and a time-of-use electricity tariff model was employed to estimate the cost of energy consumption accurately, accounting for fluctuating peak and off-peak hours. Standing costs, such as connection and fixed charges, were excluded from the assessment as they are typically independent of the heating system used. By using the previously established electricity and gas usage metrics from Tbls. 5.1 and 5.2, and respective energy costs, the total cost of space heating was evaluated and the most cost-effective hybrid operation temperature window for the system was identified.

6.1.1 *Cost of Energy*

For the Irish market case study, the price of gas was taken to be a constant at 12.06 cent, which is the figure provided by the Household Energy Price Index (HEPI) in their February 2023 monthly update [80]. For the generalised analysis, varying values of gas price will be used of course.

6.1.1.1 *Electricity Tme-of-Use Tariff*

A time-of-use tariff electricity price was utilised to calculate the cost of the electricity used in heating the dwelling at a given time. The tariff price comprised three tiers, namely peak rate, standard rate, and night rate, with each tier representing different costs. The peak rate was the most expensive, followed by the standard rate, with the night rate being the least expensive. By utilising the time-of-use tariff, the study accounted for the variation in electricity prices across different times of the day, thereby providing a more accurate representation of the energy costs associated with the operation of the HHS. Tbl. 6.1 shows the price breakdown by tier for the electricity, provided by Electric Ireland.

Table 6.1: Time-of-Use Electricity tariffs [81]

Time-band name	Interval	Cost [cents]
Night	23:00 →08:00	22.39
Day	08:00 →17:00 & 19:00 →23:00	44.50
Peak	17:00 →19:00	47.47

6.1.2 *Irish Market Case Study*

When the product of the gas and electricity usage rates for all of the different parameter-level combinations from Tbls. 5.1 and 5.2, and the energy prices are taken, as explained in Subsec. 6.1.1 and Subsubsec. 6.1.1.1, using the formula Eq. 3.2 is used, Tbl. 6.2 is obtained. This table is the annual cost of the HHS for the different bivalent operation temperature window combinations in Euro.

Table 6.2: Total annual cost of HHS for different parameter-level combinations [€ yr^{-1}]

T_{cut} \ T_{biv}	−2	−1	0	1	2	3	4
10	1896	1878	1861	1846	1852	1860	1877
9	1870	1857	1840	1826	1831	1840	1853
8	1845	1832	1813	1801	1805	1815	1825
7	1813	1801	1782	1767	1770	1787	1799
6	1785	1776	1757	1744	1747	1757	1772
5	1749	1738	1724	1708	1713	1718	1733

As can be seen from the table the {1, 5} parameter-level combination is the combination with the lowest annual operating costs, with a total cost of €1707.88. While {−2, 10} is the combination resulting in the highest annual cost of €1889.62. Generally, the worst performing combinations reside in the {∼ , 9 → 10} band, while the best performing combinations reside in the {∼ , 5 → 6} band. A sort of horseshoe-shaped pattern can be identified from the heatmap, with all gradients leading towards the lowest cost

combination. There are no other local minima. This carpet plot can be thought of as a superposition of Tbls. 5.1 and 5.2, along with a transformation due to the fixed cost of gas and fluctuating cost of electricity.

This may be interpreted in the following way: the highest cost combinations are those where the boiler is allowed to operate at very high temperatures, i.e., the cut-off temperature is high. This means the HP, which coincidentally, has its greatest COPs at these temperatures, is denied from providing the entire heating demand of the dwelling. At the lower cut-off temperatures, the HP is permitted to provide all the heating demand at lower temperatures. As for the changes in the cost in the bivalent temperature direction of the heatmap, this can be explained by recalling that the electricity usage increases dramatically towards the lower bivalent temperature values.

The resulting values in this heatmap are very fickle, and are very sensitive to the prices of gas and electricity, as was also determined by Rauschkolb, Modi and Culligan [21]. It is also worth noting that the ratio between the maximum and minimum cost is 10.66%, which is not negligible, but perhaps not the single greatest cost saving measure implementable in a heating system. It is clear from Keogh [31] that a deep retrofit would decrease the total energy usage of the dwelling for space heating by about a third, which would have a much greater affect on the annual heating bill, however, at a high upfront cost.

6.1.3 *Generalised Economic Analysis*

Due to how sensitive the results from the Irish market case study total annual heating costs were on the prices of natural gas and electricity, it is worth considering how the analysis changes depending on how the prices change. For this reason, two diametrically opposed parameter-level combinations were chosen

which vary in their make-up of electrical and gas distribution, $\{-2, 10\}$ and $\{4, 5\}$. These combinations have different compositions of gas and electrical usage as can be seen from Tbls. 5.1 and 5.2. These two combinations had their electrical cost and gas cost varied systematically. The gas cost was varied from 0.06 cents to 0.18 cents per kilowatt-hour, using the 12.06 cents per kilowatt-hour found in Ireland as a pivot point, linearly increasing and decreasing by 3 steps in 0.02 cent increments. The electrical cost was varied from 30% of the Irish price to 130% of the Irish price. Ireland currently has the highest electricity cost in Europe [80], while the lowest electrical prices can be found in Hungary and Ukraine at 9.33 cents and 4.3 cents per kilowatt-hour respectively. Eq. 3.2 was used to calculate the cost for each new gas and electricity cost combination and divided by the Irish price, in order to see relative change.

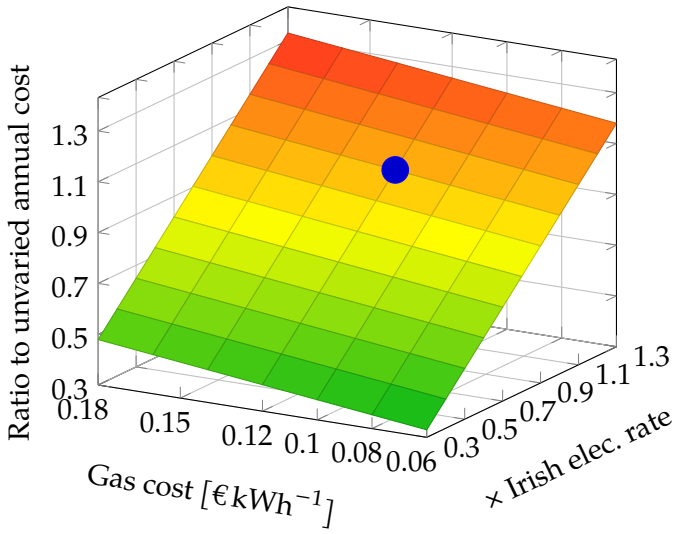

Figure 6.1: Varying gas price from 6 ¢ kWh^{-1} to 18 ¢ kWh^{-1} and electricity from 30% to 130% of Irish prices for parameter-level combination $\{-2, 10\}$

Figs. 6.1 and 6.2 show two surface plots. The electrical cost per unit is varied along the x-axis and the gas cost is varied along the y-axis. The resulting total annual cost is divided by the non-

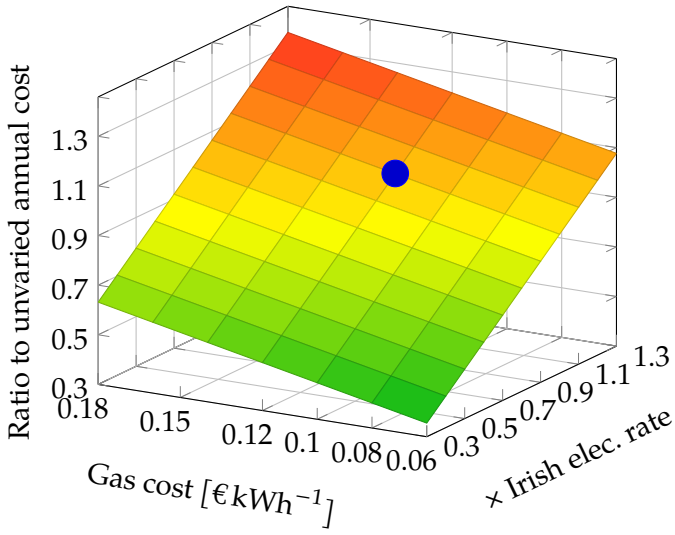

Figure 6.2: Varying gas price from 6 ¢ kWh^{-1} to 18 ¢ kWh^{-1} and electricity from 30% to 130% of Irish prices for parameter-level combination {4, 5}

varied total price (i.e., 12.06 ¢ kWh^{-1} of gas and the time-of-use electrical tariffs from Tbl. 6.1) to obtain a ratio, where less than unity is cheaper and vice-versa. A blue sphere is placed at the "original" Irish price for that particular combination for reference. Comparing the incline of the surface along the the varying gas cost at 30% of the Irish electricity rate, one can see that Fig. 6.2 is steeper than Fig. 6.1, with the former reaching a ratio of 0.63 while the latter reaches 0.47. Along the incline of of gas cost fixed at 0.06 €/kWh] and varying electricity rate, once again Fig. 6.2 is steeper than Fig. 6.1, with ratios of 1.17 and 1.07 respectively. The highest ratios of 1.32 and 1.35 for Fig. 6.1 and Fig. 6.2 respectively, are of course achieved when the electricity is 130% of Irish prices and the gas is at the greatest price of 0.18 €/kWh].

The $\{-2, 10\}$ parameter-level combination is less sensitive to price increases or decreases than the $\{4, 5\}$ combination. This could be possibly due to the how the gas and electricity usage

totals from Tbl. 5.1 and Tbl. 5.2 for those combinations are interacting with the with the price changes. The price of electricity seems to affect the annual price much more than the price of gas. Even though the gas is being varied by half and almost double, it has a much shallower incline than the electricity.

6.2 ECOLOGICAL ASSESSMENT

A similar sequence of steps to Sec. 6.1 will be carried out for the ecological assessment, where first the Irish market is used a case study, and then an attempt to generalise the analysis is made.

6.2.1 *Irish Market Case Study*

Similarly to the how the total annual cost of the heating system was calculated, the total annual carbon emissions from the heating system was calculated by finding the sum of the product of the gas and electricity usage by their respective carbon intensity figures. The carbon intensity figure for natural gas was placed at 202.9 g kWh^{-1}, as is suggested by SEAI [82]. The carbon intensity figure for electricity is however as constantly changing variable due to how the grid operates.

The carbon intensity of electrical grids is subject to fluctuations resulting from factors such as variable renewable energy sources, changing electricity demand, and the availability of backup power sources. In the case of the Irish grid, wind energy is a significant contributor to electricity generation, and its variability can cause fluctuations in carbon intensity. These fluctuations are influenced by weather conditions, including wind speed and direction. During periods of peak electricity demand, more power may need to be generated, resulting in a higher carbon intensity if more fossil fuel-based power plants are used. Finally, backup power sources, such as hydroelectric or gas-fired power

plants, may need to be utilised in times of supply disruption, resulting in a higher carbon intensity.

The carbon intensity figure for electricity was placed at 296 g kWh^{-1}, as this is the figure determined by SEAI [48], and is a historic low for the annual carbon intensity for Ireland.

Tbl. 6.3 shows the results for the annual carbon emissions generated by the heating system. Once again, the parameter-level combination {1, 5} is the combination which performs the best, with a carbon emissions value of 1638 kg, while the {4, 10} combination performs the worst with a carbon emissions value of 1899 kg. The ratio between these figures comes to 15.93%.

Table 6.3: Irish Case Study: Total annual CO_2 emissions from HHS [kg]

T_{cut} \ T_{biv}	−2	−1	0	1	2	3	4
10	1765	1749	1727	1708	1747	1812	1899
9	1756	1739	1718	1700	1739	1802	1879
8	1745	1727	1707	1685	1724	1792	1859
7	1729	1712	1689	1669	1702	1783	1849
6	1710	1698	1676	1648	1687	1765	1840
5	1697	1683	1663	1638	1671	1747	1825

6.2.2 *Generalised Ecological Analysis*

It was decided to perform a 3-case-scenario analysis for the generalised ecological analysis. Since the carbon intensity of the natural gas is almost entirely fixed, the variable in this analysis will be the the carbon intensity of the electricity. Worst case, middle case and best case scenarios will be devised and compared.

Using the *Explore the Smart Grid Dashboard* [83] utility provided by Eirgrid Group, the highest carbon intensity experienced in 2023 was 454 g kWh^{-1} which occurred on the 3rd of March, while the lowest figure was 131 g kWh^{-1} on 28th of March. It

could also be noted that France, due to its high number of nuclear plants has typical carbon intensity figures of 58 g kWh^{-1}, with lows around the 20 g kWh^{-1} [84].

Therefore, for the best case scenario a carbon intensity of 58 g kWh^{-1} was chosen, as although that is lofty goal for Ireland to reach in the near future, it may be a possibility once the Ireland-France interconnector is completed and more renewable energy sources are installed on the island. The middle case scenario assumed a carbon intensity of 131 g kWh^{-1} as this figure has been achieved as of recent and is a very achievable average carbon intensity figure for the Irish grid in the coming years. The worst case scenario used a carbon intensity figure of 454 g kWh^{-1}, as this value represents the worst carbon emissions of the Irish grid as of recent, and a middling value of 296 g kWh^{-1} was already used in Subsec. 6.2.1.

Table 6.4: Best Case (58 g kWh^{-1}): Total annual CO_2 emissions from HHS [kg]

T_{cut} \ T_{biv}	−2	−1	0	1	2	3	4
10	730.5	720.4	711.1	701.9	764.3	883.1	1024.1
9	730.2	719	709.7	702.6	765.7	883.2	1005.6
8	733.7	721.9	715.3	696.2	759.8	885.5	990.5
7	732.9	719.1	712.8	698.3	751.9	898.8	998.8
6	725	718.5	711.8	684.4	746.9	893.8	1007.5
5	728.1	719.1	714.2	692.2	742.3	889.4	1009.5

Tbls. 6.4 to 6.6 show the three resulting tables from the best, middle and worst case scenarios. As it turns out, Tbls. 6.4 and 6.5 look much more similar to Tbl. 6.3 than Tbl. 6.6 does to any of the other three. A change can be seen where around the Irish value of 296 g kWh^{-1} where the emissions resulting from the gas boiler seem to dominate heavily as this figure begins to decrease. The parameter-level combinations of $\{3 \to 4, \sim\}$ are consistently the highest compared to the rest, and recalling the consumption

Table 6.5: Middle Case ($131\,\mathrm{g\,kWh^{-1}}$): Total annual CO_2 emissions from HHS [kg]

T_{cut} \ T_{biv}	−2	−1	0	1	2	3	4
10	1048	1036	1023	1011	1066	1168	1292
9	1045	1032	1019	1008	1064	1165	1273
8	1044	1030	1020	999	1055	1164	1257
7	1038	1023	1012	996	1043	1170	1259
6	1027	1019	1008	980	1035	1161	1263
5	1025	1015	1005	982	1027	1152	1260

Table 6.6: Worst Case ($454\,\mathrm{g\,kWh^{-1}}$): Total annual CO_2 emissions from HHS [kg]

T_{cut} \ T_{biv}	−2	−1	0	1	2	3	4
10	2452	2431	2402	2377	2400	2428	2479
9	2438	2416	2387	2361	2384	2413	2458
8	2416	2395	2366	2341	2363	2394	2435
7	2391	2370	2338	2313	2333	2370	2413
6	2364	2348	2317	2288	2311	2344	2392
5	2341	2323	2294	2266	2287	2317	2366

distributions from Tbls. 5.1 and 5.2 along with the decreasing value of carbon emissions of the middle and best case, it make sense that the $\{3 \rightarrow 4, \sim\}$ dominate as the electricity carbon intensity is decreased.

As the carbon intensity of the electricity increases, it appears as though low cut-off temperatures and middling bivalent temperatures give the lowest carbon emissions, as was the case for the Irish case study in Subsec. 6.2.1 and Tbl. 6.6. While for low electricity carbon intensities, parameter-level combinations where less gas is used is preferable, due to the electricity being more ecologically friendly.

7

CONCLUSIONS

7.1 CONCLUSIONS

This thesis set out to determine the optimal hybrid operation temperature window of a HHS in the Irish climate, a temperate oceanic climate in a residential dwelling. The hybrid operation window was to be optimised along two dimensions, minimising annual carbon emissions, and minimising annual heating costs. The analysis was based off of an in-situ HHS implemented in a residential dwelling in a town in Ireland, which was used to create the initial `EnergyPlus` building model. A `Modelica` HHS model was built, and the composite model was calibrated using experimental data collected from the in-situ heating system.

The model then was used in a parametric study, where the bivalent temperature of the HP and cut-off temperature of the conventional gas boiler were varied, resulting in 42 simulation runs. The system behaviour was analysed, and an ecological-economic assessment was carried out.

The main results from the thesis are:

- A decrease in the bivalent temperature generally meant that the HP operated more frequently and longer overall over the course of year, even though frosting caused the HP to have to shut down for periods of time during colder weather. A lower bivalent temperature also resulted in the HP using up to 25% more energy than higher bivalent

temperatures, partially due to the decrease in SCOP accompanying the lower temperature operation.

- The effect of frosting on the HP caused it to have up to 50% increase in number of on-off cycles over the course of a year, which can negatively affect the performance of the HP.
- The distribution of gas consumption and electricity consumption for different bivalent and cut-off temperatures are very different. Gas consumption peaks at high bivalent temperatures, with a steep drop of and levelling at lower bivalent temperatures. While electricity consumption peaks at low bivalent temperatures and high cut-off temperatures, and decreasing linearly to a low at high bivalent temperatures and low cut-off temperatures.
- SCOP values do not change very much with varying bivalent and cut-off temperatures. This is most likely due to the mild Irish climate modelled, which does not offer many opportunities for good weather to massively increase the SCOP, nor for cold weather to negatively affect the SCOP.
- The annual total cost of heating depends very much on the price of gas and electricity, with it being particularly sensitive to electricity rates. Higher bivalent and lower cut-off temperatures seem to be more sensitive to price changes than the inverse.
- Annual carbon emissions from the HHS are also very sensitive to the carbon intensity of electricity. At low electricity carbon intensities, the higher bivalent temperatures result in much greater carbon emissions due to the higher usage of gas. While at higher electricity carbon intensities, a combination of low cut-off temperatures and middling bivalent temperatures result in the lowest carbon emissions.

- Finally, for the Irish climate studied, it appears as though a bivalent temperature of 1 °C and a cut-off temperature of 5 °C resulted in the lowest carbon emissions and the lowest annual cost simultaneously.

7.2 FUTURE WORK

There are many avenues to pursue in regard to potential future work in the HHPS field. Although a great effort was made to investigate the issue of varying bivalent temperature operation windows, there is always more to study, science is never finished. A brief list of areas of potential future research which could be fruitful includes:

- Improve the frosting model implemented in this thesis. The frosting model described in Subsubsec. 4.5.1.1 is perhaps not the most developed or accurate model, a more nuanced model may include a model which tracks ice build up as a function both temperature and r.h. The data required for this may be too sparse to accurately model this behaviour however. A full reversing-flow capable hydronic system would also increase accuracy.
- Different constructions, perhaps a model representing a dwelling having undergone a deep retrofit could be investigated. The resulting improved thermal properties of the house would result in less heating demand overall and would surely alter the dynamics of the boiler-HP relationship.
- Calibration was only performed for one of the temperature windows, namely a bivalent temperature of 7 °C and a cut-off temperature of 2 °C. It would better if a second operation window was experimentally measured and calibrated with.

- More climates could be investigated. The Irish climate is perhaps under researched in the field of HHPS, however, there are also other climates which could be researched to further generalise the optimisation of the operation window.
- DHW production was omitted in the simulation of this thesis, however it could be of merit to inquire into how DHW production would alter the dynamics of the HP and boiler, given the boiler were not the sole producer of hot water.
- Scrutinise whether parallel vs. in-series HP and boiler makes a difference in the analysis.
- Finally, smart, real-time bivalent operation temperature window shifting and dilating could be a very interesting topic to pursue.

BIBLIOGRAPHY

[1] International Energy Agency. *The Future of Cooling*. https://www.iea.org/reports/the-future-of-cooling. 2018. (1).

[2] International Energy Agency. *Space Cooling*. https://www.iea.org/reports/space-cooling. 2022. (1).

[3] Eurostat. *Final energy consumption in the residential sector by use, EU-27*. 2018. URL: https://ec.europa.eu/eurostat/statistics-explained/index.php?title=File:Final_energy_consumption_in_the_residential_sector_by_use,_EU-27,_2018.png. (1).

[4] Eurostat. *Energy consumption in households*. 2020. URL: https://ec.europa.eu/eurostat/statistics-explained/index.php?title=Energy_consumption_in_households. (1).

[5] M. Owen, R. American Society of Heating and A.-C. Engineers. *2009 ASHRAE Handbook: Fundamentals*. 2009 Ashrae Handbook - Fundamentals. American Society of Heating, Refrigeration and Air-Conditioning Engineers, 2009. ISBN: 978-1-933742-55-7. URL: https://books.google.ie/books?id=D65XPgAACAAJ. (1, 19, 24, 25, 36, 38).

[6] Pakalolo. *Europe's heatwave is "the most extreme event ever seen in European climatology."* Jan. 2023. URL: https://www.dailykos.com/stories/2023/1/4/2145284/-Europe-s-heatwave-is-the-most-extreme-event-ever-seen-in-European-climatology. (2).

[7] The European Heat Pump Association AISBL (EHPA). *European Heat Pump Market and Statistics Report 2015 - EHPA*. 2015. URL: https://www.ehpa.org/fileadmin/red/07._Market_Data/2014/EHPA_European_Heat_Pump_Market_and_Statistics_Report_2015_-_executive_Summary.pdf. (2, 12).

[8] T. Nowak. *Heat Pumps – Integrating technologies to decarbonize heating and cooling*. EHPA, 2018. URL: https://help.leonardo-energy.org/hc/article_attachments/360010981780/ehpa-white-paper-111018.pdf. (2, 11, 13, 27).

[9] S. Heinen, D. Burke and M. O'Malley. 'Electricity, gas, heat integration via residential hybrid heating technologies – An investment model assessment'. In: *Energy* 109 (15th Aug. 2016), pp. 906–919. ISSN: 0360-5442. DOI: 10.1016/j.energy.2016.04.126. URL: https://www.sciencedirect.com/science/article/pii/S0360544216305461. (2, 7, 17).

[10] C. Vuillecard, C. E. Hubert, R. Contreau, A. mazzenga, P. Stabat and J. Adnot. 'Small scale impact of gas technologies on electric load management – μCHP & hybrid heat pump'. In: *Energy* 36.5 (1st May 2011), pp. 2912–2923. ISSN: 0360-5442. DOI: 10.1016/j.energy.2011.02.034. URL: https://www.sciencedirect.com/science/article/pii/S0360544211001125. (2).

[11] G. Thomaßen, K. Kavvadias and J. P. Jiménez Navarro. 'The decarbonisation of the EU heating sector through electrification: A parametric analysis'. In: *Energy Policy* 148 (1st Jan. 2021), p. 111929. ISSN: 0301-4215. DOI: 10.1016/j.enpol.2020.111929. URL: https://www.sciencedirect.com/science/article/pii/S0301421520306406. (2).

[12] Central Statistics Office. *Housing Stock*. 2020. URL: https://www.cso.ie/en/releasesandpublications/ep/p-cp1hii/cp1hii/hs/. (3).

[13] K. Klein, K. Huchtemann and D. Müller. 'Numerical study on hybrid heat pump systems in existing buildings'. In: *Energy and Buildings* 69 (1st Feb. 2014), pp. 193–201. ISSN: 0378-7788. DOI: 10.1016/j.enbuild.2013.10.032. URL: https://www.sciencedirect.com/science/article/pii/S0378778813006798. (3, 7, 11, 18–20, 25, 54).

[14] M. Dongellini, C. Naldi and G. L. Morini. 'Influence of sizing strategy and control rules on the energy saving potential of heat pump hybrid systems in a residential building'. In: *Energy*

Conversion and Management 235 (1st May 2021), p. 114022. ISSN: 0196-8904. DOI: 10.1016/j.enconman.2021.114022. URL: https://www.sciencedirect.com/science/article/pii/S0196890421001989. (3, 7, 16, 17, 20, 54).

[15] Sustainable Enegry Authority of Ireland. *SEAI Data and Insights*. 2020. URL: https://www.seai.ie/data-and-insights/seai-statistics/energy-data/. (3, 4).

[16] Y. A. Çengel, M. A. Boles and M. Kanoglu. *Thermodynamics: an engineering approach*. English. 9th in SI units. Singapore: McGraw Hill, 2020. ISBN: 9813157879. (3, 14, 15).

[17] C. Di Perna, G. Magri, G. Giuliani and G. Serenelli. 'Experimental assessment and dynamic analysis of a hybrid generator composed of an air source heat pump coupled with a condensing gas boiler in a residential building'. In: *Applied Thermal Engineering* 76 (5th Feb. 2015), pp. 86–97. ISSN: 1359-4311. DOI: 10.1016/j.applthermaleng.2014.10.007. URL: https://www.sciencedirect.com/science/article/pii/S1359431114008783. (4, 7, 21, 31).

[18] G. Li. 'Parallel loop configuration for hybrid heat pump – gas fired water heater system with smart control strategy'. In: *Applied Thermal Engineering* 138 (25th June 2018), pp. 807–818. ISSN: 1359-4311. DOI: 10.1016/j.applthermaleng.2018.04.087. URL: https://www.sciencedirect.com/science/article/pii/S1359431118302886. (7).

[19] J. Y. Jang, H. H. Bae, S. J. Lee and M. Y. Ha. 'Continuous heating of an air-source heat pump during defrosting and improvement of energy efficiency'. In: *Applied Energy* 110 (1st Oct. 2013), pp. 9–16. ISSN: 0306-2619. DOI: 10.1016/j.apenergy.2013.04.030. URL: https://www.sciencedirect.com/science/article/pii/S0306261913003255. (7).

[20] H. Park, K. H. Nam, G. H. Jang and M. S. Kim. 'Performance investigation of heat pump–gas fired water heater hybrid system and its economic feasibility study'. In: *Energy and Buildings* 80 (1st Sept. 2014), pp. 480–489. ISSN: 0378-7788. DOI: 10.1016/j.e

nbuild.2014.05.052. URL: https://www.sciencedirect.com/science/article/pii/S0378778814004769. (7, 16).

[21] N. Rauschkolb, V. Modi and P. Culligan. 'Cost-Optimal Sizing and Operation of a Hybrid Heat Pump System Using Numerical Simulation'. In: *ASHRAE Transactions* 126 (2020), pp. 134–143. ISSN: 00012505. URL: https://www.proquest.com/docview/2414052984/abstract/D9A56D8BC8F44C6CPQ/1. (7, 16, 25, 39, 85).

[22] G. Bagarella, R. Lazzarin and M. Noro. 'Annual simulation, energy and economic analysis of hybrid heat pump systems for residential buildings'. In: *Applied Thermal Engineering* 99 (25th Apr. 2016), pp. 485–494. ISSN: 1359-4311. DOI: 10.1016/j.applthermaleng.2016.01.089. URL: https://www.sciencedirect.com/science/article/pii/S1359431116300394. (7, 16, 22, 23, 31).

[23] E. Roccatello, A. Prada, P. Baggio and M. Baratieri. 'Analysis of the Influence of Control Strategy and Heating Loads on the Performance of Hybrid Heat Pump Systems for Residential Buildings'. In: *Energies* 15.3 (2022). Num Pages: 732 Place: Basel, Switzerland Publisher: MDPI AG, p. 732. DOI: 10.3390/en15030732. URL: https://www.proquest.com/docview/2627555758/abstract/55D08F93CBA943A6PQ/1. (7, 19, 20, 31, 54).

[24] T. S. Amirkhizi and I. G. Jensen. 'Cost comparison and optimization of gas electric hybrid heat pumps'. In: *WIREs Energy and Environment* 9.3 (2020), e370. ISSN: 2041-840X. DOI: 10.1002/wene.370. URL: https://onlinelibrary.wiley.com/doi/abs/10.1002/wene.370. (7).

[25] SEAI and R. E.
bibinitperiod Environment. *Heat Pump Implementation Guide*. SEAI, 2020, p. 55. URL: https://www.seai.ie/publications/Heat-Pump-Implementation-Guide.pdf. (11, 13).

[26] Council of European Union. *Commission Decision of 1 March 2013 establishing the guidelines for Member States on calculating renewable energy from heat pumps from different heat pump technologies pursuant to Article 5 of Directive 2009/28/EC of the European Parliament and of the Council*. English. 2013. URL: https://eur-lex.europa

.eu/legal-content/EN/TXT/?uri=CELEX%3A02013D0114-20130306. (11).

[27] A. Mustafa Omer. 'Ground-source heat pumps systems and applications'. English. In: *Renewable & sustainable energy reviews* 12.2 (2008), pp. 344–371. (11).

[28] K. Ochsner. *Geothermal heat pumps*. Planning and Installing. London, England: Earthscan, Nov. 2007. (11).

[29] E. Bee, A. Prada, P. Baggio and E. Psimopoulos. 'Air-source heat pump and photovoltaic systems for residential heating and cooling: Potential of self-consumption in different European climates'. In: *Building Simulation* 12.3 (1st June 2019), pp. 453–463. ISSN: 1996-8744. DOI: 10.1007/s12273-018-0501-5. URL: https://doi.org/10.1007/s12273-018-0501-5. (12).

[30] J. Haeger. *Heat Pumps: Engineering and Installation*. Stiebel Eltron GmbH & Co. KG. Holzminden, Germany, 2012, p. 108. (12, 19).

[31] D. Keogh. 'A Technical and Economic Assessment of Hybrid Gas Heat Pump Systems as a Retrofit Measure for the Irish Residential Building Stock'. MA thesis. 2018, p. 123. (13, 41, 55, 85).

[32] C. Blackman, K. R. Gluesenkamp, M. Malhotra and Z. Yang. 'Study of optimal sizing for residential sorption heat pump system'. In: *Applied Thermal Engineering* 150 (5th Mar. 2019), pp. 421–432. ISSN: 1359-4311. DOI: 10.1016/j.applthermaleng.2018.12.151. URL: https://www.sciencedirect.com/science/article/pii/S1359431118351007. (15, 25).

[33] T. Buday. 'Reduction of environmental impacts of heat pump usage with special regard on systems with borehole heat exchangers'. In: *Acta Geographica Debrecina Landscape & Environment* 8 (Dec. 2014), pp. 66–77. (17–19).

[34] F. D'Ettorre, M. De Rosa, P. Conti, E. Schito, D. Testi and D. P. Finn. 'Economic assessment of flexibility offered by an optimally controlled hybrid heat pump generator: a case study for residential building'. In: *Energy Procedia*. ATI 2018 - 73rd Conference of the Italian Thermal Machines Engineering Association 148

(1st Aug. 2018), pp. 1222–1229. ISSN: 1876-6102. DOI: 10.1016/j.egypro.2018.08.008. URL: https://www.sciencedirect.com/science/article/pii/S1876610218302935. (19).

[35] A. Mugnini, G. Coccia, F. Polonara and A. Arteconi. 'Variable-Load Heat Pumps: Impact of the Design and Control Parameters on the Actual Operation Conditions'. In: *TECNICA ITALIANA-Italian Journal of Engineering Science* (2021). DOI: 10.18280/ti-ijes.652-434. (19, 31).

[36] M. Dongellini and G. L. Morini. 'On-off cycling losses of reversible air-to-water heat pump systems as a function of the unit power modulation capacity'. In: *Energy Conversion and Management* 196 (2019), pp. 966–978. ISSN: 0196-8904. DOI: https://doi.org/10.1016/j.enconman.2019.06.022. URL: https://www.sciencedirect.com/science/article/pii/S0196890419306934. (20, 79).

[37] G. Bagarella, R. M. Lazzarin and B. Lamanna. 'Cycling losses in refrigeration equipment: An experimental evaluation'. In: *International Journal of Refrigeration* 36.8 (1st Dec. 2013), pp. 2111–2118. ISSN: 0140-7007. DOI: 10.1016/j.ijrefrig.2013.07.020. URL: https://www.sciencedirect.com/science/article/pii/S0140700713001989. (20, 79).

[38] C. Sandström. 'Frosting and Defrosting on Air Source Heat Pump Evaporators'. MA thesis. 2021. URL: http://urn.kb.se/resolve?urn=urn:nbn:se:kth:diva-299880. (20, 64).

[39] T. Kropas, G. Streckienė and J. Bielskus. 'Experimental Investigation of Frost Formation Influence on an Air Source Heat Pump Evaporator'. In: *Energies* 14.18 (Jan. 2021), p. 5737. ISSN: 1996-1073. DOI: 10.3390/en14185737. URL: https://www.mdpi.com/1996-1073/14/18/5737. (21).

[40] E. Bee, A. Prada and P. Baggio. 'Variable-Speed Air-to-Water Heat Pumps for Residential Buildings: Evaluation of the Performance in Northern Italian Climate'. In: *CLIMA 2016 - Proceedings of the 12th REHVA World Congress*. Vol. 3. Aalborg University, 2016, pp. 22–25. (21).

[41] L. Zhang, Y. Jiang, J. Dong, Y. Yao and S. Deng. 'An experimental study of frost distribution and growth on finned tube heat exchangers used in air source heat pump units'. In: *Applied Thermal Engineering* 132 (5th Mar. 2018), pp. 38–51. ISSN: 1359-4311. DOI: 10.1016/j.applthermaleng.2017.12.047. URL: https://www.sciencedirect.com/science/article/pii/S1359431117360969. (21).

[42] M. Amer and C.-C. Wang. 'Review of defrosting methods'. In: *Renewable and Sustainable Energy Reviews* 73 (1st June 2017), pp. 53–74. ISSN: 1364-0321. DOI: 10.1016/j.rser.2017.01.120. URL: https://www.sciencedirect.com/science/article/pii/S1364032117301302. (22).

[43] J. Dong, S. Deng, Y. Jiang, L. Xia and Y. Yao. 'An experimental study on defrosting heat supplies and energy consumptions during a reverse cycle defrost operation for an air source heat pump'. In: *Applied Thermal Engineering* 37 (2012), pp. 380–387. ISSN: 1359-4311. DOI: https://doi.org/10.1016/j.applthermaleng.2011.11.052. URL: https://www.sciencedirect.com/science/article/pii/S1359431111006806. (23).

[44] Chartered Institution of Building Services Engineers. *Environmental Design: CIBSE Guide A*. 7th. CIBSE guide. Chartered Institution of Building Services Engineers, 2006. ISBN: 978-1-903287-66-8. URL: https://books.google.ie/books?id=IxXKAAAACAAJ. (23, 24).

[45] BizEE Software. *Degree Days*. https://www.degreedays.net/. Accessed: 2022-10-25. (24).

[46] M. Todorović, M. J. Banjac, T. S. Bajc and M. R. Ristanović. 'Achieving savings by implementation of efficient hybrid heating systems'. In: *Thermal Science* 23 (2019), S1683–S1693. ISSN: 0354-9836. DOI: 10.2298/TSCI180726176T. URL: https://www.proquest.com/docview/2429069502/abstract/4760FEA1CBED4F5EPQ/1. (25).

[47] V. Bianco, F. Scarpa and L. A. Tagliafico. 'Estimation of primary energy savings by using heat pumps for heating purposes in

the residential sector'. In: *Applied Thermal Engineering* 114 (Mar. 2017), pp. 938–947. ISSN: 13594311. DOI: 10.1016/j.applthermaleng.2016.12.058. URL: https://linkinghub.elsevier.com/retrieve/pii/S1359431116340625. (27, 28, 31).

[48] SEAI. *Energy in Ireland 2021 Report*. 2021. URL: https://www.seai.ie/publications/Energy-in-Ireland-2021_Final.pdf. (28, 30, 89).

[49] J. Sachs, C. Kroll, G. Lafortune, G. Fuller and F. Woelm. *Sustainable development report 2022*. Cambridge University Press, 2022. (29).

[50] European Commission. 'An EU Strategy on Heating and Cooling'. In: *COM* 51 (2016). (29).

[51] EPRI. 'US national electrification assessment'. In: *Technical Report 3002013582* (2018). (30).

[52] G. F. Franklin, J. D. Powell and A. Emami-Naeini. *Feedback control of dynamic systems*. 7th ed. Upper Saddle River, NJ: Pearson, Apr. 2014. (31, 34).

[53] T. J. A. d. Vries, W. J. R. Velthuis and J. v. Amerongen. 'Learning Feed-Forward Control: A Survey and Historical Note'. In: *IFAC Proceedings Volumes* 33.26 (2000), pp. 881–886. ISSN: 1474-6670. DOI: https://doi.org/10.1016/S1474-6670(17)39256-X. URL: https://www.sciencedirect.com/science/article/pii/S1474766701739256X. (31).

[54] R. Panda and V. Sujath. 'Identification and control of multivariable systems – role of relay feedback'. In: *Introduction to PID Controllers - Theory, Tuning and Application to Frontier Areas*. InTech, Feb. 2012. DOI: 10.5772/2422. (31, 33, 34).

[55] G. Demirezen and A. S. Fung. 'Feasibility of Cloud Based Smart Dual Fuel Switching System (SDFSS) of Hybrid Residential Space Heating Systems for Simultaneous Reduction of Energy Cost and Greenhouse Gas Emission'. In: *Energy and Buildings* 250 (1st Nov. 2021), p. 111237. ISSN: 0378-7788. DOI: 10.1016/j.enbuild.2021.111237. URL: https://www.sciencedirect.com/science/article/pii/S0378778821005211. (31, 32).

[56] elprofessor. *TikZ: Create bounding box in tikz picture of control system diagram*. TeX - LaTeX Stack Exchange. 30th June 2019. URL: https://tex.stackexchange.com/q/498105/239962. (32).

[57] mmm. *Left and right align inside one TiKZ rectangular node*. TeX - LaTeX Stack Exchange. 9th May 2012. URL: https://tex.stackexchange.com/q/55093/239962. (32).

[58] R. Judkoff, D. Wortman, B. O'Doherty and J. Burch. *Methodology for Validating Building Energy Analysis Simulations*. NREL/TP-550-42059, 928259. 1st Apr. 2008, NREL/TP–550–42059, 928259. DOI: 10.2172/928259. URL: http://www.osti.gov/servlets/purl/928259-CqoQMI/. (35).

[59] G. R. Ruiz and C. F. Bandera. 'Validation of Calibrated Energy Models: Common Errors'. In: *Energies* 10.10 (Oct. 2017). Number: 10 Publisher: Multidisciplinary Digital Publishing Institute, p. 1587. ISSN: 1996-1073. DOI: 10.3390/en10101587. URL: https://www.mdpi.com/1996-1073/10/10/1587. (35).

[60] D. Coakley, P. Raftery and M. Keane. 'A review of methods to match building energy simulation models to measured data'. In: *Renewable and Sustainable Energy Reviews* 37 (1st Sept. 2014), pp. 123–141. ISSN: 1364-0321. DOI: 10.1016/j.rser.2014.05.007. URL: https://www.sciencedirect.com/science/article/pii/S1364032114003232. (35–37).

[61] S. de Wit and G. Augenbroe. 'Analysis of uncertainty in building design evaluations and its implications'. In: *Energy and Buildings* 34.9 (2002). A View of Energy and Bilding Performance Simulation at the start of the third millennium, pp. 951–958. ISSN: 0378-7788. DOI: https://doi.org/10.1016/S0378-7788(02)00070-1. URL: https://www.sciencedirect.com/science/article/pii/S0378778802000701. (35).

[62] T. Farhang and M. Ardeshir. 'Monitoring-based optimization-assisted calibration of the thermal performance model of an office building'. In: International Conference on Architecture and Urban Design. 2012. (36).

[63] A. G. P. C. 14. 'ASHRAE Guideline 14-2014'. In: (2014). ISSN: 1049-894X. URL: https://upgreengrade.ir/admin_panel/assets/images/books/ASHRAE%20Guideline%2014-2014.pdf. (36–38, 44, 46).

[64] E. Lucas Segarra, H. Du, G. Ramos Ruiz and C. Fernández Bandera. 'Methodology for the quantification of the impact of weather forecasts in predictive simulation models'. In: *Energies* 12.7 (2019), p. 1309. (36).

[65] S. Makridakis. 'Accuracy measures: theoretical and practical concerns'. In: *International Journal of Forecasting* 9.4 (1993), pp. 527–529. ISSN: 0169-2070. DOI: https://doi.org/10.1016/0169-2070(93)90079-3. URL: https://www.sciencedirect.com/science/article/pii/0169207093900793. (37).

[66] C. Tofallis. 'A better measure of relative prediction accuracy for model selection and model estimation'. In: *Journal of the Operational Research Society* 66.8 (1st Aug. 2015). Publisher: Taylor & Francis, pp. 1352–1362. ISSN: 0160-5682. DOI: 10.1057/jors.2014.103. URL: https://doi.org/10.1057/jors.2014.103. (37).

[67] F. Khendek and R. Gotzhein, eds. *System Analysis and Modeling. Languages, Methods, and Tools for Systems Engineering: 10th International Conference, SAM 2018, Copenhagen, Denmark, October 15–16, 2018, Proceedings*. Vol. 11150. Lecture Notes in Computer Science. Cham: Springer International Publishing, 2018. ISBN: 978-3-030-01042-3. DOI: 10.1007/978-3-030-01042-3. URL: http://link.springer.com/10.1007/978-3-030-01042-3. (37).

[68] S. Kim and H. Kim. 'A new metric of absolute percentage error for intermittent demand forecasts'. In: *International Journal of Forecasting* 32 (1st July 2016), pp. 669–679. DOI: 10.1016/j.ijforecast.2015.12.003. (37).

[69] A. Bloess, W.-P. Schill and A. Zerrahn. 'Power-to-heat for renewable energy integration: A review of technologies, modeling approaches, and flexibility potentials'. In: *Applied Energy* 212 (15th Feb. 2018), pp. 1611–1626. ISSN: 0306-2619. DOI: 10.1016/j

.apenergy.2017.12.073. URL: https://www.sciencedirect.com/science/article/pii/S0306261917317889. (39).

[70] M. Wetter, W. Zuo, T. Nouidui and X. Pang. 'Modelica Buildings library'. In: *Journal of Building Performance Simulation* 7 (4th July 2014). DOI: 10.1080/19401493.2013.765506. (41, 64, 65).

[71] M. Wetter, K. Benne and B. Ravache. 'Software Architecture and Implementation of Modelica Buildings Library Coupling for Spawn of EnergyPlus'. In: *Modelica Conferences*. 2021, pp. 325–334. (41).

[72] OneBuilding. *climate.onebuilding.org*. URL: https://climate.onebuilding.org/. (43).

[73] Daikin. *Daikin Altherma 3 Product catalogue 2018*. 2018. URL: https://www.daikin-ce.com/en_us/product-group/air-to-water-heat-pump-low-temperature/daikin_altherma_3_r.html. (49).

[74] Lawrence Berkeley National Laboratory. *User Guide — Buildings Library User Guide*. 2022. URL: https://simulationresearch.lbl.gov/modelica/userGuide/. (54).

[75] G. Buttitta and D. P. Finn. 'A high-temporal resolution residential building occupancy model to generate high-temporal resolution heating load profiles of occupancy-integrated archetypes'. In: *Energy and Buildings* 206 (1st Jan. 2020), p. 109577. ISSN: 0378-7788. DOI: 10.1016/j.enbuild.2019.109577. URL: https://www.sciencedirect.com/science/article/pii/S0378778819322170. (58, 59).

[76] ASHRAE. 'ANSI/ASHRAE Standard 55-2010: Thermal Environmental Conditions for Human Occupancy'. In: (2010), p. 44. ISSN: 1041-2336. (60).

[77] Technical Committee ISO/TC 163. *Energy performance of buildings — Indoor environmental quality*. Standard. Geneva, CH: International Organization for Standardization, June 2017, p. 60. (61, 62).

[78] F. Jorissen, G. Reynders, R. Baetens, D. Picard, D. Saelens and L. Helsen. 'Implementation and verification of the IDEAS building

energy simulation library'. In: *Journal of Building Performance Simulation* 11.6 (2nd Nov. 2018), pp. 669–688. ISSN: 1940-1493. DOI: 10.1080/19401493.2018.1428361. URL: https://doi.org/10.1080/19401493.2018.1428361. (63).

[79] Daikin Europe N.V. *Technical Data — ERYQ005-007A, EKHBH007A / EKHBX007A, EKSWW150-300*. Ostend, Belguim, 2006. URL: http://www.pacenr.free.fr/doc/daikin_altherma_bt_tech_spec/TD_ERYQ005-007A_EKHBH-X007A_EN.pdf. (64).

[80] Household Energy Price Index. *Price Data*. HEPI. Mar. 2023. URL: https://www.energypriceindex.com/price-data. (83, 86).

[81] Electric Ireland. *Time-of-Use Tariffs*. 2023. URL: https://www.electricireland.ie/residential/help/smart-electricity-meters/time-of-use-tariffs-for-residential-customers. (83, 84).

[82] SEAI. *Conversion Factors*. Sustainable Energy Authority Of Ireland. URL: https://www.seai.ie/data-and-insights/seai-statistics/conversion-factors/. (88).

[83] Eirgrid Group. *Explore the Smart Grid Dashboard*. Smart Grid Dashboard. 2023. URL: https://smartgriddashboard.com/. (89).

[84] International Energy Agency. 'World energy statistics and balances, IEA'. In: *France* (2019). (90).

A

MODELICA CODE LISTING

Listing 1: `Modelica` source code for final HHS model. Source available at https://github.com/daniel-jakob/ThesisModelica

```
within Thesis_Project.Experiments;
model HHSFinalModel "Model of a hydronic heating system with energy storage"
extends Modelica.Icons.Example;
replaceable package MediumA = Buildings.Media.Air(T_default=293.15) "Medium model for air";
replaceable package MediumW = Buildings.Media.Water "Medium model";
constant Modelica.Units.SI.Volume RoomVols[:] = {29.85, 13.5, 6, 13.5, 78.625, 61.2, 30.225, 15.7*2.5, 4.83*2.5, 5.85*2.5, 10.14*2.5, 13.72*2.5, 14.06*2.5};
constant Modelica.Units.SI.Volume TotRoomVols = sum(RoomVols) - RoomVols[3];
parameter Modelica.Units.SI.MassFlowRate m_flow_nominal[:]=1.29*0.8/3600*RoomVols[:] "Design massflow rate";
parameter Modelica.Units.SI.Power Q_flow_nominal=7000 "Nominal power of heating plant";
// Due to the night setback, in which the radiator do not provide heat input into the room, // we scale the design power of the radiator loop
parameter Real scaFacRad = 1.5 "Scaling factor to scale the power (and massflow rate) of the radiator loop";
parameter Modelica.Units.SI.Temperature TSup_nominal=273.15 + 40 + 5 "Nominal supply temperature for radiators";
parameter Modelica.Units.SI.Temperature TRet_nominal=273.15 + 30 + 5 "Nominal return temperature for radiators";
parameter Modelica.Units.SI.Temperature THPSup_nominal=273.15 + 32 + 5 "Nominal supply temperature for radiators";
parameter Modelica.Units.SI.Temperature THPRet_nominal=273.15 + 22 + 5 "Nominal return temperature for radiators";
parameter Modelica.Units.SI.Temperature dTRad_nominal=TSup_nominal -
TRet_nominal "Nominal temperature difference for radiator loop";
parameter Modelica.Units.SI.Temperature dTBoi_nominal=20 "Nominal temperature difference for boiler loop";
parameter Modelica.Units.SI.MassFlowRate mRad_flow_nominal=scaFacRad*
Q_flow_nominal/dTRad_nominal/4200 "Nominal massflow rate of radiator loop";
parameter Modelica.Units.SI.MassFlowRate mBoi_flow_nominal=scaFacRad*
Q_flow_nominal/dTBoi_nominal/4200 "Nominal massflow rate of boiler loop";
parameter Modelica.Units.SI.PressureDifference dpPip_nominal=10000 "Pressure difference of pipe (without valve)";
```

```
parameter Modelica.Units.SI.PressureDifference dpVal_nominal=6000 "Pressure difference of valve";
parameter Modelica.Units.SI.PressureDifference dpRoo_nominal=6000 "Pressure difference of flow leg that serves a room";
parameter Modelica.Units.SI.PressureDifference dpThrWayVal_nominal=6000 "Pressure difference of three-way valve";
parameter Modelica.Units.SI.PressureDifference dp_nominal=dpPip_nominal +
dpVal_nominal + dpRoo_nominal + dpThrWayVal_nominal "Pressure difference of loop";
// Room model
parameter Modelica.Units.SI.Temperature TempBlockBoi= 273.15 + 7;
parameter Modelica.Units.SI.Temperature TempBlockHP = 273.15 - 2;
Buildings.Fluid.Movers.SpeedControlled_y pumBoi(
redeclare package Medium = MediumW, per(pressure(V_flow=mBoi_flow_nominal/1000*{0.5, 1}, dp=(3000 + 2000)*{2, 1})), use_inputFilter=false, energyDynamics=Modelica.Fluid.Types.Dynamics.SteadyState) "Pump for boiler circuit";
Buildings.Fluid.Movers.SpeedControlled_y pumRad(
redeclare package Medium = MediumW, per(pressure(V_flow=mRad_flow_nominal/1000*{0, 2}, dp=dp_nominal*{2, 0})), energyDynamics=Modelica.Fluid.Types.Dynamics.SteadyState) "Pump that serves the radiators";
Buildings.Fluid.Boilers.BoilerPolynomial boi(
allowFlowReversal=false, a={0.93}, effCur=Buildings.Fluid.Types.EfficiencyCurves.Constant, redeclare package Medium = MediumW, Q_flow_nominal=Q_flow_nominal, m_flow_nominal=mBoi_flow_nominal, fue=Buildings.Fluid.Data.Fuels.HeatingOilLowerHeatingValue(), dp_nominal=3000 + 2000, energyDynamics=Modelica.Fluid.Types.Dynamics.FixedInitial, T_start=293.15) "Boiler"
Modelica.Thermal.HeatTransfer.Sensors.TemperatureSensor TRoo1
Buildings.Controls.OBC.CDL.Continuous.PIDWithReset conPum(
yMax=1, Td=60, yMin=0.05, k=0.5, Ti=15) "Controller for pump"
Buildings.Fluid.Sensors.RelativePressure dpSen(redeclare package Medium =
MediumW)
; Buildings.Fluid.Actuators.Valves.TwoWayEqualPercentage val1(
redeclare package Medium = MediumW, allowFlowReversal=false, dpValve_nominal(displayUnit="Pa") = dpVal_nominal, m_flow_nominal=mRad_flow_nominal*(RoomVols[1] /TotRoomVols), dpFixed_nominal=dpRoo_nominal, from_dp=true, use_inputFilter=false) "Radiator valve"
Buildings.Controls.OBC.CDL.Continuous.PID conRoo1(
yMax=1, yMin=0, Ti=60, Td=60, controllerType=Modelica.Blocks.Types.SimpleController.P, k=0.5) "Controller for room temperature"
Modelica.Thermal.HeatTransfer.Sensors.TemperatureSensor TRoo2
Buildings.Fluid.Actuators.Valves.TwoWayEqualPercentage val2(
redeclare package Medium = MediumW, allowFlowReversal=false, dpValve_nominal(displayUnit="Pa") = dpVal_nominal, m_flow_nominal=mRad_flow_nominal*(RoomVols[2] /TotRoomVols), dpFixed_nominal=dpRoo_nominal, from_dp=true, use_inputFilter=false) "Radiator valve"
```

```
48 Buildings.Controls.OBC.CDL.Continuous.PID conRoo2(
49 yMax=1, yMin=0, Ti=60, Td=60,
    ↪ controllerType=Modelica.Blocks.Types.SimpleController.P,
    ↪ k=0.5) "Controller for room temperature"
50 Buildings.Fluid.HeatExchangers.Radiators.RadiatorEN442_2 rad2(
51 redeclare package Medium = MediumW, allowFlowReversal=false,
    ↪ fraRad=0, Q_flow_nominal= scaFacRad
    ↪ *Q_flow_nominal(RoomVols[2] /TotRoomVols),
    ↪ energyDynamics=Modelica.Fluid.Types.Dynamics.FixedInitial,
    ↪ T_a_nominal=323.15, T_b_nominal=313.15, n=1.3) "Radiator"
52 Buildings.Fluid.HeatExchangers.Radiators.RadiatorEN442_2 rad1(
53 redeclare package Medium = MediumW, allowFlowReversal=false,
    ↪ fraRad=0, Q_flow_nominal= scaFacRad
    ↪ *Q_flow_nominal(RoomVols[1] /TotRoomVols),
    ↪ energyDynamics=Modelica.Fluid.Types.Dynamics.FixedInitial,
    ↪ T_a_nominal=323.15, T_b_nominal=313.15, n=1.3)   "Radiator"
54 Buildings.Fluid.Actuators.Valves.ThreeWayEqualPercentageLinear
    ↪ thrWayVal(
55 redeclare package Medium = MediumW,
    ↪ dpValve_nominal=dpThrWayVal_nominal, l={0.01, 0.01}, tau=10,
    ↪ m_flow_nominal=mRad_flow_nominal, dpFixed_nominal={100, 0},
    ↪ use_inputFilter=false,
    ↪ energyDynamics=Modelica.Fluid.Types.Dynamics.SteadyState)
    ↪ "Three-way valve"
56 ; Buildings.Controls.OBC.CDL.Continuous.PIDWithReset conVal(
57 yMax=1, yMin=0, xi_start=1, Td=60, k=0.1, Ti=120) "Controller
    ↪ for pump"
58 Buildings.Fluid.Storage.Stratified tan(
59 allowFlowReversal=true, m_flow_nominal=mRad_flow_nominal,
    ↪ dIns=0.10, redeclare package Medium = MediumW, hTan=1.7,
    ↪ nSeg=10, show_T=true, VTan=0.5,
    ↪ energyDynamics=Modelica.Fluid.Types.Dynamics.FixedInitial)
    ↪ "Storage tank"
60 Modelica.Thermal.HeatTransfer.Sensors.TemperatureSensor
    ↪ tanTemBot "Tank bottom temperature"
61 Modelica.Thermal.HeatTransfer.Sensors.TemperatureSensor
    ↪ tanTemTop "Tank top temperature"
62 Buildings.Controls.OBC.CDL.Continuous.GreaterThreshold
    ↪ greThrBoi(t=
63 TSup_nominal + 5) "Check for temperature at the bottom of the
    ↪ tank"
64 Buildings.Controls.OBC.CDL.Conversions.BooleanToReal booToReaPum
    ↪ "Signal converter for pump"
65 Buildings.Controls.OBC.CDL.Continuous.Greater lesThr "Check for
    ↪ temperature at the top of the tank"
66 Buildings.Fluid.Sensors.TemperatureTwoPort temSup(
67 redeclare package Medium = MediumW, allowFlowReversal=false,
    ↪ m_flow_nominal=mRad_flow_nominal)
68 ; Buildings.Fluid.Sensors.TemperatureTwoPort temRet(
69 redeclare package Medium = MediumW, allowFlowReversal=false,
    ↪ m_flow_nominal=mRad_flow_nominal)
70 ; Buildings.Controls.SetPoints.SupplyReturnTemperatureReset
    ↪ heaChaBoi(
71 TRoo_nominal=296.15, dTOutHeaBal=3, use_TRoo_in=true,
    ↪ TSup_nominal=TSup_nominal, TRet_nominal=TRet_nominal,
    ↪ TOut_nominal=268.15)
72 Buildings.Controls.SetPoints.OccupancySchedule
    ↪ occSch(occupancy=3600*{7, 19})"Occupancy schedule"
73 Buildings.Controls.OBC.CDL.Continuous.Switch swi "Switch to
    ↪ select set point"
74 Buildings.Controls.OBC.CDL.Continuous.Sources.Constant
    ↪ TRooNig(k=273.15 + 18) "Room temperature set point at night"
```

```
75 Buildings.Controls.OBC.CDL.Continuous.Sources.Constant
    ↪ TRooSet(k=273.15 + 24)
76 Buildings.Controls.OBC.CDL.Continuous.MultiMax mulMax(nin=12)
    ↪ "Maximum radiator valve position" ));
77 Buildings.Controls.OBC.CDL.Continuous.Hysteresis
    ↪ hysPum(uLow=0.01, uHigh=0.20) "Hysteresis for pump"
78 Modelica.Blocks.MathBoolean.Or pumOnSig(nu=4) "Signal for pump
    ↪ being on"
79 Buildings.Controls.OBC.CDL.Continuous.Sources.Constant
    ↪ dTThr(k=1) "Threshold to switch boiler off"
80 Buildings.Controls.OBC.CDL.Continuous.Subtract sub1
81 Buildings.Controls.OBC.CDL.Continuous.Sources.Constant
    ↪ TRooOff(k=273.15 - 5) "Low room temperature set point to
    ↪ switch heating off"
82 Buildings.Controls.OBC.CDL.Continuous.Switch swi1 "Switch to
    ↪ select set point"
83 Modelica.Blocks.Logical.OnOffController onOff(bandwidth=2)
    ↪ "On/off switch"
84 Buildings.Controls.OBC.CDL.Continuous.Sources.Constant
    ↪ TOutSwi(k=16 + 293.15) "Outside air temperature to switch
    ↪ heating on or off"
85 Buildings.Fluid.Sources.Boundary_pT bou1(
86 T=288.15, nPorts=1, redeclare package Medium = MediumW) "Fixed
    ↪ boundary condition, needed to provide a pressure in the
    ↪ system"
87 Buildings.Controls.OBC.CDL.Continuous.MultiplyByParameter
    ↪ gain(k=1/dp_nominal) "Gain used to normalize pressure
    ↪ measurement signal"
88 Buildings.Fluid.FixedResistances.Junction splVal(
89 dp_nominal={dpPip_nominal, 0, 0},
    ↪ m_flow_nominal=mRad_flow_nominal*{1, -1, -1}, redeclare
    ↪ package Medium = MediumW,
    ↪ energyDynamics=Modelica.Fluid.Types.Dynamics.SteadyState)
    ↪ "Flow splitter"; Buildings.Fluid.FixedResistances.Junction
    ↪ splVal1(
90 m_flow_nominal=mRad_flow_nominal*{1, -1, -1}, redeclare package
    ↪ Medium = MediumW, dp_nominal={0, 0, 0},
    ↪ energyDynamics=Modelica.Fluid.Types.Dynamics.SteadyState)
    ↪ "Flow splitter"; Buildings.Fluid.FixedResistances.Junction
    ↪ splVal2(
91 m_flow_nominal=mRad_flow_nominal*{1, -1, -1}, redeclare package
    ↪ Medium = MediumW, dp_nominal={0, 0, 0},
    ↪ energyDynamics=Modelica.Fluid.Types.Dynamics.SteadyState)
    ↪ "Flow splitter"; Modelica.Blocks.Logical.LessThreshold
    ↪ lesThrTRoo(threshold=19 + 273.15) "Test to block boiler pump
    ↪ if room air temperature is sufficiently high"
92 Buildings.Controls.OBC.CDL.Logical.And and1 "Logical test to
    ↪ enable pump and subsequently the boiler"
93 Modelica.StateGraph.TransitionWithSignal T1 "Transition to pump
    ↪ on"
94 Modelica.StateGraph.StepWithSignal pumOn(nOut=1, nIn=1) "Pump
    ↪ on"
95 Modelica.StateGraph.StepWithSignal boiOn(nIn=1, nOut=1) "Boiler
    ↪ on"
96 Modelica.StateGraph.TransitionWithSignal T2(enableTimer=false,
    ↪ waitTime=300) "Transition that switches HP off"
97 Modelica.StateGraph.StepWithSignal pumOn2(        nIn=1, nOut=1)
    ↪ "Pump on"
98 Modelica.StateGraph.Transition T4(enableTimer=true, waitTime=10)
    ↪ "Transition to boiler on"
99 inner Modelica.StateGraph.StateGraphRoot stateGraphRoot "Root of
    ↪ the state graph"
```

```
Buildings.Controls.OBC.CDL.Conversions.BooleanToReal booToRea "Conversion from boolean to real signal"
Buildings.Controls.OBC.CDL.Continuous.MovingAverage aveTOut(delta=12*3600) "Time averaged outdoor air temperature"
inner Buildings.ThermalZones.EnergyPlus_9_6_0.Building building(
idfName="E:/Documents/ThesisNumericalSim/Reference_Home/Irish_Reference_Home(v960)_Minimal.idf",
epwName="E:/Documents/ThesisNumericalSim/Weather/Clones/IRL_Clones.039740_IWEC.epw",
weaName="E:/Documents/ThesisNumericalSim/Weather/Clones/IRL_Clones.039740_IWEC.mos", usePrecompiledFMU=false,
computeWetBulbTemperature=false) "Building model"
Buildings.BoundaryConditions.WeatherData.Bus weaBus;
Building.irishReferenceHouse
irishReferenceHouse(zone1_floor1(zoneName="zone1_floor1"))
Buildings.Fluid.Sources.MassFlowSource_WeatherData bou[13](
redeclare package Medium = MediumA, m_flow=m_flow_nominal,
nPorts=13) "Boundary condition"
Buildings.Fluid.Sources.Outside out(redeclare package Medium =
MediumA, nPorts=
1) "Outside condition"
Modelica.Thermal.HeatTransfer.Celsius.FromKelvin fromKelvin
Modelica.Thermal.HeatTransfer.Celsius.PrescribedTemperature
prescribedTemperature
Buildings.Fluid.FixedResistances.Junction splVal3(
m_flow_nominal=mRad_flow_nominal*{1, -1, -1}, redeclare package
Medium = MediumW, dp_nominal={0, 0, 0},
energyDynamics=Modelica.Fluid.Types.Dynamics.SteadyState)
"Flow splitter";
Buildings.Fluid.Actuators.Valves.TwoWayEqualPercentage val4(
redeclare package Medium = MediumW, allowFlowReversal=false,
dpValve_nominal(displayUnit="Pa") = dpVal_nominal,
m_flow_nominal=mRad_flow_nominal*(RoomVols[4] /TotRoomVols),
dpFixed_nominal=dpRoo_nominal, from_dp=true,
use_inputFilter=false) "Radiator valve"
Buildings.Fluid.HeatExchangers.Radiators.RadiatorEN442_2 rad4(
redeclare package Medium = MediumW, allowFlowReversal=false,
fraRad=0, Q_flow_nominal=scaFacRad*
Q_flow_nominal*(RoomVols[4] /TotRoomVols),
energyDynamics=Modelica.Fluid.Types.Dynamics.FixedInitial,
T_a_nominal=323.15, T_b_nominal=313.15, n=1.3) "Radiator"
Buildings.Fluid.FixedResistances.Junction splVal5(
m_flow_nominal=mRad_flow_nominal*{1, -1, -1}, redeclare package
Medium = MediumW, dp_nominal={0, 0, 0},
energyDynamics=Modelica.Fluid.Types.Dynamics.SteadyState)
"Flow splitter"
; Buildings.Fluid.FixedResistances.Junction splVal4(
m_flow_nominal=mRad_flow_nominal*{1, -1, -1}, redeclare package
Medium = MediumW, dp_nominal={0, 0, 0},
energyDynamics=Modelica.Fluid.Types.Dynamics.SteadyState)
"Flow splitter"; Buildings.Fluid.FixedResistances.Junction
splVal6(
m_flow_nominal=mRad_flow_nominal*{1, -1, -1}, redeclare package
Medium = MediumW, dp_nominal={0, 0, 0},
energyDynamics=Modelica.Fluid.Types.Dynamics.SteadyState)
"Flow splitter";
Modelica.Thermal.HeatTransfer.Sensors.TemperatureSensor
TRoo4
Buildings.Controls.OBC.CDL.Continuous.PID conRoo4(
yMax=1, yMin=0, Ti=60, Td=60,
controllerType=Modelica.Blocks.Types.SimpleController.P,
k=0.5) "Controller for room temperature"
```

```
Buildings.Fluid.FixedResistances.Junction splVal7(
m_flow_nominal=mRad_flow_nominal*{1, -1, -1}, redeclare package
 ↪  Medium = MediumW, dp_nominal={0, 0, 0},
 ↪  energyDynamics=Modelica.Fluid.Types.Dynamics.SteadyState)
 ↪  "Flow splitter"; Buildings.Fluid.FixedResistances.Junction
 ↪  splVal8(
m_flow_nominal=mRad_flow_nominal*{1, -1, -1}, redeclare package
 ↪  Medium = MediumW, dp_nominal={0, 0, 0},
 ↪  energyDynamics=Modelica.Fluid.Types.Dynamics.SteadyState)
 ↪  "Flow splitter";
 ↪  Buildings.Fluid.Actuators.Valves.TwoWayEqualPercentage val5(
redeclare package Medium = MediumW, allowFlowReversal=false,
 ↪  dpValve_nominal(displayUnit="Pa") = dpVal_nominal,
 ↪  m_flow_nominal=mRad_flow_nominal*(RoomVols[5] /TotRoomVols),
 ↪  dpFixed_nominal=dpRoo_nominal, from_dp=true,
 ↪  use_inputFilter=false) "Radiator valve"
Buildings.Fluid.HeatExchangers.Radiators.RadiatorEN442_2 rad5(
redeclare package Medium = MediumW, allowFlowReversal=false,
 ↪  fraRad=0, Q_flow_nominal = scaFacRad * Q_flow_nominal *
 ↪  (RoomVols[5] / TotRoomVols),
 ↪  energyDynamics=Modelica.Fluid.Types.Dynamics.FixedInitial,
 ↪  T_a_nominal=323.15, T_b_nominal=313.15, n=1.3) "Radiator"
Modelica.Thermal.HeatTransfer.Sensors.TemperatureSensor TRoo5
Buildings.Controls.OBC.CDL.Continuous.PID conRoo5(
yMax=1, yMin=0, Ti=60, Td=60,
 ↪  controllerType=Modelica.Blocks.Types.SimpleController.P,
 ↪  k=0.5) "Controller for room temperature"
Buildings.Fluid.FixedResistances.Junction splVal9(
m_flow_nominal=mRad_flow_nominal*{1, -1, -1}, redeclare package
 ↪  Medium = MediumW, dp_nominal={0, 0, 0},
 ↪  energyDynamics=Modelica.Fluid.Types.Dynamics.SteadyState)
 ↪  "Flow splitter"; Buildings.Fluid.FixedResistances.Junction
 ↪  splVal10(
m_flow_nominal=mRad_flow_nominal*{1, -1, -1}, redeclare package
 ↪  Medium = MediumW, dp_nominal={0, 0, 0},
 ↪  energyDynamics=Modelica.Fluid.Types.Dynamics.SteadyState)
 ↪  "Flow splitter";
 ↪  Buildings.Fluid.Actuators.Valves.TwoWayEqualPercentage val6(
redeclare package Medium = MediumW, allowFlowReversal=false,
 ↪  dpValve_nominal(displayUnit="Pa") = dpVal_nominal,
 ↪  m_flow_nominal=mRad_flow_nominal*(RoomVols[6] /TotRoomVols),
 ↪  dpFixed_nominal=dpRoo_nominal, from_dp=true,
 ↪  use_inputFilter=false) "Radiator valve"
Buildings.Fluid.HeatExchangers.Radiators.RadiatorEN442_2 rad6(
redeclare package Medium = MediumW, allowFlowReversal=false,
 ↪  fraRad=0, Q_flow_nominal=scaFacRad* Q_flow_nominal*
 ↪  (RoomVols[6] / TotRoomVols),
 ↪  energyDynamics=Modelica.Fluid.Types.Dynamics.FixedInitial,
 ↪  T_a_nominal=323.15, T_b_nominal=313.15, n=1.3) "Radiator"
Modelica.Thermal.HeatTransfer.Sensors.TemperatureSensor TRoo6
Buildings.Controls.OBC.CDL.Continuous.PID conRoo6(
yMax=1, yMin=0, Ti=60, Td=60,
 ↪  controllerType=Modelica.Blocks.Types.SimpleController.P,
 ↪  k=0.5) "Controller for room temperature"
Buildings.Fluid.FixedResistances.Junction splVal11(
m_flow_nominal=mRad_flow_nominal*{1, -1, -1}, redeclare package
 ↪  Medium = MediumW, dp_nominal={0, 0, 0},
 ↪  energyDynamics=Modelica.Fluid.Types.Dynamics.SteadyState)
 ↪  "Flow splitter"; Buildings.Fluid.FixedResistances.Junction
 ↪  splVal12(
m_flow_nominal=mRad_flow_nominal*{1, -1, -1}, redeclare package
 ↪  Medium = MediumW, dp_nominal={0, 0, 0},
```

```
148 energyDynamics=Modelica.Fluid.Types.Dynamics.SteadyState) "Flow
    ↪ splitter";
    ↪ Buildings.Fluid.Actuators.Valves.TwoWayEqualPercentage val7(
149 redeclare package Medium = MediumW, allowFlowReversal=false,
    ↪ dpValve_nominal(displayUnit="Pa") = dpVal_nominal,
    ↪ m_flow_nominal=mRad_flow_nominal*(RoomVols[7] /TotRoomVols),
    ↪ dpFixed_nominal=dpRoo_nominal, from_dp=true,
    ↪ use_inputFilter=false) "Radiator valve"
150 Buildings.Fluid.HeatExchangers.Radiators.RadiatorEN442_2 rad7(
151 redeclare package Medium = MediumW, allowFlowReversal=false,
    ↪ fraRad=0, Q_flow_nominal= scaFacRad *Q_flow_nominal
    ↪ *(RoomVols[7] /TotRoomVols),
    ↪ energyDynamics=Modelica.Fluid.Types.Dynamics.FixedInitial,
    ↪ T_a_nominal=323.15, T_b_nominal=313.15, n=1.3) "Radiator"
152 Modelica.Thermal.HeatTransfer.Sensors.TemperatureSensor TRoo7
153 Buildings.Controls.OBC.CDL.Continuous.PID conRoo7(
154 yMax=1, yMin=0, Ti=60, Td=60,
    ↪ controllerType=Modelica.Blocks.Types.SimpleController.P,
    ↪ k=0.5) "Controller for room temperature"
155 Buildings.Fluid.FixedResistances.Junction splVal13(
156 m_flow_nominal=mRad_flow_nominal*{1, -1, -1}, redeclare package
    ↪ Medium = MediumW, dp_nominal={0, 0, 0},
    ↪ energyDynamics=Modelica.Fluid.Types.Dynamics.SteadyState)
    ↪ "Flow splitter"; Buildings.Fluid.FixedResistances.Junction
    ↪ splVal14(
157 m_flow_nominal=mRad_flow_nominal*{1, -1, -1}, redeclare package
    ↪ Medium = MediumW, dp_nominal={0, 0, 0},
    ↪ energyDynamics=Modelica.Fluid.Types.Dynamics.SteadyState)
    ↪ "Flow splitter";
    ↪ Buildings.Fluid.Actuators.Valves.TwoWayEqualPercentage val8(
158 redeclare package Medium = MediumW, allowFlowReversal=false,
    ↪ dpValve_nominal(displayUnit="Pa") = dpVal_nominal,
    ↪ m_flow_nominal=mRad_flow_nominal*(RoomVols[8] /TotRoomVols),
    ↪ dpFixed_nominal=dpRoo_nominal, from_dp=true,
    ↪ use_inputFilter=false) "Radiator valve"
159 Buildings.Fluid.HeatExchangers.Radiators.RadiatorEN442_2 rad8(
160 redeclare package Medium = MediumW, allowFlowReversal=false,
    ↪ fraRad=0, Q_flow_nominal= scaFacRad
    ↪ *Q_flow_nominal(RoomVols[8] /TotRoomVols),
    ↪ energyDynamics=Modelica.Fluid.Types.Dynamics.FixedInitial,
    ↪ T_a_nominal=323.15, T_b_nominal=313.15, n=1.3) "Radiator"
161 Modelica.Thermal.HeatTransfer.Sensors.TemperatureSensor TRoo8
162 Buildings.Controls.OBC.CDL.Continuous.PID conRoo8(
163 yMax=1, yMin=0, Ti=60, Td=60,
    ↪ controllerType=Modelica.Blocks.Types.SimpleController.P,
    ↪ k=0.5) "Controller for room temperature"
164 Buildings.Fluid.FixedResistances.Junction splVal15(
165 m_flow_nominal=mRad_flow_nominal*{1, -1, -1}, redeclare package
    ↪ Medium = MediumW, dp_nominal={0, 0, 0},
    ↪ energyDynamics=Modelica.Fluid.Types.Dynamics.SteadyState)
    ↪ "Flow splitter"; Buildings.Fluid.FixedResistances.Junction
    ↪ splVal16(
166 m_flow_nominal=mRad_flow_nominal*{1, -1, -1}, redeclare package
    ↪ Medium = MediumW, dp_nominal={0, 0, 0},
    ↪ energyDynamics=Modelica.Fluid.Types.Dynamics.SteadyState)
    ↪ "Flow splitter";
    ↪ Buildings.Fluid.Actuators.Valves.TwoWayEqualPercentage val9(
167 redeclare package Medium = MediumW, allowFlowReversal=false,
    ↪ dpValve_nominal(displayUnit="Pa") = dpVal_nominal,
    ↪ m_flow_nominal=mRad_flow_nominal*(RoomVols[9] /TotRoomVols),
    ↪ dpFixed_nominal=dpRoo_nominal, from_dp=true,
    ↪ use_inputFilter=false) "Radiator valve"
```

```
Buildings.Fluid.HeatExchangers.Radiators.RadiatorEN442_2 rad9(
redeclare package Medium = MediumW, allowFlowReversal=false,
  fraRad=0, Q_flow_nominal= scaFacRad
  *Q_flow_nominal(RoomVols[9] /TotRoomVols),
energyDynamics=Modelica.Fluid.Types.Dynamics.FixedInitial,
  T_a_nominal=323.15, T_b_nominal=313.15, n=1.3) "Radiator"
Modelica.Thermal.HeatTransfer.Sensors.TemperatureSensor TRoo9
Buildings.Controls.OBC.CDL.Continuous.PID conRoo9(
yMax=1, yMin=0, Ti=60, Td=60,
  controllerType=Modelica.Blocks.Types.SimpleController.P,
  k=0.5) "Controller for room temperature"
Buildings.Fluid.FixedResistances.Junction splVal17(
m_flow_nominal=mRad_flow_nominal*{1, -1, -1}, redeclare package
  Medium = MediumW, dp_nominal={0, 0, 0},
  energyDynamics=Modelica.Fluid.Types.Dynamics.SteadyState)
  "Flow splitter"; Buildings.Fluid.FixedResistances.Junction
  splVal18(
m_flow_nominal=mRad_flow_nominal*{1, -1, -1}, redeclare package
  Medium = MediumW, dp_nominal={0, 0, 0},
  energyDynamics=Modelica.Fluid.Types.Dynamics.SteadyState)
  "Flow splitter";
  Buildings.Fluid.Actuators.Valves.TwoWayEqualPercentage
  val10(
redeclare package Medium = MediumW, allowFlowReversal=false,
  dpValve_nominal(displayUnit="Pa") = dpVal_nominal,
  m_flow_nominal=mRad_flow_nominal*(RoomVols[10]
  /TotRoomVols), dpFixed_nominal=dpRoo_nominal, from_dp=true,
  use_inputFilter=false) "Radiator valve"
Buildings.Fluid.HeatExchangers.Radiators.RadiatorEN442_2 rad10(
redeclare package Medium = MediumW, allowFlowReversal=false,
  fraRad=0, Q_flow_nominal= scaFacRad
  *Q_flow_nominal(RoomVols[10] /TotRoomVols),
  energyDynamics=Modelica.Fluid.Types.Dynamics.FixedInitial,
  T_a_nominal=323.15, T_b_nominal=313.15, n=1.3) "Radiator"
Modelica.Thermal.HeatTransfer.Sensors.TemperatureSensor TRoo10
Buildings.Controls.OBC.CDL.Continuous.PID conRoo10(
yMax=1, yMin=0, Ti=60, Td=60,
  controllerType=Modelica.Blocks.Types.SimpleController.P,
  k=0.5) "Controller for room temperature"
Buildings.Fluid.FixedResistances.Junction splVal20(
m_flow_nominal=mRad_flow_nominal*{1, -1, -1}, redeclare package
  Medium = MediumW, dp_nominal={0, 0, 0},
  energyDynamics=Modelica.Fluid.Types.Dynamics.SteadyState)
  "Flow splitter";
  Buildings.Fluid.Actuators.Valves.TwoWayEqualPercentage
  val11(
redeclare package Medium = MediumW, allowFlowReversal=false,
  dpValve_nominal(displayUnit="Pa") = dpVal_nominal,
  m_flow_nominal=mRad_flow_nominal*(RoomVols[11]
  /TotRoomVols), dpFixed_nominal=dpRoo_nominal, from_dp=true,
  use_inputFilter=false) "Radiator valve"
Buildings.Fluid.HeatExchangers.Radiators.RadiatorEN442_2 rad11(
redeclare package Medium = MediumW, allowFlowReversal=false,
  fraRad=0, Q_flow_nominal= scaFacRad
  *Q_flow_nominal(RoomVols[11] /TotRoomVols),
  energyDynamics=Modelica.Fluid.Types.Dynamics.FixedInitial,
  T_a_nominal=323.15, T_b_nominal=313.15, n=1.3) "Radiator"
Modelica.Thermal.HeatTransfer.Sensors.TemperatureSensor TRoo11
Buildings.Controls.OBC.CDL.Continuous.PID conRoo11(
yMax=1, yMin=0, Ti=60, Td=60,
  controllerType=Modelica.Blocks.Types.SimpleController.P,
  k=0.5) "Controller for room temperature"
```

```
191 Buildings.Fluid.Actuators.Valves.TwoWayEqualPercentage val12(
192 redeclare package Medium = MediumW, allowFlowReversal=false,
    ↪ dpValve_nominal(displayUnit="Pa") = dpVal_nominal,
    ↪ m_flow_nominal=mRad_flow_nominal*(RoomVols[12]
    ↪ /TotRoomVols), dpFixed_nominal=dpRoo_nominal, from_dp=true,
    ↪ use_inputFilter=false) "Radiator valve"
193 Buildings.Fluid.HeatExchangers.Radiators.RadiatorEN442_2 rad12(
194 redeclare package Medium = MediumW, allowFlowReversal=false,
    ↪ fraRad=0, Q_flow_nominal= scaFacRad
    ↪ *Q_flow_nominal(RoomVols[12] /TotRoomVols),
    ↪ energyDynamics=Modelica.Fluid.Types.Dynamics.FixedInitial,
    ↪ T_a_nominal=323.15, T_b_nominal=313.15, n=1.3) "Radiator"
195 Modelica.Thermal.HeatTransfer.Sensors.TemperatureSensor TRoo12
196 Buildings.Controls.OBC.CDL.Continuous.PID conRoo12(
197 yMax=1, yMin=0, Ti=60, Td=60,
    ↪ controllerType=Modelica.Blocks.Types.SimpleController.P,
    ↪ k=0.5) "Controller for room temperature"
198 Buildings.Fluid.FixedResistances.Junction splVal19(
199 m_flow_nominal=mRad_flow_nominal*{1, -1, -1}, redeclare package
    ↪ Medium = MediumW, dp_nominal={0, 0, 0},
    ↪ energyDynamics=Modelica.Fluid.Types.Dynamics.SteadyState)
    ↪ "Flow splitter";
    ↪ Buildings.Fluid.Actuators.Valves.TwoWayEqualPercentage
    ↪ val13(
200 redeclare package Medium = MediumW, allowFlowReversal=false,
    ↪ dpValve_nominal(displayUnit="Pa") = dpVal_nominal,
    ↪ m_flow_nominal=mRad_flow_nominal*(RoomVols[13]
    ↪ /TotRoomVols), dpFixed_nominal=dpRoo_nominal, from_dp=true,
    ↪ use_inputFilter=false) "Radiator valve"
201 Buildings.Fluid.HeatExchangers.Radiators.RadiatorEN442_2 rad13(
202 redeclare package Medium = MediumW, allowFlowReversal=false,
    ↪ fraRad=0, Q_flow_nominal= scaFacRad
    ↪ *Q_flow_nominal(RoomVols[13] /TotRoomVols),
    ↪ energyDynamics=Modelica.Fluid.Types.Dynamics.FixedInitial,
    ↪ T_a_nominal=323.15, T_b_nominal=313.15, n=1.3) "Radiator"
203 Modelica.Thermal.HeatTransfer.Sensors.TemperatureSensor TRoo13
204 Buildings.Controls.OBC.CDL.Continuous.PID conRoo13(
205 yMax=1, yMin=0, Ti=60, Td=60,
    ↪ controllerType=Modelica.Blocks.Types.SimpleController.P,
    ↪ k=0.5) "Controller for room temperature"
206 Buildings.Fluid.FixedResistances.Junction splVal21(
207 m_flow_nominal=mRad_flow_nominal*{1, -1, -1}, redeclare package
    ↪ Medium = MediumW, dp_nominal={0, 0, 0},
    ↪ energyDynamics=Modelica.Fluid.Types.Dynamics.SteadyState)
    ↪ "Flow splitter"; Buildings.Fluid.FixedResistances.Junction
    ↪ splVal22(
208 m_flow_nominal=mRad_flow_nominal*{1, -1, -1}, redeclare package
    ↪ Medium = MediumW, dp_nominal={0, 0, 0},
    ↪ energyDynamics=Modelica.Fluid.Types.Dynamics.SteadyState)
    ↪ "Flow splitter"; Modelica.Blocks.Continuous.Integrator
    ↪ TESQLossIntegrator
209 Modelica.Thermal.HeatTransfer.Sources.PrescribedTemperature
    ↪ TReturn
210 Buildings.Controls.OBC.CDL.Continuous.Sources.Constant
    ↪ HPOnSetpoint(k=
211 THPSup_nominal + 5) "Setpoint HP"
212 Buildings.Controls.OBC.CDL.Continuous.Switch swi2 "Switch for HP
    ↪ setpoint"
213 Buildings.Controls.OBC.CDL.Continuous.Sources.Constant
    ↪ HPOffSetpoint(k=273.15 -
214 10) "Setpoint HP"
215 Components.HP_AirWater_TSet hP_AirWater_TSet(
```

```
redeclare package Medium = MediumW, QNom=7000, tauHeatLoss=3600, mWater=3, cDry=4000, m_flow_nominal=mBoi_flow_nominal, betaFactor=0.65, modulation_min=5, modulation_start=12.5)
; inner IDEAS.BoundaryConditions.SimInfoManager sim(filNam="E:/Documents/ThesisNumericalSim/Weather/Clones/IRL_Clones.039740_IWEC.mos" )
Buildings.Fluid.Sensors.TemperatureTwoPort TempPreHP(redeclare package Medium
= MediumW, allowFlowReversal=falsem_flow_nominal=mBoi_flow_nominal); Buildings.Fluid.Sensors.TemperatureTwoPort TemPostHP(redeclare package Medium
= MediumW, allowFlowReversal=falsem_flow_nominal=mBoi_flow_nominal); Modelica.Blocks.Logical.LessThreshold lesThrTOut(threshold=TempBlockBoi) "Test to block boiler if TOut > 7C"
Modelica.StateGraph.TransitionWithSignal T3(enableTimer=true, waitTime=10) "Transition to boiler on"
Modelica.Blocks.Logical.GreaterThreshold greaterThreshold(threshold=
TempBlockHP) "Block\acsfont{HP}if TOut is less than 2C"
Buildings.Controls.OBC.CDL.Continuous.Switch swi3 "Switch for Supply Temp setpoint"
Buildings.Controls.SetPoints.SupplyReturnTemperatureReset heaChaHP(
TRoo_nominal=296.15, dTOutHeaBal=6, use_TRoo_in=true, TSup_nominal=THPSup_nominal, TRet_nominal=THPRet_nominal, TOut_nominal=268.15) "Supply Temp Calc for HP"
Modelica.StateGraph.StepWithSignal HPOn(nIn=1, nOut=1) "HP on"
Modelica.StateGraph.TransitionWithSignal T5(enableTimer=true, waitTime=10) "Transition to HP on"
Buildings.Controls.OBC.CDL.Logical.Switch logSwi
Buildings.Controls.OBC.CDL.Continuous.GreaterThreshold greThrHP(t=
THPSup_nominal + 3) "Check for temperature at the bottom of the tank"
Modelica.StateGraph.TransitionWithSignal T6(enableTimer=false, waitTime=300) "Transition that switches boiler off"
Modelica.StateGraph.StepWithSignal pumOn1(nIn=1, nOut=1) "Pump on"
Modelica.StateGraph.StepWithSignal pumOn3(nOut=1, nIn=1) "Pump on"
Modelica.StateGraph.Transition T7(enableTimer=true, waitTime=10) "Transition to boiler on"
Modelica.StateGraph.TransitionWithSignal T8 "Transition to pump on"
Buildings.Controls.OBC.CDL.Continuous.Less les
Buildings.Controls.OBC.CDL.Logical.And and2 "Boiler on if <7C & TPostHP > TSupplySetpoint"
; Modelica.StateGraph.InitialStepWithSignal off(nOut=1, nIn=1) "Pump and furnace off"
Modelica.StateGraph.InitialStepWithSignal off1(nOut=1, nIn=1) "Pump and furnace off"
Buildings.Controls.OBC.CDL.Logical.Nor Nor
Buildings.Controls.OBC.CDL.Logical.And and3
Buildings.Utilities.Math.Average roomAvgTemp(nin=11)
; Modelica.Blocks.MathBoolean.Or pumOnSig1(nu=3) "Signal for pump being on"
Modelica.Blocks.Logical.GreaterThreshold greaterThreshold1(threshold=
TempBlockBoi) "Block HP if TOut is less than 2C"
```

```
Buildings.Controls.OBC.CDL.Continuous.GreaterThreshold greThr(t=0.1)
; Buildings.Controls.OBC.CDL.Continuous.LessThreshold lesThr1(t=273.15 + 2)
; Buildings.Controls.OBC.CDL.Logical.And and4;
 Buildings.Controls.OBC.CDL.Logical.TimerAccumulating accTim(t=60*60)
; Buildings.Controls.OBC.CDL.Logical.Timer tim(t=5*60) ;
 Buildings.Controls.OBC.CDL.Continuous.GreaterThreshold greThr1(t=273.15 + 3)
; Buildings.Controls.OBC.CDL.Logical.TrueHoldWithReset truHol(duration=10*60)
Buildings.Controls.OBC.CDL.Logical.Not not1
Buildings.Controls.OBC.CDL.Logical.And and5
Buildings.Controls.OBC.CDL.Continuous.PID BoiPI(
yMax=1, yMin=0, Ti=60, Td=60,
 controllerType=Buildings.Controls.OBC.CDL.Types.
 SimpleController.PID, k=0.25) "Controller for room
 temperature"
Buildings.Controls.OBC.CDL.Continuous.Switch swi4
Buildings.Controls.OBC.CDL.Continuous.Sources.Constant dTThr1(k=0) "Threshold to switch boiler off"
Buildings.Controls.OBC.CDL.Logical.Pre pre
Buildings.Controls.OBC.CDL.Logical.Or or2
Buildings.Fluid.Boilers.BoilerPolynomial boi1(
allowFlowReversal=false, a={0.93},
 effCur=Buildings.Fluid.Types.EfficiencyCurves.Constant,
 redeclare package Medium = MediumW, Q_flow_nominal=832,
 m_flow_nominal=mBoi_flow_nominal,
 fue=Buildings.Fluid.Data.Fuels.
 HeatingOilLowerHeatingValue(), dp_nominal=3000 + 2000,
 energyDynamics=Modelica.Fluid.Types.Dynamics.FixedInitial,
 T_start=293.15) "Boiler"
Buildings.Controls.OBC.CDL.Conversions.BooleanToReal booToReaPum1 "Signal converter for pump"
Buildings.Fluid.Sources.Boundary_pT bou2(
T=288.15, nPorts=1, redeclare package Medium = MediumW) "Fixed
 boundary condition, needed to provide a pressure in the
 system"
Buildings.Fluid.Sources.Boundary_pT bou3(
T=288.15, nPorts=1, redeclare package Medium = MediumW) "Fixed
 boundary condition, needed to provide a pressure in the
 system"
Buildings.Fluid.Movers.SpeedControlled_y pumBoi1(
redeclare package Medium = MediumW,
 per(pressure(V_flow=mBoi_flow_nominal/1000*{0.5, 1},
 dp=(3000 + 2000)*{2, 1})), use_inputFilter=false,
 energyDynamics=Modelica.Fluid.Types.Dynamics.SteadyState)
 "Pump for boiler circuit";
connect(pumRad.port_b, dpSen.port_a)
connect(val2.port_b, rad2.port_a);
connect(val1.port_b, rad1. port_a);
connect(conRoo2.y, val2.y);
connect(conRoo1.y, val1.y);
connect(pumRad.port_a, thrWayVal.port_2)
connect(boi.port_b, pumBoi. port_a);
connect(tan.heaPorVol[1], tanTemTop.port);
connect(tanTemBot.port, tan.heaPorVol[tan.nSeg]);
connect(temSup.T, conVal.u_m);
connect(mulMax.y, hysPum.u);
connect(conRoo2.y, mulMax.u[1]);
connect(conRoo1.y, mulMax.u[2]);
```

```
connect(conVal.y, thrWayVal.y);
connect(booToReaPum.y, pumBoi.y);
connect(swi.y, heaChaBoi.TRoo_in);
connect(pumRad.port_b, temSup.port_a);
connect(sub1.y, lesThr.u2);
connect(tanTemTop.T, sub1.u1);
connect(dTThr.y, sub1.u2);
connect(tanTemBot.T, greThrBoi.u);
connect(TRooSet.y, swi1.u1);
connect(swi1.u2, occSch.occupied);
connect(TRooNig.y, swi1.u3);
connect(TOutSwi.y, onOff.reference);
connect(swi1.y, swi.u1);
connect(onOff.y, swi.u2);
connect(TRooOff.y, swi.u3);
connect(conPum.y, pumRad.y);
connect(TRoo2.T, conRoo2. u_m);
connect(TRoo1.T, conRoo1.u_m);
connect(bou1.ports[1], boi.port_a);
connect(gain.u, dpSen.p_rel);
connect(gain.y, conPum.u_m);
connect(pumBoi.port_b, tan.port_a);
connect(pumBoi.port_b, thrWayVal.port_1);
connect(temRet.port_b, splVal.port_1);
connect(thrWayVal.port_3, splVal.port_3);
connect(splVal.port_2, tan.port_b);
connect(splVal1.port_3, $15$al1. port_a);
connect(splVal1.port_1, temSup.port_b);
connect(temRet.port_a, splVal2.port_1);
connect(splVal2.port_3, rad1. port_b);
connect(lesThr.y, and1.u2);
connect(lesThrTRoo.y, and1.u1);
connect(and1.y, T1.condition);
connect(pumOn2.active, pumOnSig.u[1]);
connect(pumOn.active, pumOnSig.u[2]);
connect(hysPum.y, conPum.trigger);
connect(hysPum.y, booToRea.u)
connect(booToRea.y, conPum.u_s)
connect(conVal.trigger, hysPum.y);
connect(onOff.u, aveTOut.y);
connect(weaBus, building. weaBus);
connect(weaBus.TDryBul, aveTOut. u);
connect(weaBus.TDryBul, heaChaBoi.TOut);
connect(weaBus, bou[1].weaBus);
connect(weaBus, bou[2].weaBus);
connect(weaBus, bou[3].weaBus);
connect(weaBus, bou[4].weaBus);
connect(weaBus, bou[5].weaBus);
connect(weaBus, bou[6].weaBus);
connect(weaBus, bou[7].weaBus);
connect(weaBus, bou[8].weaBus);
connect(weaBus, bou[9].weaBus);
connect(weaBus, bou[10].weaBus);
connect(weaBus, bou[11].weaBus);
connect(weaBus, bou[12].weaBus);
connect(weaBus, bou[13].weaBus);
connect(irishReferenceHouse.port_a, bou.ports[1]);
connect(irishReferenceHouse.port_b, out.ports[1]);
connect(out.weaBus, weaBus);
connect(rad2.heatPortCon, irishReferenceHouse.heat_port_a[2]);
connect(rad1.heatPortCon, irishReferenceHouse.heat_port_a[1]);
connect(TRoo1.port, irishReferenceHouse.heat_port_a[1]);
```

```
connect(TRoo2.port, irishReferenceHouse.heat_port_a[2]);
connect(fromKelvin.Kelvin, irishReferenceHouse.TAir[3]);
connect(fromKelvin.Celsius, prescribedTemperature.T)
connect(prescribedTemperature.port, boi.heatPort);
connect(prescribedTemperature.port, tan.heaPorTop);
connect(prescribedTemperature.port, tan.heaPorBot);
connect(prescribedTemperature.port, tan.heaPorSid);
connect(splVal1.port_2, splVal3.port_1)
connect(splVal3.port_3, val2.port_a);
connect(splVal3.port_2, splVal5.port_1)
connect(splVal5.port_3, val4.port_a)
connect(val4.port_b, rad4.port_a);
connect(splVal2.port_2, splVal4. port_1);
connect(rad2.port_b, splVal4. port_3);
connect(rad4.port_b, splVal6.port_3);
connect(splVal6.port_1, splVal4. port_2);
connect(TRoo4.port, irishReferenceHouse.heat_port_a[4]);
connect(TRoo4.T, conRoo4.u_m);
connect(swi.y, conRoo4.u_s);
connect(conRoo4.y, val4.y);
connect(conRoo4.y, mulMax.u[3]);
connect(rad4.heatPortCon, irishReferenceHouse.heat_port_a[4]);
connect(swi.y, conRoo2.u_s);
connect(swi.y, conRoo1.u_s);
connect(splVal8.port_1, splVal6.port_2);
connect(splVal5.port_2, splVal7.port_1);
connect(splVal7.port_3, val5.port_a);
connect(val5.port_b, rad5.port_a);
connect(rad5.port_b, splVal8.port_3);
connect(TRoo5.T, conRoo5.u_m);
connect(conRoo5.y, val5.y);
connect(TRoo5.port, irishReferenceHouse.heat_port_a[5]);
connect(rad5.heatPortCon, irishReferenceHouse.heat_port_a[5])
connect(conRoo5.u_s, swi.y);
connect(conRoo5.y, mulMax.u[4]);
connect(conRoo6.y, val6.y);
connect(TRoo6.port, irishReferenceHouse.heat_port_a[6]);
connect(rad6.heatPortCon, irishReferenceHouse.heat_port_a[6]);
connect(conRoo6.u_s, swi.y);
connect(conRoo6.y, mulMax.u[5]);
connect(val6.port_b, rad6.port_a);
connect(TRoo6.T, conRoo6.u_m);
connect(conRoo7.y, val7.y);
connect(TRoo7.port, irishReferenceHouse.heat_port_a[7]);
connect(rad7.heatPortCon, irishReferenceHouse.heat_port_a[7]);
connect(conRoo7.u_s, swi.y);
connect(conRoo7.y, mulMax.u[6]);
connect(val7.port_b, rad7.port_a);
connect(TRoo7.T, conRoo7.u_m);
connect(conRoo8.y, val8.y);
connect(TRoo8.port, irishReferenceHouse.heat_port_a[8]);
connect(rad8.heatPortCon, irishReferenceHouse.heat_port_a[8]);
connect(conRoo8.u_s, swi.y);
connect(conRoo8.y, mulMax.u[7]);
connect(val8.port_b, rad8.port_a);
connect(TRoo8.T, conRoo8.u_m);
connect(conRoo9.y, val9.y);
connect(TRoo9.port, irishReferenceHouse.heat_port_a[9]);
connect(rad9.heatPortCon, irishReferenceHouse.heat_port_a[9]);
connect(conRoo9.u_s, swi.y);
connect(conRoo9.y, mulMax.u[8]);
connect(val9.port_b, rad9.port_a);
```

```
connect(TRoo9.T, conRoo9.u_m);
connect(conRoo10.y, val10.y);
connect(TRoo10.port, irishReferenceHouse.heat_port_a[10]);
connect(rad10.heatPortCon, irishReferenceHouse.heat_port_a[10]);
connect(conRoo10.u_s, swi.y);
connect(conRoo10.y, mulMax.u[9]);
connect(val10.port_b, rad10.port_a);
connect(TRoo10.T, conRoo10.u_m);
connect(conRoo11.y, val11.y);
connect(TRoo11.port, irishReferenceHouse.heat_port_a[11]);
connect(rad11.heatPortCon, irishReferenceHouse.heat_port_a[11]);
connect(conRoo11.u_s, swi.y);
connect(conRoo11.y, mulMax.u[10]);
connect(val11.port_b, rad11.port_a);
connect(TRoo11.T, conRoo11.u_m);
connect(conRoo12.y, val12.y);
connect(TRoo12.port, irishReferenceHouse.heat_port_a[12]);
connect(rad12.heatPortCon, irishReferenceHouse.heat_port_a[12]);
connect(conRoo12.u_s, swi.y);
connect(conRoo12.y, mulMax.u[11]);
connect(val12.port_b, rad12.port_a);
connect(TRoo12.T, conRoo12.u_m);
connect(conRoo13.y, val13.y);
connect(TRoo13.port, irishReferenceHouse.heat_port_a[13]);
connect(rad13.heatPortCon, irishReferenceHouse.heat_port_a[13]);
connect(conRoo13.u_s, swi.y);
connect(conRoo13.y, mulMax.u[12]);
connect(val13.port_b, rad13.port_a);
connect(TRoo13.T, conRoo13.u_m);
connect(splVal8.port_2, splVal10.port_1);
connect(splVal10.port_2, splVal12.port_1);
connect(splVal12.port_2, splVal14.port_1);
connect(splVal14.port_2, splVal16.port_1);
connect(splVal16.port_2, splVal18.port_1);
connect(splVal18.port_2, splVal20.port_1);
connect(splVal7.port_2, splVal9.port_1);
connect(splVal9.port_2, splVal11.port_1);
connect(splVal11.port_2, splVal13.port_1);
connect(splVal13.port_2, splVal15.port_1);
connect(splVal15.port_2, splVal17.port_1);
connect(rad11.port_b, splVal20.port_3);
connect(rad10.port_b, splVal18.port_3);
connect(rad9.port_b, splVal16.port_3);
connect(rad8.port_b, splVal14.port_3);
connect(rad7.port_b, splVal12.port_3);
connect(rad6.port_b, splVal10.port_3);
connect(splVal9.port_3, val6.port_a);
connect(splVal11.port_3, val7.port_a);
connect(splVal13.port_3, val8.port_a);
connect(splVal15.port_3, val9.port_a);
connect(splVal17.port_3, val10.port_a);
connect(splVal17.port_2, splVal19.port_1);
connect(splVal19.port_3, val11.port_a);
connect(splVal20.port_2, splVal22.port_1);
connect(splVal19.port_2, splVal21.port_1);
connect(splVal21.port_2, val13.port_a);
connect(splVal22.port_2, rad13.port_b);
connect(splVal21.port_3, val12.port_a);
connect(rad12.port_b, splVal22.port_3);
connect(TESQLossIntegrator.u, tan.Ql_flow);
connect(weaBus.TDryBul, TReturn.T);
connect(HPOnSetpoint.y, swi2.u1);
```

```
connect(HPOffSetpoint.y, swi2.u3);
connect(swi2.y, hP_AirWater_TSet.TSet);
connect(TReturn.port, hP_AirWater_TSet.heatPort);
connect(hP_AirWater_TSet.port_a, TempPreHP.port_b)
connect(TempPreHP.port_a, tan.port_b);
connect(hP_AirWater_TSet.port_b, TemPostHP.port_a)
connect(TemPostHP.port_b, boi.port_a);
connect(weaBus.TDryBul, lesThrTOut.u);
connect(weaBus.TDryBul, greaterThreshold.u);
connect(swi3.y, lesThr.u1);
connect(swi.y, heaChaHP.TRoo_in);
connect(weaBus.TDryBul, heaChaHP.TOut);
connect(swi3.y, conVal.u_s);
connect(T5.outPort, HPOn.inPort[1])
connect(greaterThreshold.y, T5.condition);
connect(tanTemBot.T, greThrHP.u);
connect(logSwi.y, T2.condition);
connect(T3.outPort, boiOn.inPort[1])
connect(T6.condition, logSwi.y);
connect(boiOn.outPort[1], T6.inPort)
connect(HPOn.outPort[1], T2.inPort)
connect(pumOn1.active, pumOnSig.u[3]);
connect(T2.outPort, pumOn1.inPort[1])
connect(pumOn.outPort[1], T3.inPort)
connect(T6.outPort, pumOn2.inPort[1])
connect(pumOn3.outPort[1], T5.inPort)
connect(pumOn3.active, pumOnSig.u[4]);
connect(pumOn2.outPort[1], T4.inPort)
connect(pumOn1.outPort[1], T7.inPort);
connect(T1.outPort, pumOn.inPort[1])
connect(T8.outPort, pumOn3.inPort[1])
connect(and1.y, T8.condition);
connect(greaterThreshold.y, logSwi.u2);
connect(greThrBoi.y, logSwi.u3);
connect(heaChaHP.TSup, swi3.u1);
connect(heaChaBoi.TSup, swi3.u3);
connect(greThrHP.y, logSwi.u1);
connect(les.u1, TemPostHP.T);
connect(swi3.y, les.u2);
connect(lesThrTOut.y, and2.u2);
connect(les.y, and2.u1);
connect(and2.y, T3.condition);
connect(off.outPort[1], T1.inPort)
connect(T4.outPort, off.inPort[1]));
connect(T8.inPort, off1.outPort[1])
connect(T7.outPort, off1.inPort[1]));
connect(off.active, Nor.u1);
connect(off1.active, Nor.u2);
connect(and3.u1, pumOnSig.y);
connect(Nor.y, and3.u2);
connect(roomAvgTemp.y, lesThrTRoo.u);
connect(TRoo1.T, roomAvgTemp.u[1]);
connect(TRoo2.T, roomAvgTemp.u[2]);
connect(TRoo4.T, roomAvgTemp.u[3]);
connect(TRoo5.T, roomAvgTemp.u[4]);
connect(TRoo6.T, roomAvgTemp.u[5]);
connect(TRoo7.T, roomAvgTemp.u[6]);
connect(TRoo8.T, roomAvgTemp.u[7]);
connect(TRoo9.T, roomAvgTemp.u[8]);
connect(TRoo10.T, roomAvgTemp.u[9]);
connect(TRoo11.T, roomAvgTemp.u[10]);
connect(TRoo12.T, roomAvgTemp.u[11]);
```

```
connect(pumOnSig1.y, booToReaPum.u));
connect(pumOnSig1.u[1], and3.y);
connect(boiOn.active, pumOnSig1.u[2]);
connect(weaBus.TDryBul, greaterThreshold1.u);
connect(greaterThreshold1.y, swi3.u2);
connect(hP_AirWater_TSet.HPCOP, greThr.u));
connect(weaBus.TDryBul, lesThr1.u);
connect(lesThr1.y, and4.u1);
connect(greThr.y, and4.u2)
connect(and4.y, accTim.u)
connect(tim.u, greThr1.y)
connect(weaBus.TDryBul, greThr1.u);
connect(accTim.passed, truHol.u);
connect(truHol.y, not1.u);
connect(not1.y, and5.u2);
connect(HPOn.active, and5.u1);
connect(and5.y, swi2.u2);
connect(and5.y, pumOnSig1.u[3]);
connect(TemPostHP.T, BoiPI.u_m);
connect(swi3.y, BoiPI.u_s);
connect(boiOn.active, swi4.u2);
connect(BoiPI.y, swi4.u1);
connect(swi4.u3, dTThr1.y);
connect(accTim.passed, pre.u);
connect(tim.passed, or2.u1);
connect(pre.y, or2.u2);
connect(or2.y, accTim.reset);
connect(swi4.y, boi.y);
connect(truHol.y, booToReaPum1.u);
connect(booToReaPum1.y, boi1.y);
connect(boi1.port_b, bou3.ports[1]);
connect(bou2.ports[1], pumBoi1.port_a);
connect(pumBoi1.port_b, boi1.port_a);
connect(booToReaPum1.y, pumBoi1.y);
connect(prescribedTemperature.port, boi1.heatPort);
), Icon(
coordinateSystem(extent={{-100, -360}, {760, 1080}})),
 ↪  experiment(
StopTime=31536000Tolerance=1e-06__Dymola_Algorithm="Radau"),
 ↪  __Dymola_experimentFlags( Advanced(
 ↪  GenerateVariableDependencies = false,
 ↪  OutputModelicaCode=false) Evaluate =
 ↪  falseOutputCPUtime=falseOutputFlatModelica =false));
end HHSFinalModel;
```

B

MODELICA HHPS MODEL BREAKDOWN

Fig. B.1 shows the section of the model with many components relating to the boiler, HP, various control related blocks and the composite block containing the reference home. The `building` block on the left connects the `.idf`-file and `.epw`-file to the `Modelica` model via `Spawn of EnergyPlus`, acting as the interface between the two softwares. the `weaBus` block directly to the right of the `building` block is the weather bus block, essentially allowing weather data to be passed to other blocks. The `bou[]` block and the block directly beneath it act as boundary condition blocks, converting the climatic data to infiltrating and exiting air to the conditioned zones. The `pumBOi` and `pumRad` blocks are the two pumps of the hydronic system. the `boi` block towards the bottom left is the boiler block described in Subsec. 4.5.4. The `tan` block bottom center is the tank model described in Subsec. 4.5.3. The various `temSup`, `temRet`, `tanTemTop`, `tankTemBot`, `temPostHP` and `tempPreHP` block are water temperature sensors. The information from the sensors are used in the control system. The `swi` blocks are logical switches. The `heaChaBoi` and `heaChaHP` blocks are the blocks which compute the supply temperature for the radiators using the curves from Fig. 4.4. The various `splVal` blocks are splitting valves. The block directly left of the `splVal` block is a controllable three way splitter, being controlled by the PI-controller block `conVal`, the output of which is determined by the `temSup` sensor, and the `swi3` block (which switches between the two demand curves depending on outdoor conditions, as per the `greaterOut` block).

The HP model block is located bottom centre, directly next to the `TReturn` boundary condition block.

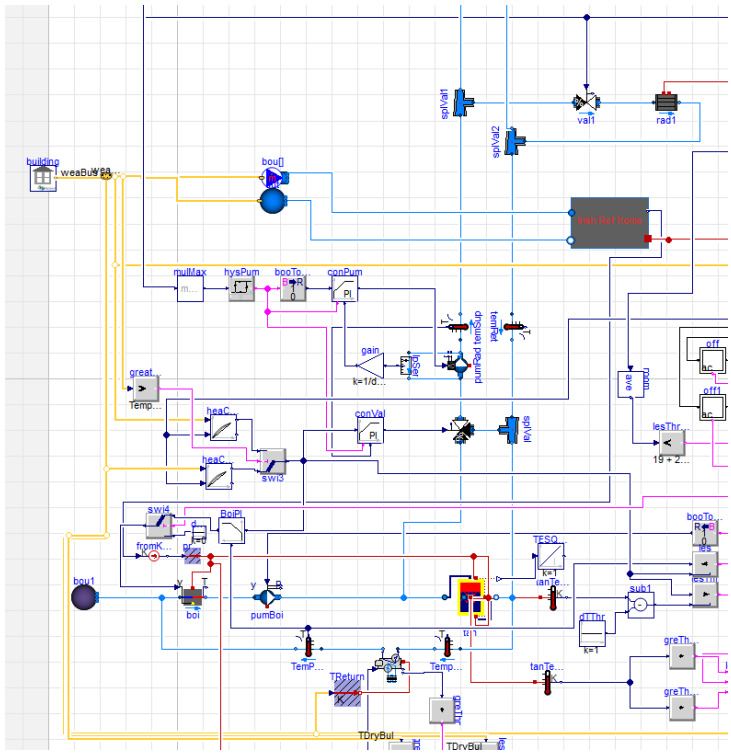

Figure B.1: Boiler and HP section of the `Modelica` model

In Fig. B.2, just north of the centre is the day-night setback control section. The `TRooSet` and `TRooNig` constant integer outputs are switched by the `occSch` and `swi1` blocks. This feeds into the supply temperature demand block. In the centre of the figure is the state machine portion of the control system, comprised of the various `pumOn` step blocks and `T1`, `T2`, etc. transition blocks. The top loop control the boiler and the bottom one controls the HP. The `stateGraphRoot` block on the right is necessary for `Modelica` to keep track of the state machine. There are many `and` and `or` blocks connected to the inputs and outputs of the `Modelica.StateGraph.StepWithSignal` blocks. In the bottom centre two blocks connected by yellow lines can be seen, these

are the inequality blocks to test for the outdoor temperature to block the boiler or HP by blocking the `T3` and `T5` respectively. The `room` `Buildings.Utilities.Math.Average` block takes the temperatures of all conditioned rooms as a vector and calculates the average, and allows the `T1` and `T8` transition blocks to be unblocked if the `lesThr` block is outputting true. This block is testing whether the temperature at the top of the buffer tank is less than the demanded supply temperature.

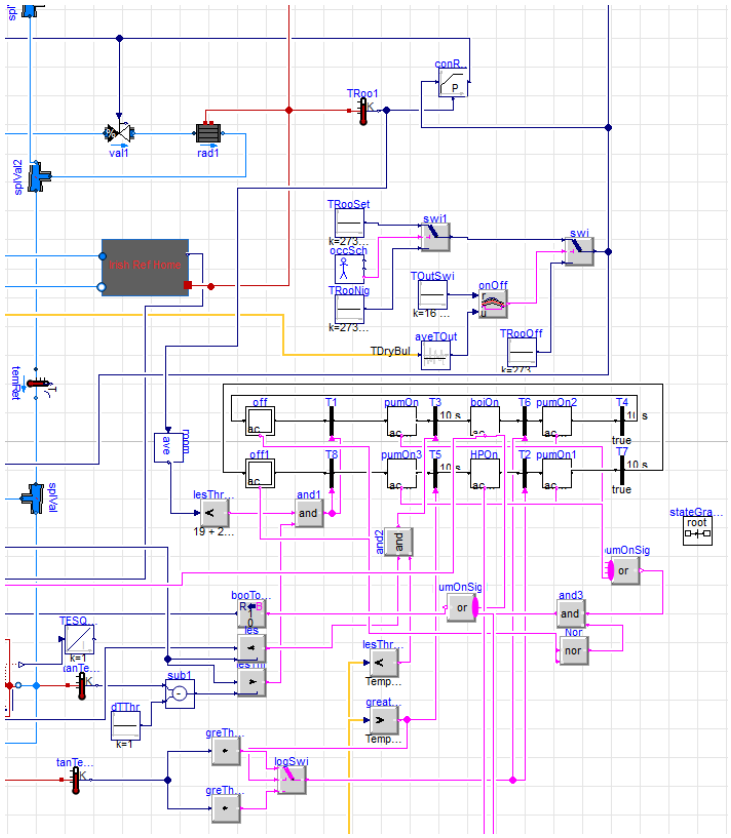

Figure B.2: Controller section of the `Modelica` model

Fig. B.3 shows the frosting model diagram. The `greThr` block tests whether the HP is on, and the `lesThr1` block tests whether it outdoor temperature is less than 2 °C, the output of these is put into the `and4` logical and block and passed to the `accTim`

time accumulating block. It is reset if the `greThr1` block activates the threshold of the `tim` timer block after a 5-minute contiguous period with $T_{ext} > 4\,°C$. The `truHol` block serves as the blocking mechanism of the HP for a 10-minute period. The second pump and boiler models are to imitate the boiler acting in reverse, the energy usage of the `boi1` model is summed with the primary boiler model to account for the energy loss due to defrosting.

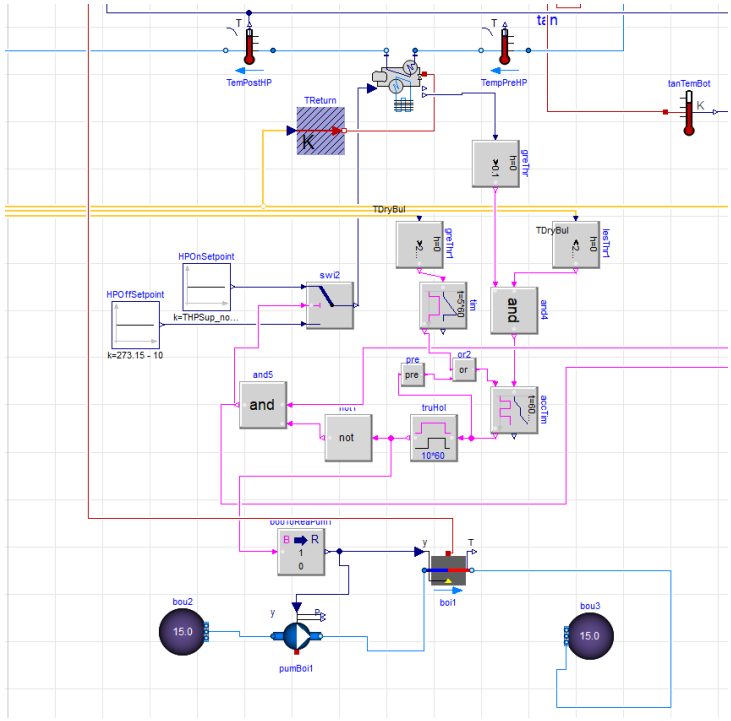

Figure B.3: Frosting model section of the `Modelica` model

Fig. B.4 shows the radiator section of the model. Not all of the connections are rendered as they were not created using the `Dymola` interface, rather, they were manually created in the underlying code in order to avoid mistakes. The `rad1`, `rad2`, etc. blocks are the radiator blocks, as described in Subsec. 4.5.2, serving each of the twelve conditioned rooms, with `rad3` omitted as the third indexed room is unconditioned. The `val1`, `val2`, etc. blocks are controllable valves, limiting the flowrate as a function of the

respective volume of the room to the total room volume, and are controlled by the `conRoo1`, `conRoo2`, etc. P-controller blocks. The P-controllers take the respective temperature of the room as input via `TRoo1`, `TRoo2`, etc. and the `swi` block from the day-night setback switch. The output of these P-controllers feeds into the `mulMax` block from Fig. B.1.

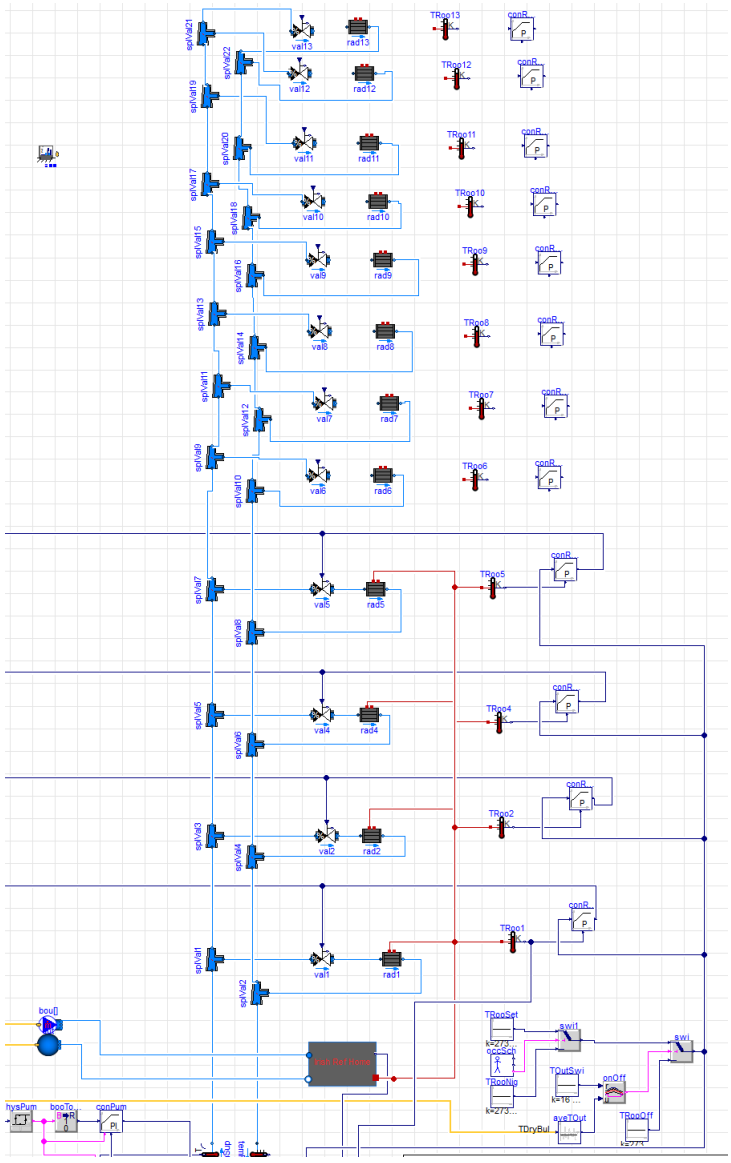

Figure B.4: Radiator section of the `Modelica` model